Sea Ice CCI+

Norwegian Meteorological Institute

ESA CCI+ CLIMATE CHANGE INITIATIVE

PHASE 1: NEW R&D ON CCI ECVS

Contract number:

4000126449/19/I-NB

esa European Space Agency

High(er) Resolution SEA ICE CONCENTRATION (SICCI-HR-SIC)

PRODUCT VALIDATION AND INTERCOMPARISON REPORT (PVIR)

Reference: D4.1

Issue: 3.0

Date: 31 January 2023

Norwegian Meteorological Institute · AWI · FMI · DTU · Danmarks Meteorologiske Institut · Max-Planck-Institut für Meteorologie · UNIS The University Centre in Svalbard

Norwegian Meteorological Institute

The Norwegian Meteorological Institute (METNO)
Henrik Mohns Plass 1
N-0313 Oslo
Norway
Phone: + 47 22 96 30 00
Fax: + 47 22 96 30 50
E-Mail: thomas.lavergne@met.no
http://www.met.no

Contract	**Deliverable**
PHASE 1 OF THE CCI+ CLIMATE CHANGE INITIATIVE NEW R&D ON CCI ECVS SEA ICE ECV	D4.1 High(er) Resolution Sea Ice Concentration Product Validation and Intercomparison Report
CLIENT	**CLIENT REFERENCE**
European Space Agency	4000126449/19/I-NB

Revision date:

31 January 2023

Principal Authors

Roberto Saldo, Technical University of Denmark - DTU Space

Thomas Lavergne, Norwegian Meteorological Institute - MET Norway

Rasmus Tonboe, Technical University of Denmark - DTU Space

Leif Toudal Pedersen, Technical University of Denmark - DTU Space

Change Record

Issue	Date	Reason for Change	Author(s)
1.0	15.03.2020	First version (Year 1)	L. Pedersen and R. Saldo
2.0	10.12.2020	Second version	L. Pedersen and R. Saldo
3.0	31.01.2023	Third version	R. Saldo, R.T. Tonboe, T. Lavergne

Document Approval

Role	Name	Signature
Written by:	R. Saldo, R.T. Tonboe, T. Lavergne	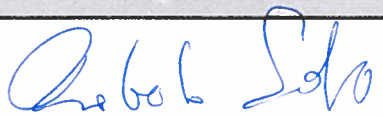
Checked by:	T. Lavergne	
Approved by:	A. M. Trofaier	

Contents

1 INTRODUCTION

1.1 Purpose

This document is the Product Validation and Intercomparison Report for High(er) Resolution Sea Ice Concentration CDR (SICCI-HR-SIC) in the Sea Ice ECV within CCI+ PHASE 1 - NEW R&D ON CCI ECVs, which is being undertaken by a METNO-led consortium.

1.2 Scope

The PVIR v3 reports on the validation of the new “High(er) Resolution” CCI+ Sea Ice Concentration data records (SICCI-HR-SIC). The validation results are compared to those obtained from the EUMETSAT OSI SAF datasets “v3” and “v2” datasets.

1.3 Document Status

This is the third and final version of the report, prepared at the end of the CCI+ Sea Ice Phase 1 project.

1.4 Reference Documents

This is the Product Validation and Intercomparison Report (PVIR) for SICCI-HR-SIC.

Reference documents are:

[RD-1] Sea Ice Concentration Algorithm Theoretical Basis Document (ATBD) for the ESA CCI datasets, D2.1, revision 3.1, available from the DOI landing page.

[RD-2] High(er) Resolution Sea Ice Concentration Product User Guide (PUG), D4.2, revision 3.0, available from the DOI landing page.

[RD-3] EUMETSAT OSI SAF Algorithm Theoretical Baseline Document (ATBD) for the Global Sea Ice Concentration Climate Data Records v3 (OSI-450-a, OSI-430-a, OSI-458), SAF/OSI/CDOP3/DMI_Met/SCI/MA/270, version v3.0, August 2022, available from https://osi-saf.eumetsat.int/products/osi-450-a

[RD-4] EUMETSAT OSI SAF Validation Report for the Global Sea Ice Concentration Climate Data Records v3 (OSI-450-a, OSI-430-a, OSI-458), SAF/OSI/CDOP3/DMI/SCI/RP/285, version v3.0, August 2022, available from https://osi-saf.eumetsat.int/products/osi-450-a

1.5 Acronyms and Abbreviations

The table below lists the acronyms and abbreviations used in this volume.

Table 1: Acronyms and Abbreviations. Acronyms for the deliverable items (URD, etc…) and partner institutions (AWI,..) are not repeated.

Acronym	Meaning
AMSR-E / AMSR2	Advanced Microwave Scanning Radiometer (for EOS / #2)
AOGCM	Arctic Ocean General Climate Model
AR5, AR6	WMO IPCC Assessment Report series
ASAR	Advanced Synthetic Aperture Radar
C3S	EU Copernicus Climate Change Service
CCI	Climate Change Initiative
CDR	Climate Data Record
CMEMS	EU Copernicus Marine Environment Monitoring Service
CMIP5, CMIP6	Coupled Model Intercomparison Project series
CMUG	Climate Modelling User Group
CRG	Climate Research Group
CS-2	ESA's CryoSat-2
DEWG	CCI Data Engineering Working Group
EASE grid	Equal-Area Scalable Earth Grid
ECMWF	European Centre for Medium-Range Weather Forecasts
ECV	Essential Climate Variable
ENVISAT	ESA's Environmental Satellite
EO	Earth Observation
ERS	European Remote Sensing Satellite
ESA	European Space Agency
ESMR	Electrically Scanning Microwave Radiometer
EUMETSAT	European Organization for the Exploitation of Meteorological Satellites
FoV (*alt* FOV)	Field-of-View
FY3	Feng Yun 3
FYI	First Year Ice
GCOS	WMO's Global Climate Observing System
GCW	WMO's Global Cryosphere Watch
ICDR	Interim Climate Data Record
IMB	Ice Mass Balance buoy
IPCC	WMO's Intergovernmental Panel on Climate Change
L1b, L2, L3C, ...	Satellite data processing Level (Level-1b, …)
MERIS	MEdium Resolution Imaging Spectrometer

EPS, EPS-SG	EUMETSAT's Polar System, EPS Second Generation
MIZ	Marginal Ice Zone
MODIS	Moderate Resolution Imaging Spectroradiometer
MTSU	Mean Total Standard Uncertainty
MWI	MicroWave Imager (EPS-SG)
MWRI	Micro-Wave Radiation Imager (Feng Yun 3)
MYI	Multi-Year Ice
NASA	National Aeronautics and Space Administration
NOAA	US National Oceanic and Atmospheric Administration
NSIDC	US National Snow and Ice Data Centre
OE	Optimal Estimation
OIB	Operation Ice Bridge
OSI SAF	EUMETSAT Ocean and Sea Ice Satellite Application Facility
OWF	Open Water Filter
PMR	Passive Microwave Radiometer
PMW	Passive Microwave
RA	Radar Altimeter
RMSE	RootMeanSquareError
RRDP	Round Robin Data Package
SIC	Sea Ice Concentration
SIT	Sea Ice Thickness
SAR	Synthetic Aperture Radar
SIRAL	Synthetic Aperture Radar (SAR) Interferometer Radar Altimeter
SOA	Service Oriented Architecture
SMMR	Scanning Multichannel Microwave Radiometer
SMOS	Soil Moisture and Ocean Salinity
SSM/I	Special Sensor Microwave/Imager
SSMIS	Special Sensor Microwave Imager/Sounder
ULS	Upward Looking Sonar
WMO	World Meteorological Organisation
WSM	Wide Swath Mode

1.6 Executive Summary

The High(er) Resolution Sea Ice Concentration Climate Data Record from ESA CCI (SICCI-HR-SIC) is a global dataset covering 30 years (1991-2020). It is processed from passive microwave imagery and Numerical Weather Prediction data through a dedicated algorithm.

SICCI-HR-SIC is an **advanced pan-sharpened version of OSI-450-a**, the most recent SIC CDR from the EUMETSAT OSI SAF. This advanced pan-sharpening approach required specific R&D and algorithms to be conducted in the CCI+ Sea Ice Phase 1 project, and resulted in a standalone dataset which is **higher resolution but shorter** than the dataset from OSI SAF. Note that ESA CCI+ Sea Ice Phase 1 also contributed R&D input to the OSI SAF processing chains.

SICCI-HR-SIC uses the high-frequency, high(er) resolution near-90 GHz imagery of the SSM/I and SSMIS satellite missions to obtain higher resolution SIC fields (12.5 km) than OSI-450-a (25 km). Such near-90 GHz imagery has only been available since 1991.

The PVIR documents the results obtained at the end of Year 3 of the CCI+ Sea Ice project for the Sea Ice Concentration (SIC) variable. The validation data is presented first (based on the SIC Round Robin Data Package RRDP developed during the previous CCI Sea Ice projects, and extended during the current), then the validation methodology (collocation and statistics).

The validation results are presented as histograms and time-series for the SICCI-HR-SIC dataset. We also compare them to the “baseline” validation results of the SIC data already published from the ESA CCI Sea Ice Phase 2 project, and the EUMETSAT OSI SAF.

Over open water (0% SIC) the Root Mean Square Error (RMSE) and the Mean Total Standard Uncertainty (MTSU) have about the same magnitude between 3 and 4% on both the Northern and Southern Hemisphere. On the Northern Hemisphere there is a nearly constant bias of 0.5% throughout the validation period, on the Southern Hemisphere the bias is near 0% throughout the validation period.

Over consolidated ice (100% SIC) the number of validation points is largest from 2016 to 2020 thanks to better SAR coverage (Sentinel-1 A&B). In the Northern Hemisphere the bias varies between 0 and -3%, and in the Southern Hemisphere the bias is between +1 and -2%. There is no bias trend as a function of time. The mean annual MTSU is nearly constant at 3% in both hemispheres while the RMSE varies between 3 and 6%.

We then present regional validation statistics over consolidated ice (100% SIC). In the Baffin Bay (mostly first year ice), and the Beaufort Sea (multiyear and first year ice), the mean annual bias is mostly positive up to +1.5 to +3.5%. There are also a few cases with a negative mean annual bias down to -1.5%. On the other hand, in the Kara Sea (first year ice), the Laptev Sea (first year ice) and in the area North of Greenland (multiyear ice) the mean annual bias is negative from 0 to about -2% with a few outliers. The overall NH SIC1 negative bias -0.5% could come from validation sites in the Western Arctic and it does not seem to be directly related to ice type.

Overall, we conclude that the advanced pan-sharpening method used to produce SICCI-HR-SIC - which was designed to improve the spatial resolution from that of the OSI SAF CDR and at the same time avoid the high noise that would result from using the near-90GHz imagery alone - is effective and that SICCI-HR-SIC has the potential to bring added value to the climate community.

2 DESCRIPTION OF THE EXTENDED SIC RRDP

The SIC Round-Robin Data Package was developed during the ESA CCI Sea Ice Phase 1 and 2 projects, and was extended during CCI+ Phase 1. It contains a variety of reference data for evaluation and tuning of SIC algorithms, but the core of the dataset is clearly the so-called SIC0 (0% SIC) and SIC1 (100% SIC) datasets.

The reference SIC0 samples are the result of filters based on location and date, while the 100% (SIC1) reference samples are derived from zones of converging sea ice motion detected by satellite synthetic aperture radar (SAR) data. See Kern et al (2019) for more information about the methods for retrieving the SIC0 and SIC1 reference data. The SIC0 samples are available from 1978 and the SIC1 samples from 2007. The SIC0 data is a static data set with fixed sample locations for each month of the year. The SIC0 samples are few, but due to the thorough retrieving method they are considered high-quality reference data. Only SIC0 samples that are located within the monthly climatological water mask are used in the validation (because those that fall outside have their SIC forced to 0% in the satellite product files). The locations of SIC0 samples used in the assessment are shown in Fig. 1.

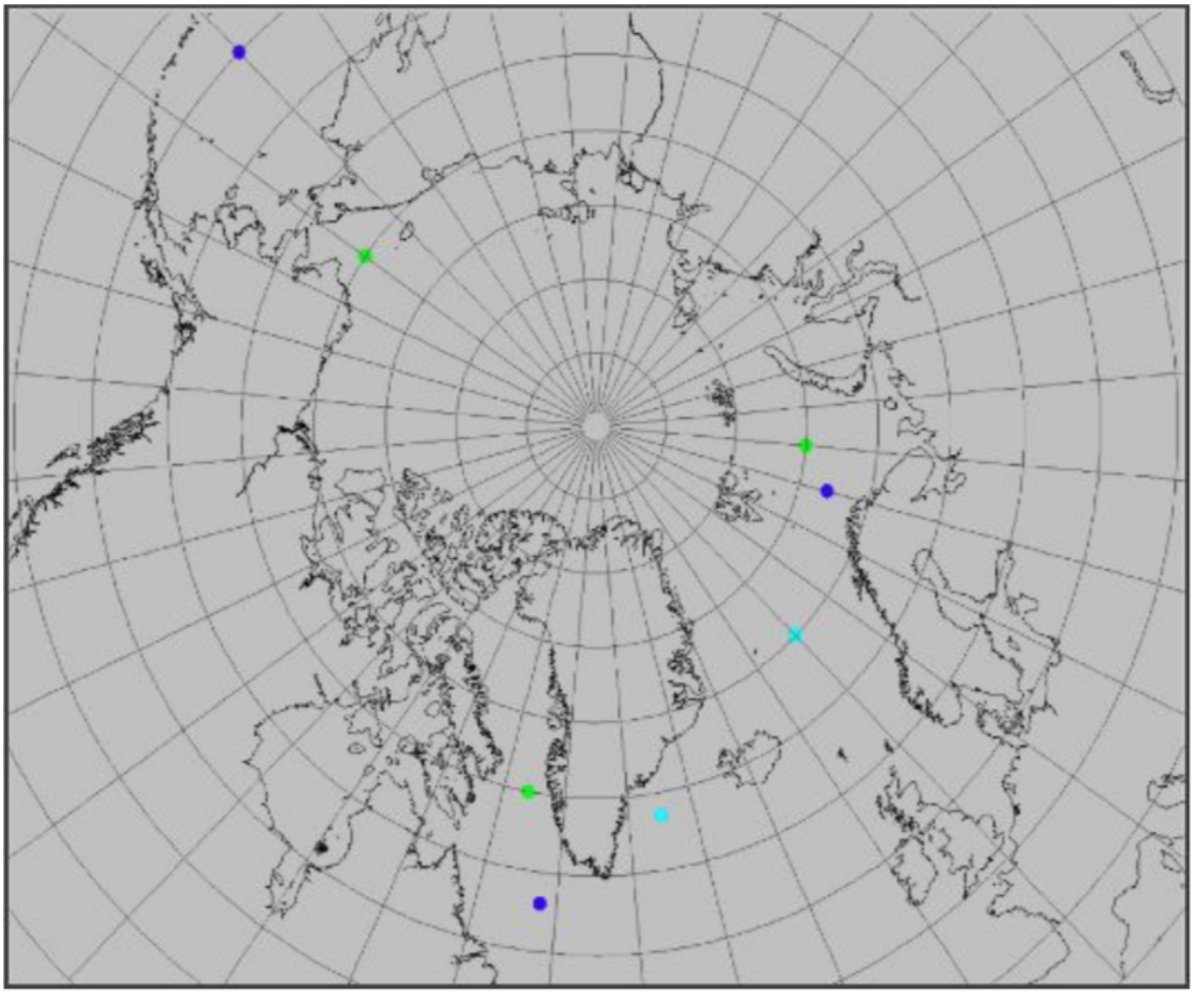

Figure 1. Location of the data points used for the open water validation (SIC0).

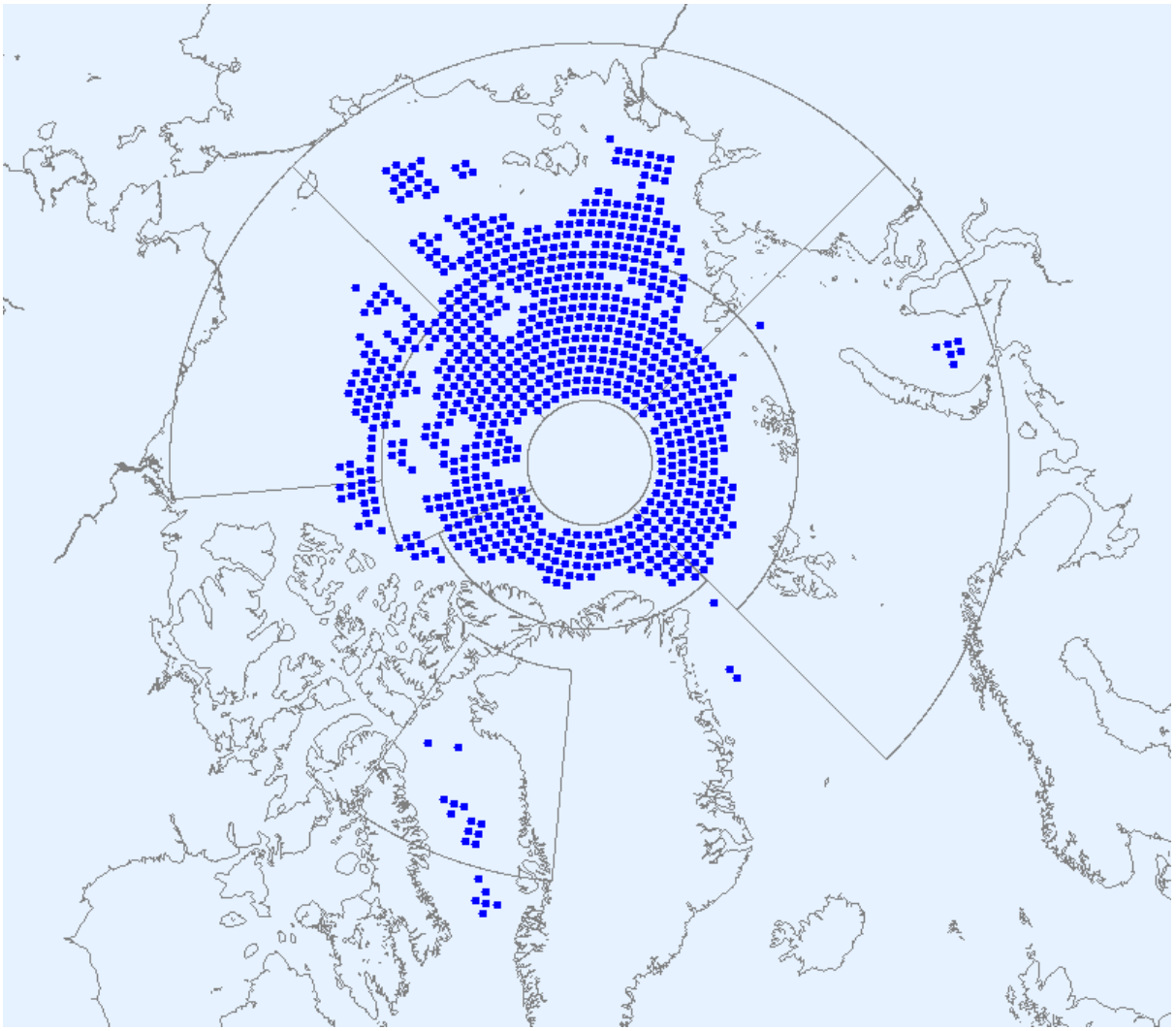

Figure 2. Visualisation of the location of data points used for the Arctic validation for compact ice (100% SIC). In addition the sub-area division is shown. The pole hole is due to the limited coverage of the Sentinel-1 SAR and hence the ice drift and deformation dataset.

The RRDP has in addition been subdivided into several geographical sub-areas in order to validate SIC performance regionally and thus for different ice type compositions.

For the Northern Hemisphere sub-areas are:

NGRL: Lat: 82-87, Lon -110 - 0

BEAUFORT-S: Lat: 70-80, Lon: -180 to -130

BEAUFORT-N: Lat: 80-87, Lon: -180 to -110

LAPTEV-S: Lat: 70-80, Lon: 90 to 180

LAPTEV-N: Lat: 80-87, Lon: 90 to 180

KARA-S: Lat: 70-80, Lon: 0 to 90

KARA-N: Lat: 80-87, Lon: 0 to 90

BAFFIN: 70-80, Lon: -80 to -50

For the Southern Ocean the sub-areas are:

Weddell: 0-60W (or 300-360E)

Ross: 130W - 160E (or 160-230E)

For the Northern Hemisphere we use SIC1 data from the winter months November through April, and for the Southern Hemisphere we use SIC1 data from the Austral winter months of May through October. A threshold for the convergence factor is applied to avoid areas which are too dynamic (that may not be fully ice covered after a day) and to avoid areas where convergence is not significantly smaller than expected noise. The divergence interval used is [0.985,0.996]. Divergence smaller than 1 corresponds to convergence (the area is shrinking).

For the open water validation we use data from the whole year.

The SIC RRDP dataset is available as:

Pedersen, Leif Toudal; Saldo, Roberto; Ivanova, Natalia; Kern, Stefan; Heygster, Georg; Tonboe, Rasmus; et al. (2019, last update Nov 2021): Reference dataset for sea ice concentration. figshare. Dataset. https://doi.org/10.6084/m9.figshare.6626549.v7

3 DESCRIPTION OF THE SIC CDRs

The main target for this report is to validate the new High(er) Resolution Sea Ice Concentration Climate Data Record from the ESA CCI+ Sea Ice Phase 1 project (SICCI-HR-SIC). The dataset has a dedicated Algorithm Theoretical Basis Document (ATBD) [RD-1] and a Product User Guide (PUG) [RD-2]. Here we briefly recall the main characteristics of the CDR.

The High(er) Resolution SIC CDR is a global dataset of daily sea-ice concentrations covering 1991 - 2020. It is presented as two polar EASE2 grids (NH and SH) with a 12.5 km grid spacing, thus a higher resolution than the OSI SAF CDRs and the previous ESA CCI (Phase 2) CDRs. The SIC is obtained using both the latest EUMETSAT OSI SAF SICs (OSI-450-a) combined with SICs (derived in CCI+) from the near-90GHz imagery of the SSM/I and SSMIS missions (hence the start in January 1991 with SSM/I F10). The processing thus involves two steps: 1) compute daily SICs at 12.5 km resolution from the near-90GHz imagery and a N90LIN algorithm including dynamic tie-points and RTM-based correction of the atmospheric noise, and 2) use these SIC fields to enhance the spatial resolution of the SICs from EUMETSAT OSI SAF (originally at 25 km resolution) with a pan-sharpening algorithm.

The resulting SICCI-HR-SIC is thus shorter than the OSI SAF CDR (1991-2020 vs 1978-2020) but brings higher resolution (12.5 km vs 25 km) without overly increasing the retrieval uncertainties (as will be documented in the results below).

We bring three more SIC CDRs in this validation report, to compare the accuracy of the SICCI-HR-SIC against that of other sources. These are:

- The older (“v2”) SIC CDR from OSI SAF (released 2017): OSI-450 (1979-2015) and its operational extension OSI-430-b (2016-2020).
- The new (“v3”) SIC CDR from OSI SAF (released 2022): OSI-450-a (1978-2020). This CDR also has an operational extension (OSI-430-a, 2020 onwards) but this is not used here.
- The new (“v3”) SIC CDR from AMSR missions (released 2022): OSI-458 (2002-2020). This CDR is the result of a Research to Operation (R2O) between ESA CCI and OSI SAF (the “v2” of this CDR was released by ESA CCI Phase 2).

Table 2: List of SIC algorithms.

Algorithm	Channels	Comment
SICCI2LF	19V, 37H, 37V	Main SIC algorithm for SICCI and OSI SAF “v2” CDR (OSI-450 and OSI-430-b)
SICCI3LF	19V, 37H, 37V	Evolution of SICCI2LF with R&D from CCI+ Phase 1 and OSI SAF. Used for all OSI SAF “v3” CDRs : OSI-450-a, OSI-430-a, and OSI-458.
N90LIN	89H, 89V	Linearised near-90GHz algorithm, used for the internal SICs in CCI+ (not distributed, not validated here).
SICCI3RELF	19V, 37H, 37V, 89H, 89V	Merger of SICCI3LF and N90LIN, using the latter for pan-sharpening the former. This is the algorithm sustaining SICCI-HR-SIC.

4 DESCRIPTION OF SEMI-AUTOMATED VALIDATION PROCEDURES

All SIC datasets from previous versions as well as new versions are in the same file format and use the same geographic projection. An automated validation procedure has been implemented that allows an easy comparison between each dataset and the reference 0% and 100% sea ice concentration datasets in the updated RRDP. For each datapoint in the reference dataset, co-located ice concentrations, uncertainties and other relevant metadata are extracted, and summary statistics are produced.

The assessment method is applied to the unfiltered, original (“raw”) sea ice concentration data as available from the product files. As a consequence of how the OSI SAF SIC algorithm works, this variable can contain unphysical ice concentration values such as

values below 0% and above 100% (this variable is available for users, who can take advantage of information with less filtering applied, e.g. via Data Assimilation techniques). Using the raw SIC values allows assessment of the bias and STD of the product near the tie-points, i.e. as it gives access to the full (symmetric) distribution of the derived SIC data-points (Kern et al., 2019).

5 EVALUATION OF SICCI-HR-SIC OVER SIC0 AND SIC1 CONDITIONS

Validation of SICCI-HR-SIC is performed covering the years from 1991 to 2020 for SIC0 (0% SIC) and 2007 to 2020 for SIC1 (100% SIC).

Figure 3 shows the number of open water validation data points together with the mean annual SIC bias (SIC - 0), the validation RMSE and the product mean total standard uncertainty (mtsu) for both the Northern and Southern Hemisphere. In 1991 there were fewer open water validation data points directly affecting the validation results by increasing both RMSE and mtsu. However, from 1992 and onwards the number of open water points is almost constant. The RMSE and the mtsu have about the same magnitude between 3% and 4% on both the Northern and Southern Hemisphere and they follow approximately the same pattern of increases and decreases as a function of time. During the validation period mtsu gradually decreases from a level near 4% to near 3%. On the Northern Hemisphere there is a nearly constant bias of 0.5% throughout the validation period, on the Southern Hemisphere the bias is near 0% throughout the validation period.

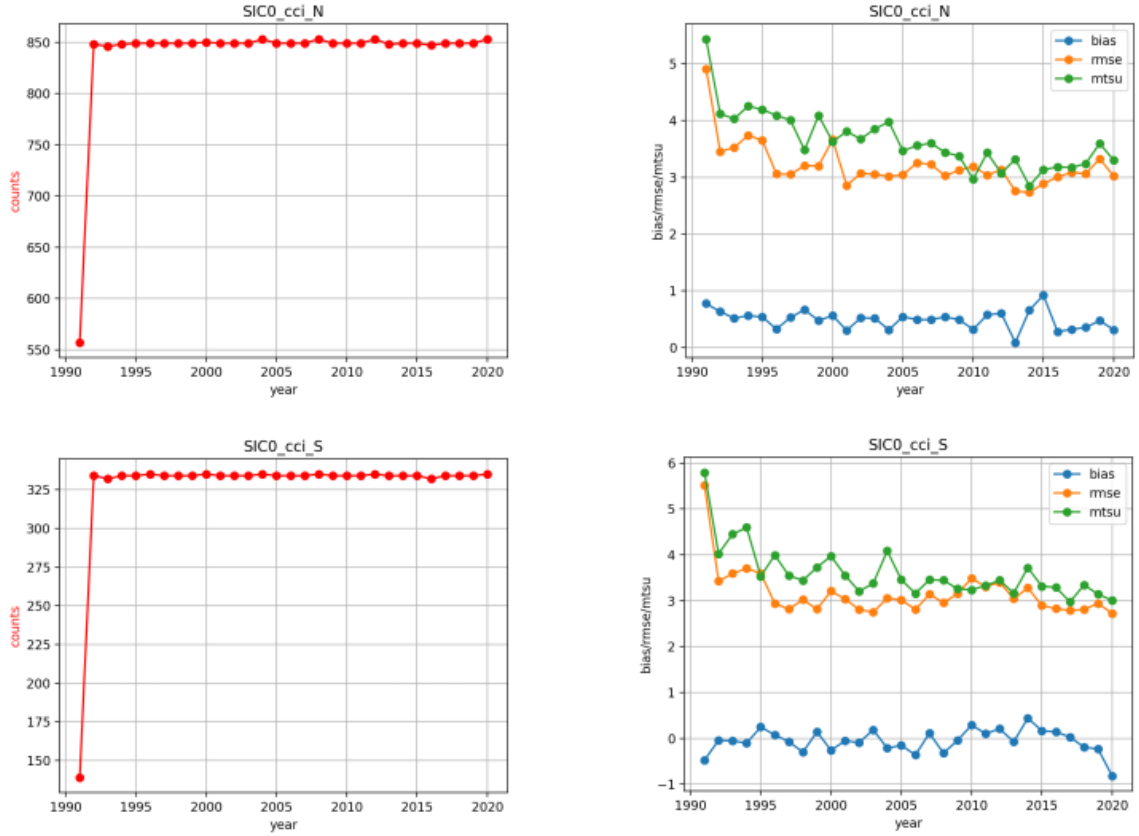

Figure 3. Time series of the SIC0 values. Note that 1991 has spotty SSM/I coverage resulting in a lower sample count.

Figure 4 summarizes the 100% sea ice validation results, showing the number of selected validations points, the mean annual RMSE, mtsu, and the bias from 2007 to 2020 for both the Northern and Southern Hemisphere. The number of annual validation points is much higher in the Northern (about 1000-13000) than the Southern Hemisphere (about 100-3000). For both hemispheres the number of validation points is largest from 2016 to 2020. On the Northern Hemisphere the bias varies between 0% and -3% and on the Southern Hemisphere the bias is between 1% and -2% and there is no bias trend as a function of time. The mean annual mtsu is nearly constant at 3% on both hemispheres while the RMSE varies between 3 and 6%.

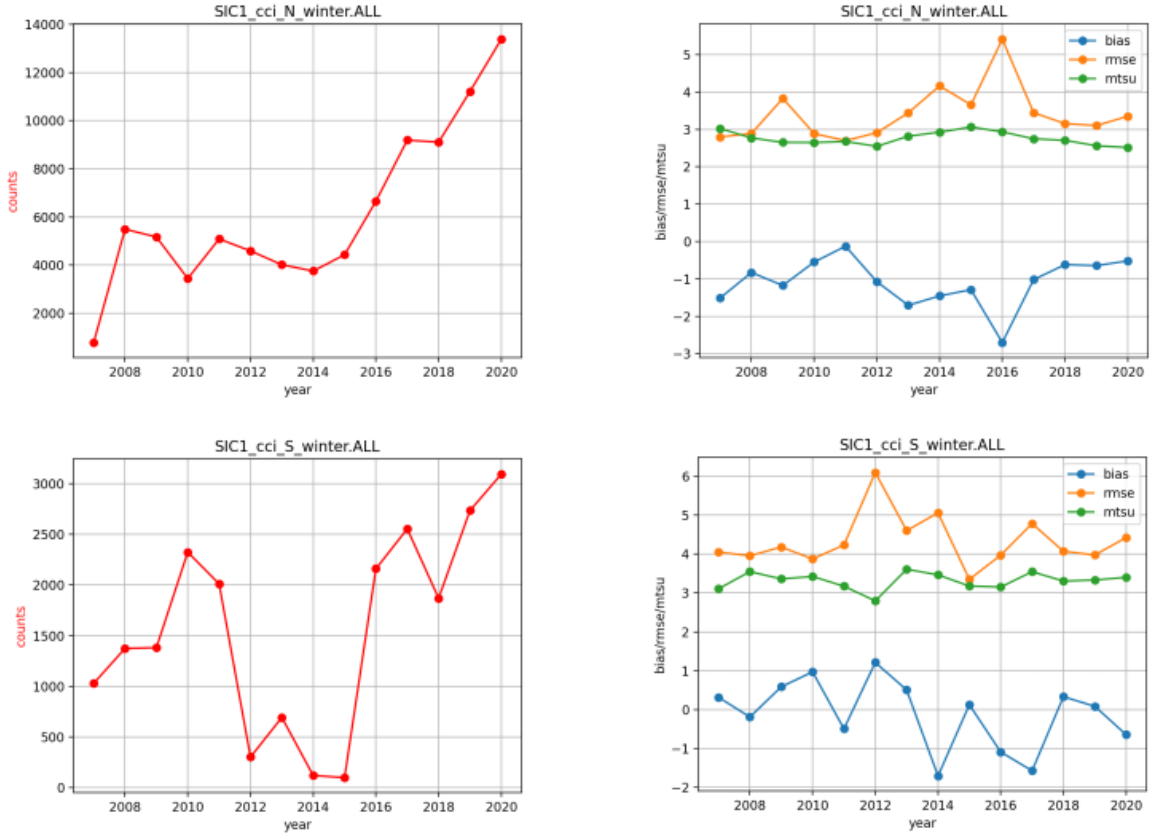

Figure 4. Time series of the SIC1 values. Note that 2012-2014 is the period in between the demise of ASAR (Envisat) on march 8th 2012 and the introduction of the Sentinel 1A in autumn 2014.

6 COMPARISON TO OTHER SIC CDRs

Fig. 5 shows the validation results for the four SIC CDRs introduced earlier. The main topic for the validation report is the SICCI-HR-SIC CDR shown in violet (and labeled CCI+ RE here). These data were already shown on Fig. 3 and 4. The validation of SICCI-HR-SIC starts in 1991 for SIC0 (because this is the start of the CDR period), and in 2007 for SIC1 (because this is the start of the SIC1 dataset). The pan-sharpening method used to produce SICCI-HR-SIC is designed to improve the spatial resolution from that of the OSI SAF CDR and at the same time avoid the high noise that would result from using the near-90GHz imagery alone. The time series shown on Fig. 5 demonstrates that this strategy is effective.

The validation against SIC0 shows that SICCI-HR-SIC has a larger but still reasonable RMSE when compared to that obtained for the OSI SAF CDRs (that only use the 19 and 37 GHz channels). The RMSE of SICCI-HR-SIC is about 3% across the timeseries, while the OSI SAF CDRs achieve between 1-2% RMSE. The bias of SICCI-HR-SIC is limited (less than 1%) in the Northern Hemisphere, as that of the OSI SAF CDRs for the same period. In the Southern Hemisphere the bias is virtually 0% over the period. One hypothesis is that the PDF of the SIC errors is skewed towards positive values in the Northern Hemisphere, leading to a positive bias. This could result from remaining un-corrected weather impact over the ocean in the Northern Hemisphere. We recall that the bias and RMSE reported here are for the un-filtered SICs (full retrieval PDF, before the application of a Open Water Filter) and

that the filtered (main) SIC field in the CDR (variable ice_conc) will still show exactly 0% over open water (thanks to the Open Water Filter). This is explained in detail in [RD-1] and [RD-2].

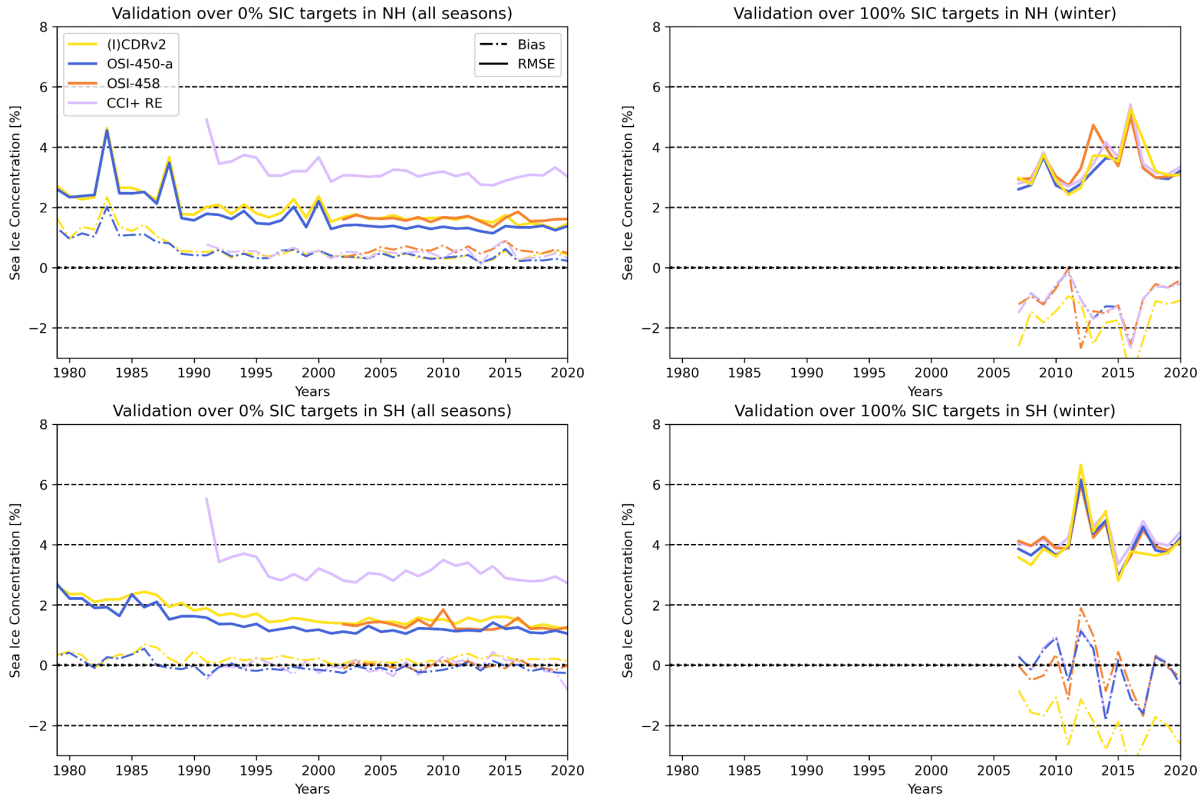

Figure 5. Time series plots of the results from the comparison of SIC0 (left plots) and SIC1 (right plots) reference data with SICCI-HR-SIC (violet line, here labeled CCI+ RE for Resolution Enhanced), the OSI SAF CDRs v3 OSI-450-a (blue line) and OSI-458 (orange line), and the OSI SAF v2 CDR+ICDR (OSI-450 and OSI-430-b, yellow line) for the Northern Hemisphere (top plots) and Southern Hemisphere (bottom plots). The figure shows the bias (dotted lines) and RMSE (solid lines). We recall that the SIC1 validation is for the winter season only, while SIC0 is year-round.

The validation against SIC1 shows that SICCI-HR-SIC achieves the same RMSE and bias as the OSI SAF CDRs. In particular, the negative bias that was observed with the “v2” CDRs (around -2%) was corrected in the “v3” CDRs (fully in SH, partly in NH). Although it uses the near-90GHz imagery, SICCI-HR-SIC does not bring additional noise (RMSE nor bias) over consolidated sea ice.

In the next section, we investigate regional SIC1 validation to see if the errors (especially the remaining bias in the Arctic) is more pronounced in certain regions, linked to different sea-ice types.

7 SIC1 REGIONAL EVALUATION NORTHERN HEMISPHERE

The following section summarizes the mean annual 100% sea ice validation for different regions in the Northern Hemisphere separately and as a function of time (2008-2020). The number of validation points vary widely from year to year and from region to region, which can explain some of the variations in the validation statistics. There are generally more data points (and more statistical significance) for the period 2016-2020.

The RMSE and the MTSU have approximately the same magnitude in all regions. On the one hand, in the Baffin Bay (mostly first year ice), and the Beaufort Sea (multiyear and first year ice), the mean annual bias is mostly positive up to 1.5% to 3.5%. There are also a few cases with a negative mean annual bias down to -1.5%. On the other hand, in the Kara Sea (first year ice), the Laptev Sea (first year ice) and in the area North of Greenland (multiyear ice) the mean annual bias is negative from 0% to about -2% with a few outliers. The overall negative hemispherical bias of about -0.5% (Fig. 4) is believed to originate from validation sites in the Western Arctic and it does not seem to be directly related to ice type.

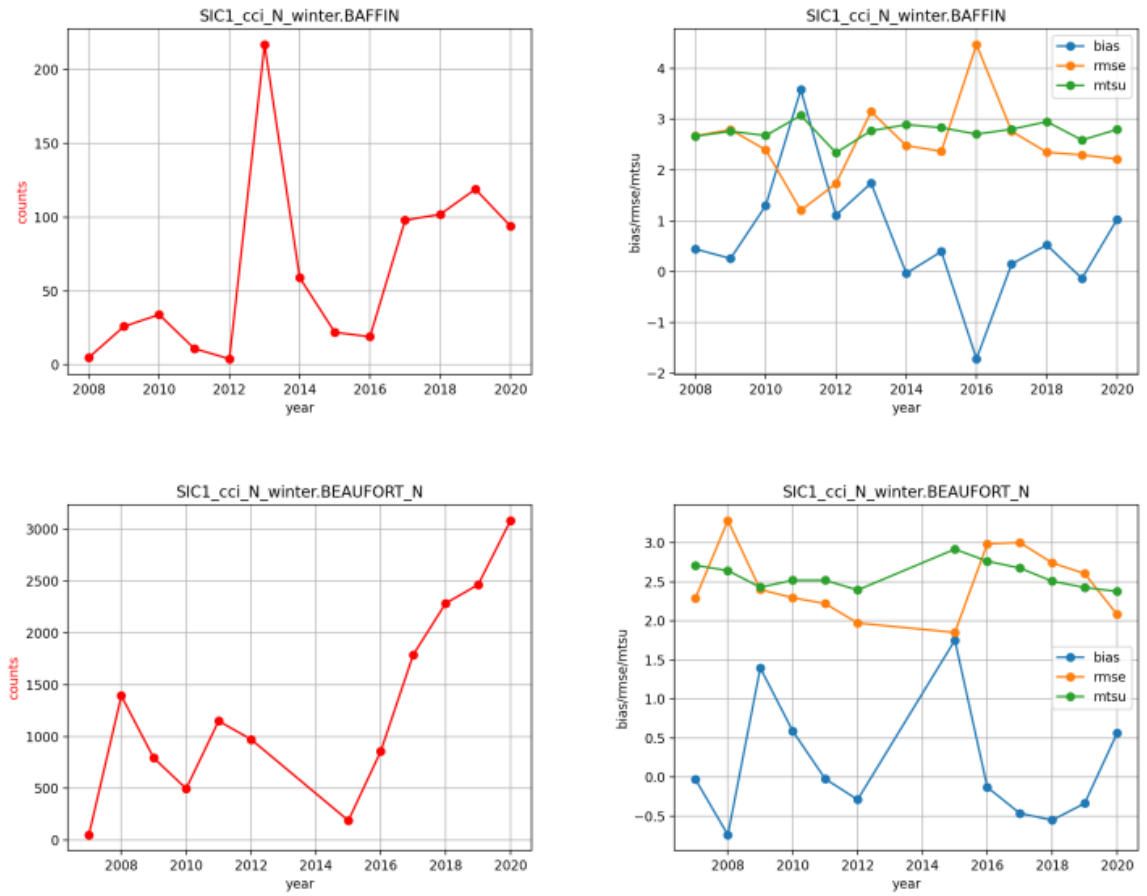

Figure 6. Regional SIC1 winter validation, Northern Hemisphere: Baffin Bay and Northern Beaufort Sea

Figure 7. Regional SIC1 winter validation, Northern Hemisphere: Southern Beaufort Sea, Northern and Southern Kara Seas.

Figure 8. Regional SIC1 winter validation, Northern Hemisphere: Northern Laptev Sea and North Greenland region.

8 SIC1 REGIONAL EVALUATION SOUTHERN HEMISPHERE

We repeat the regional SIC1 validation of SICCI-HR-SIC for two regions in the Southern Hemisphere. The bias in the SIC1 validation in the Weddell and Ross Seas is near zero when there are a sufficient number of validation points, after 2016 (Fig. 9).

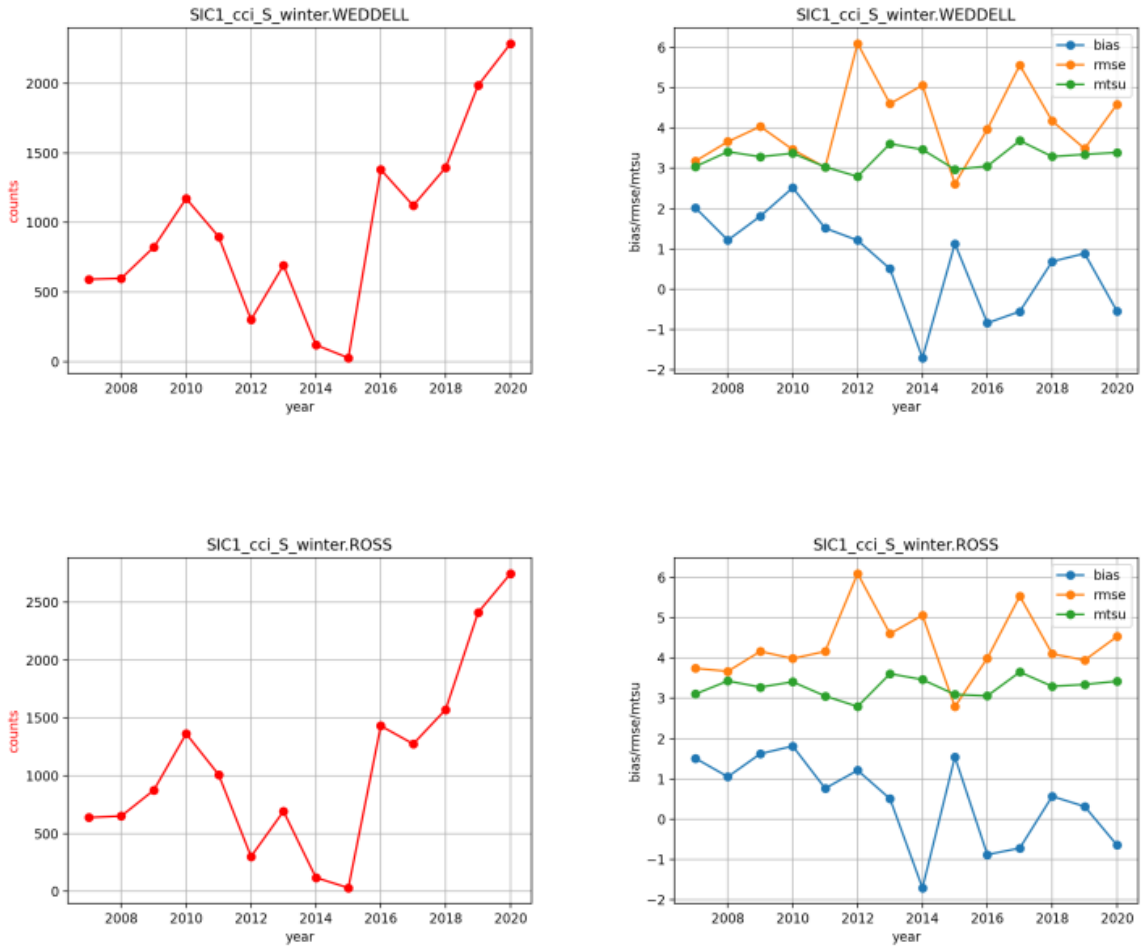

Figure 9. Regional winter validation, Southern Hemisphere: Weddell and Ross

The Weddell and Ross Sea regions show smaller bias and uncertainty numbers than for the regions in the Northern Hemisphere. Note that Antarctic sea ice is generally rather sparsely covered by SAR imagery except for these two priority regions. This translates in generally less SIC1 points in the SIC RRDP.

9 CONCLUSIONS

A semi-automatic method to perform validation of the SIC data records has been implemented based on the SIC RRDP dataset, and used to validate the new SICCI-HR-SIC CDR (1991-2020) from CCI+ Sea Ice Phase 1 project.

The validation shows good agreement between the observed RMSE (validation statistics) and the computed MTSU (uncertainties from the product files). Over open water, a small positive (+0.5%) bias is observed in the Northern Hemisphere while the bias is 0% in the Southern Hemisphere. Over consolidated ice (100% SIC) a negative bias of -1% is observed in the Northern Hemisphere which is not present in the Southern Hemisphere. The bias over 100% SIC conditions is reduced WRT what had been documented with older (v2) versions of the OSI SAF and CCI dataset.

A regional investigation of the SIC1 validation statistics in the Northern Hemisphere does not conclude that the bias is strongly related to the type/age category of sea ice (FYI vs MYI).

Overall, we conclude that the advanced pan-sharpening method used to produce SICCI-HR-SIC - which was designed to improve the spatial resolution from that of the OSI SAF CDR and at the same time avoid the high noise that would result from using the near-90GHz imagery alone - is effective and that SICCI-HR-SIC has the potential to bring added value the climate community.

Future validation exercises, including during Phase 2 of the CCI+ Sea Ice project (starting 2023) should revisit the regional validation and possibly bring auxiliary sea-ice type/age information to help with the validation and its analysis. A regional approach to the 100% SIC tie-point in the algorithm might be required.

10 REFERENCES

Ivanova, N., Pedersen, L. T., Tonboe, R. T., Kern, S., Heygster, G., Lavergne, T., Sørensen, A., Saldo, R., Dybkjær, G., Brucker, L., and Shokr, M.: Inter-comparison and evaluation of sea ice algorithms: towards further identification of challenges and optimal approach using passive microwave observations, The Cryosphere, 9, 1797–1817, https://doi.org/10.5194/tc-9-1797-2015, 2015.

Kern, S., Lavergne, T., Notz, D., Pedersen, L. T., Tonboe, R. T., Saldo, R., and Sørensen, A. M.: Satellite passive microwave sea-ice concentration data set intercomparison: closed ice and ship-based observations, The Cryosphere, 13, 3261–3307, https://doi.org/10.5194/tc-13-3261-2019, 2019.

APPENDIX A : SIC0 validation per year for the Northern Hemisphere (Histograms)

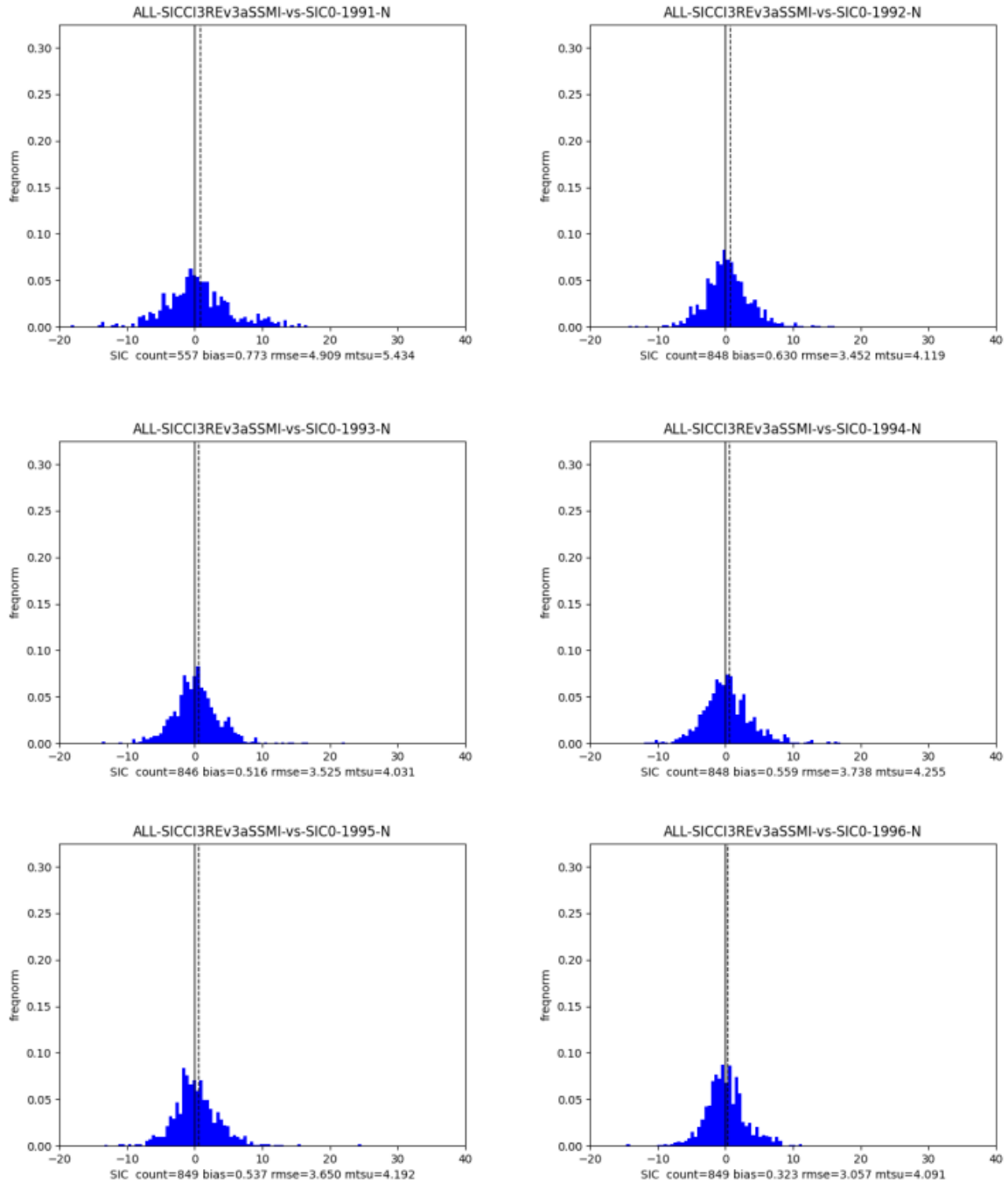

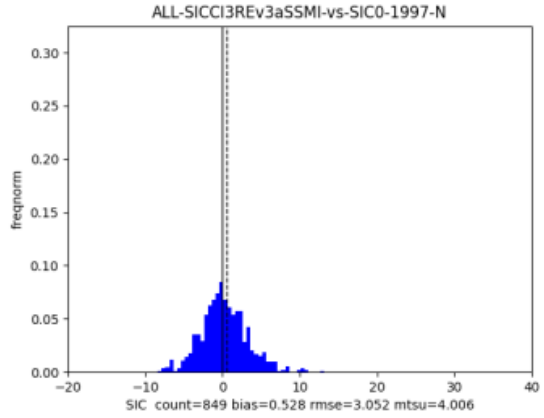
ALL-SICCI3REv3aSSMI-vs-SIC0-1997-N
freqnorm
SIC count=849 bias=0.528 rmse=3.052 mtsu=4.006

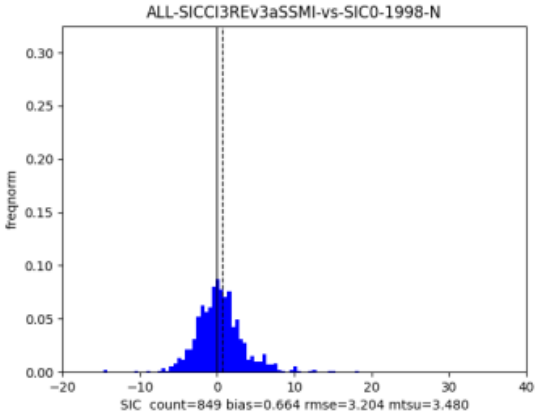
ALL-SICCI3REv3aSSMI-vs-SIC0-1998-N
freqnorm
SIC count=849 bias=0.664 rmse=3.204 mtsu=3.480

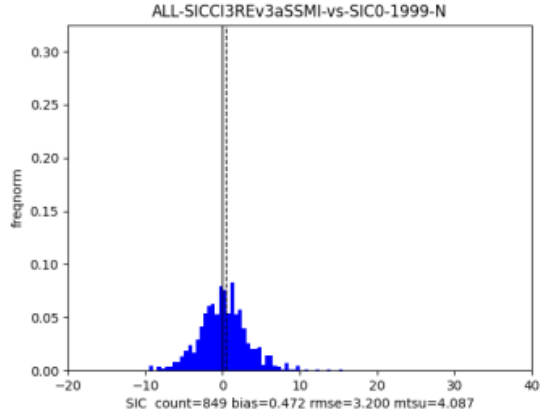
ALL-SICCI3REv3aSSMI-vs-SIC0-1999-N
freqnorm
SIC count=849 bias=0.472 rmse=3.200 mtsu=4.087

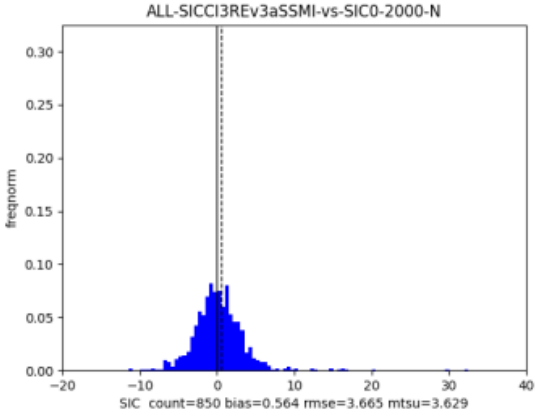
ALL-SICCI3REv3aSSMI-vs-SIC0-2000-N
freqnorm
SIC count=850 bias=0.564 rmse=3.665 mtsu=3.629

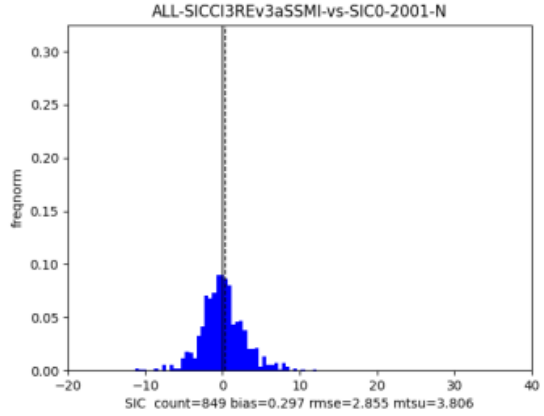
ALL-SICCI3REv3aSSMI-vs-SIC0-2001-N
freqnorm
SIC count=849 bias=0.297 rmse=2.855 mtsu=3.806

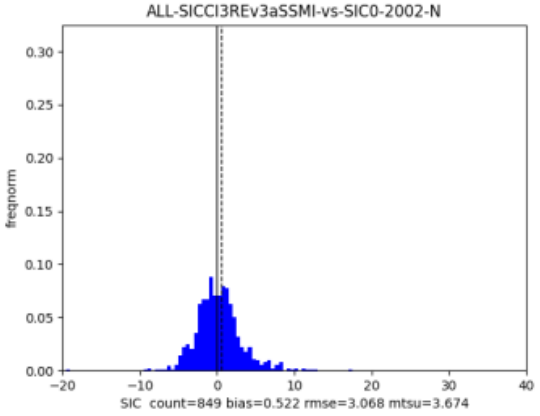
ALL-SICCI3REv3aSSMI-vs-SIC0-2002-N
freqnorm
SIC count=849 bias=0.522 rmse=3.068 mtsu=3.674

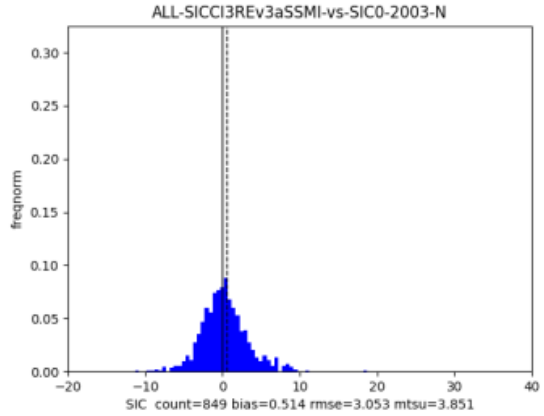
ALL-SICCI3REv3aSSMI-vs-SIC0-2003-N
freqnorm
SIC count=849 bias=0.514 rmse=3.053 mtsu=3.851

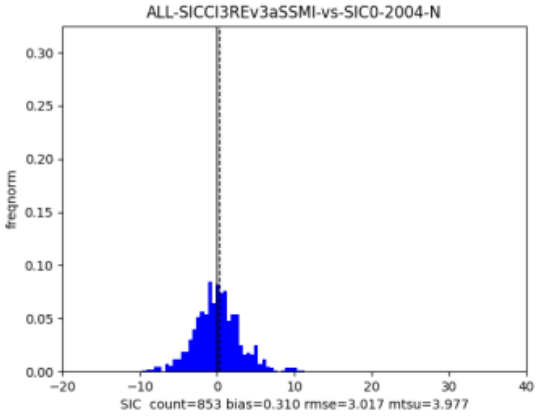
ALL-SICCI3REv3aSSMI-vs-SIC0-2004-N
freqnorm
SIC count=853 bias=0.310 rmse=3.017 mtsu=3.977

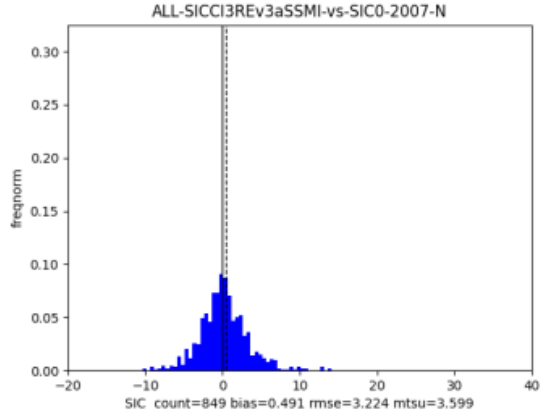
ALL-SICCI3REv3aSSMI-vs-SIC0-2007-N
freqnorm
SIC count=849 bias=0.491 rmse=3.224 mtsu=3.599

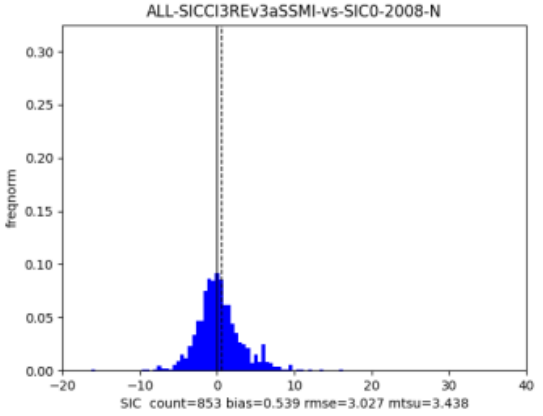
ALL-SICCI3REv3aSSMI-vs-SIC0-2008-N
freqnorm
SIC count=853 bias=0.539 rmse=3.027 mtsu=3.438

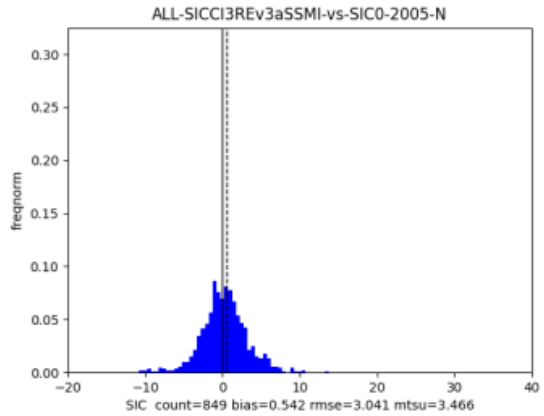
ALL-SICCI3REv3aSSMI-vs-SIC0-2005-N
freqnorm
SIC count=849 bias=0.542 rmse=3.041 mtsu=3.466

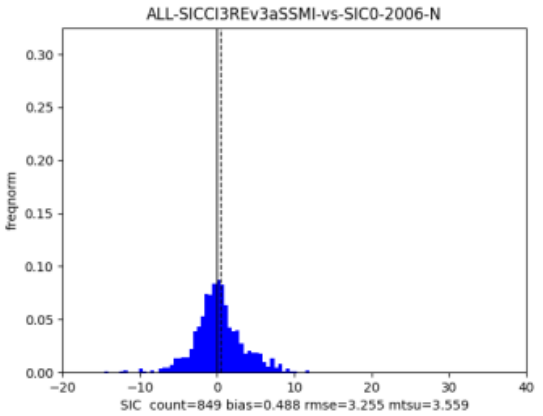
ALL-SICCI3REv3aSSMI-vs-SIC0-2006-N
freqnorm
SIC count=849 bias=0.488 rmse=3.255 mtsu=3.559

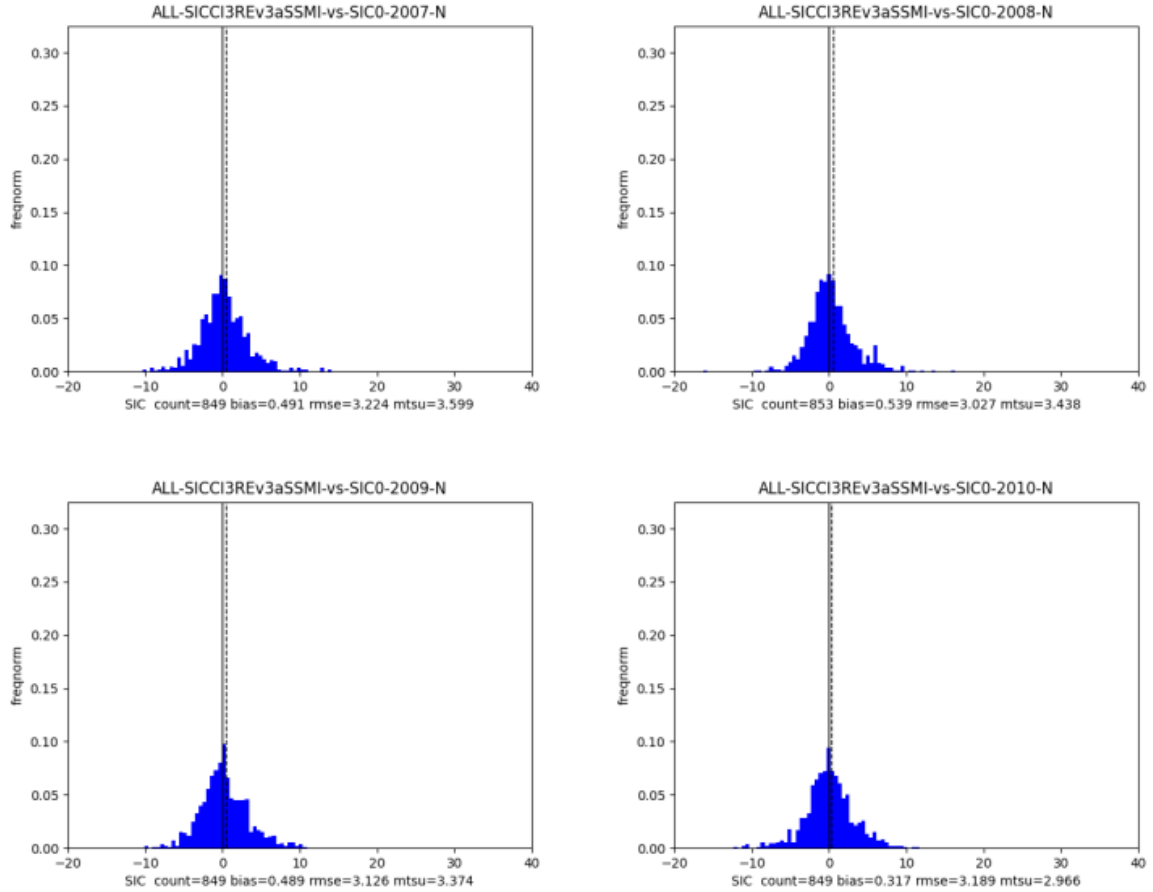

Figure 7:per year normalised histogram plots

OBJ

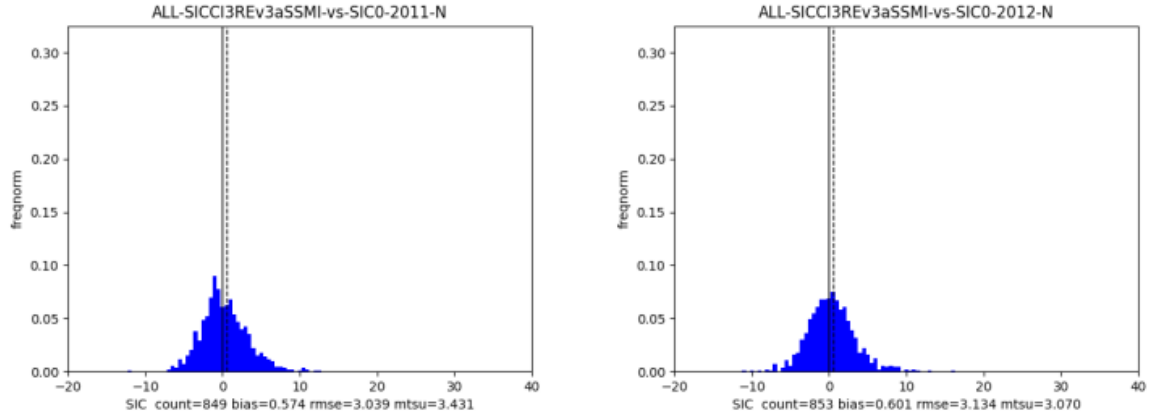

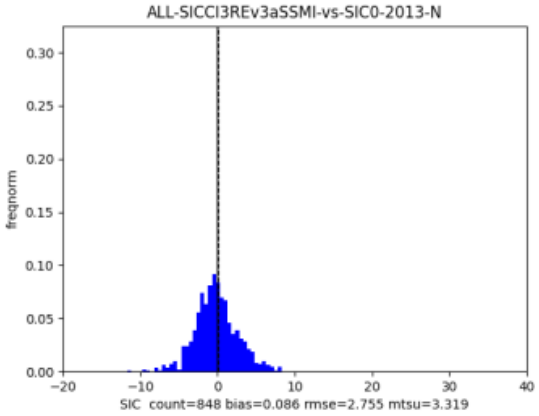
ALL-SICCI3REv3aSSMI-vs-SIC0-2013-N
freqnorm
SIC count=848 bias=0.086 rmse=2.755 mtsu=3.319

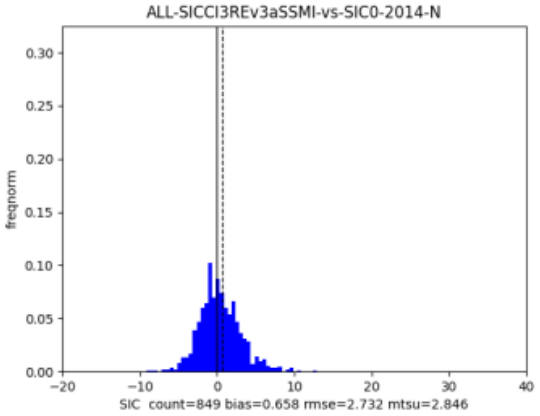
ALL-SICCI3REv3aSSMI-vs-SIC0-2014-N
freqnorm
SIC count=849 bias=0.658 rmse=2.732 mtsu=2.846

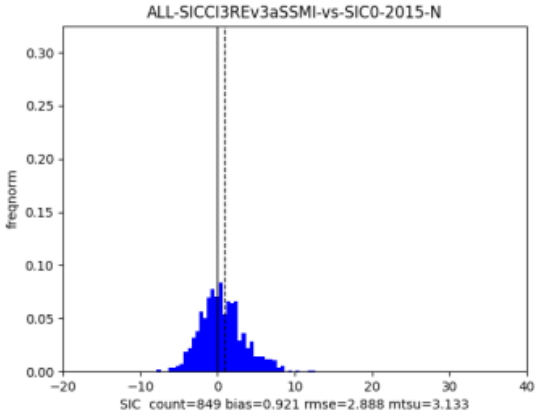
ALL-SICCI3REv3aSSMI-vs-SIC0-2015-N
freqnorm
SIC count=849 bias=0.921 rmse=2.888 mtsu=3.133

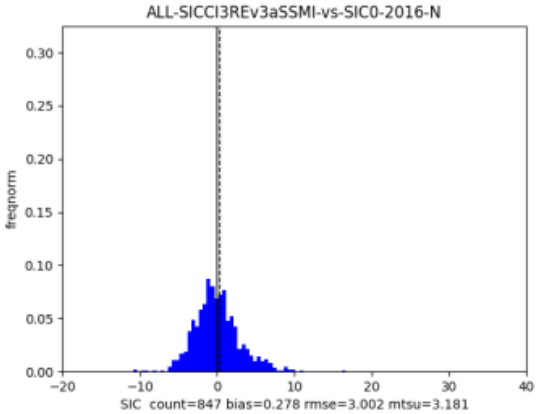
ALL-SICCI3REv3aSSMI-vs-SIC0-2016-N
freqnorm
SIC count=847 bias=0.278 rmse=3.002 mtsu=3.181

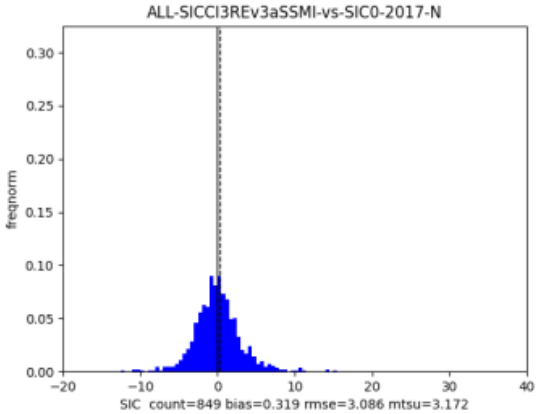
ALL-SICCI3REv3aSSMI-vs-SIC0-2017-N
freqnorm
SIC count=849 bias=0.319 rmse=3.086 mtsu=3.172

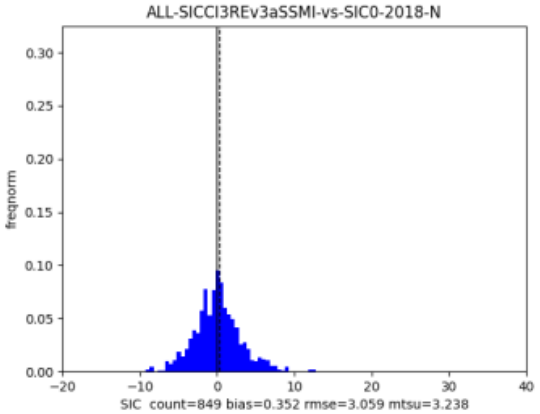
ALL-SICCI3REv3aSSMI-vs-SIC0-2018-N
freqnorm
SIC count=849 bias=0.352 rmse=3.059 mtsu=3.238

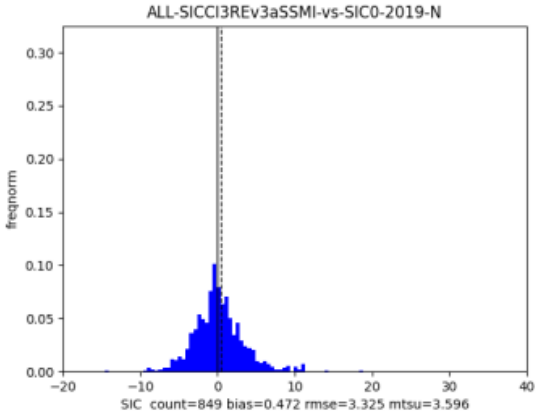
ALL-SICCI3REv3aSSMI-vs-SIC0-2019-N
freqnorm
SIC count=849 bias=0.472 rmse=3.325 mtsu=3.596

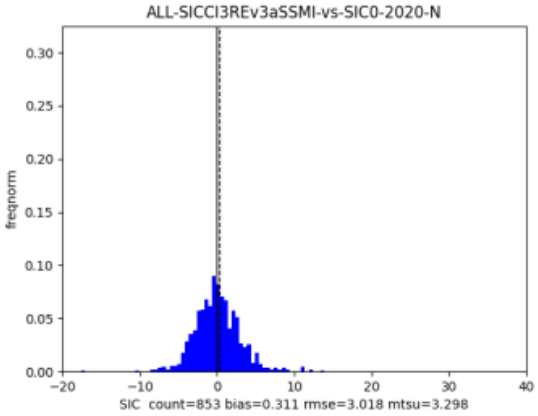
ALL-SICCI3REv3aSSMI-vs-SIC0-2020-N
freqnorm
SIC count=853 bias=0.311 rmse=3.018 mtsu=3.298

APPENDIX B : SIC0 validation per year for the Southern Hemisphere (Histograms)

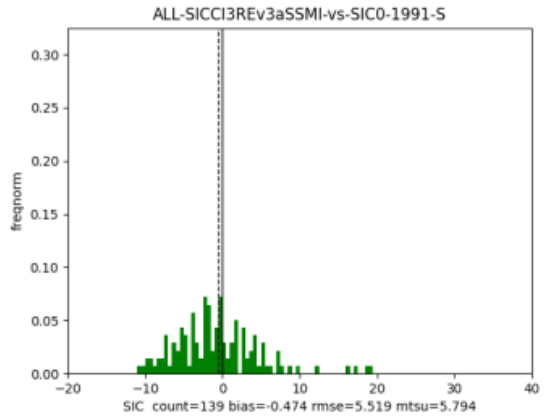

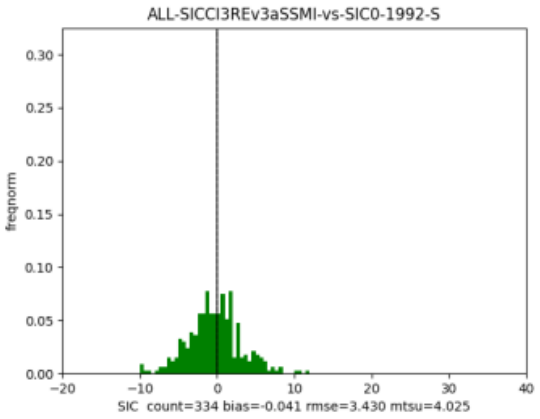

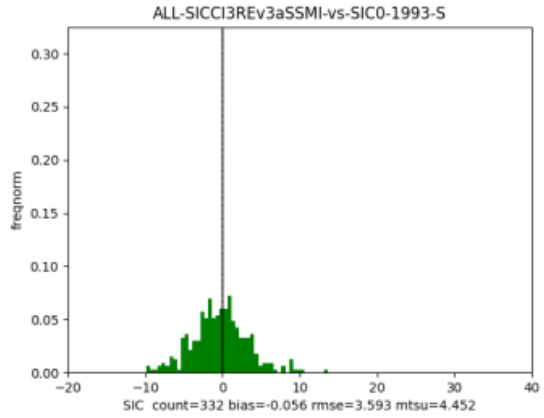

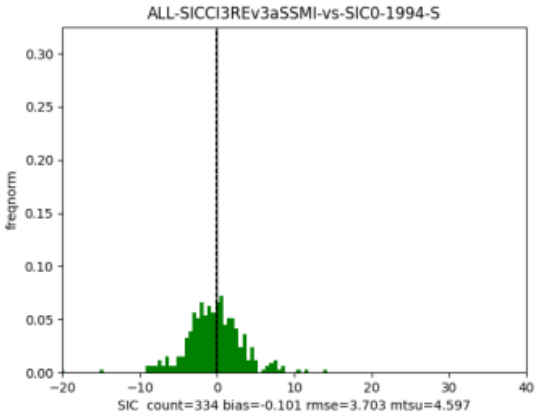

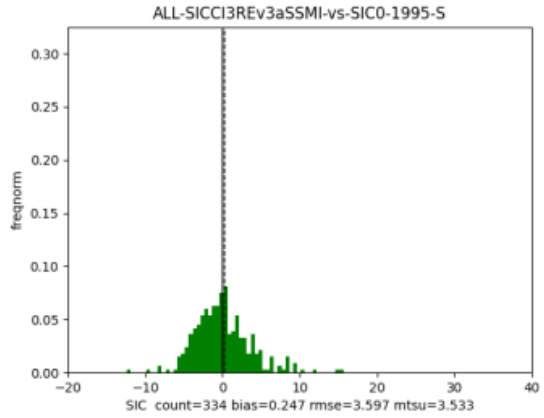

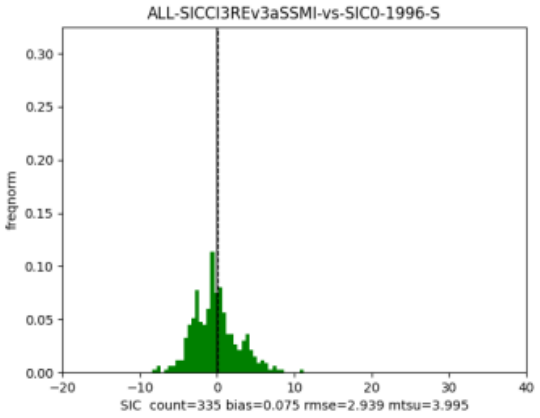

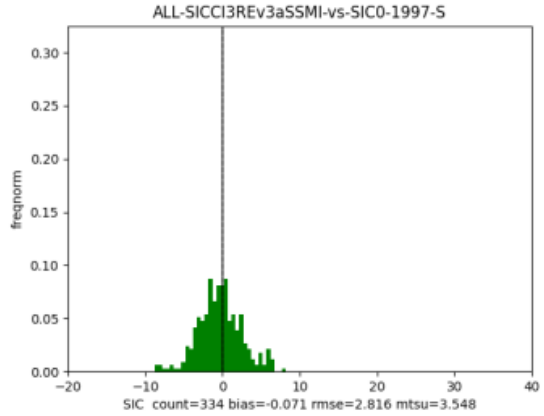
ALL-SICCI3REv3aSSMI-vs-SIC0-1997-S
freqnorm
SIC count=334 bias=-0.071 rmse=2.816 mtsu=3.548

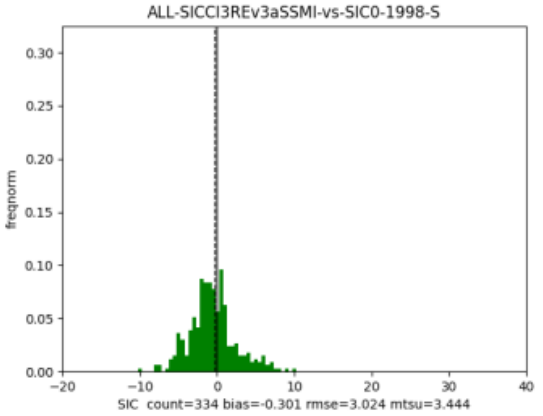
ALL-SICCI3REv3aSSMI-vs-SIC0-1998-S
freqnorm
SIC count=334 bias=-0.301 rmse=3.024 mtsu=3.444

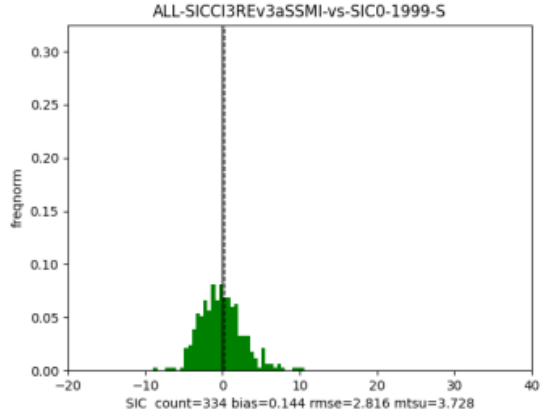
ALL-SICCI3REv3aSSMI-vs-SIC0-1999-S
freqnorm
SIC count=334 bias=0.144 rmse=2.816 mtsu=3.728

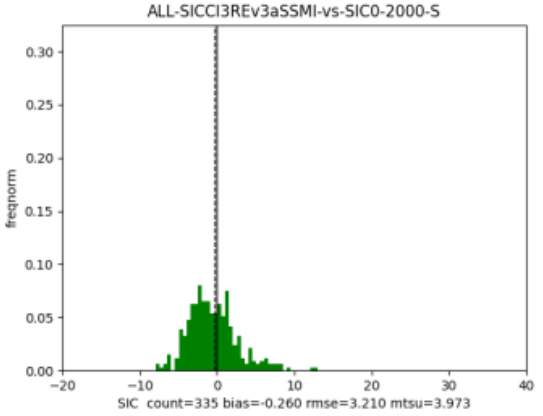
ALL-SICCI3REv3aSSMI-vs-SIC0-2000-S
freqnorm
SIC count=335 bias=-0.260 rmse=3.210 mtsu=3.973

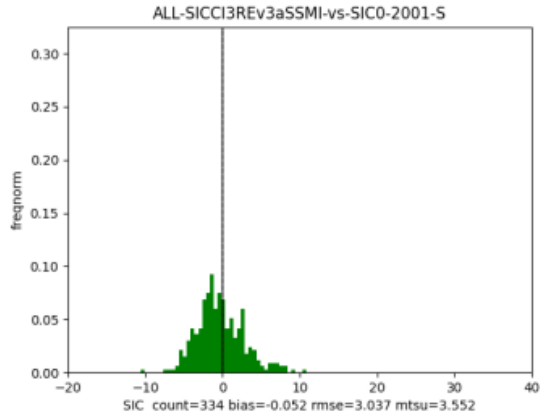
ALL-SICCI3REv3aSSMI-vs-SIC0-2001-S
freqnorm
SIC count=334 bias=-0.052 rmse=3.037 mtsu=3.552

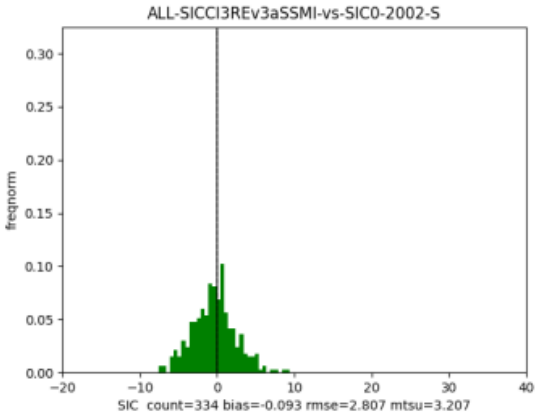
ALL-SICCI3REv3aSSMI-vs-SIC0-2002-S
freqnorm
SIC count=334 bias=-0.093 rmse=2.807 mtsu=3.207

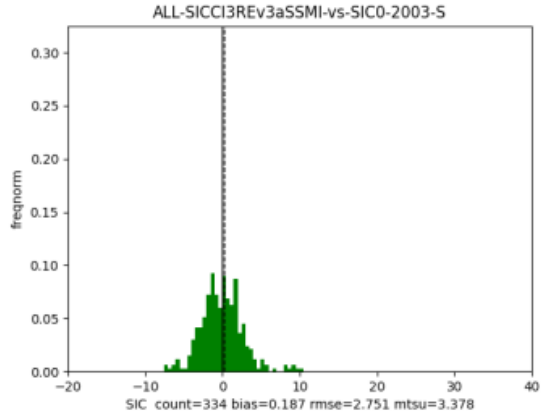
ALL-SICCI3REv3aSSMI-vs-SIC0-2003-S
freqnorm
SIC count=334 bias=0.187 rmse=2.751 mtsu=3.378

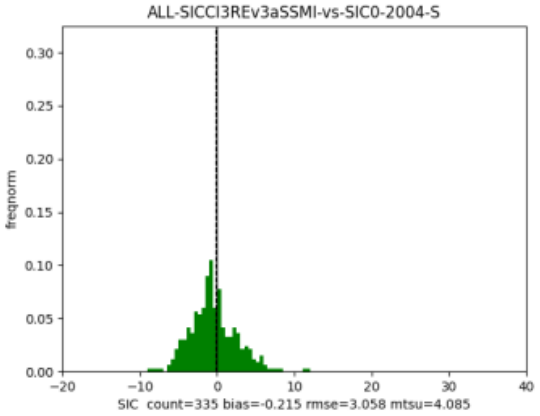
ALL-SICCI3REv3aSSMI-vs-SIC0-2004-S
freqnorm
SIC count=335 bias=-0.215 rmse=3.058 mtsu=4.085

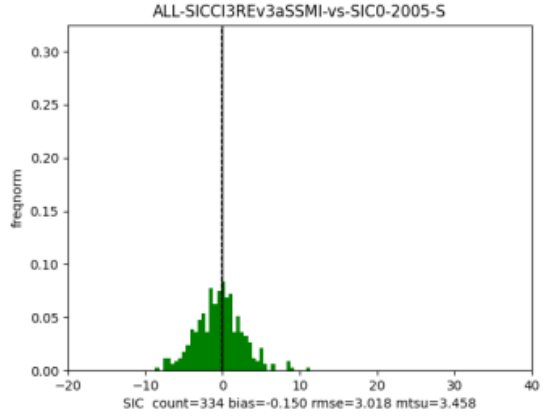
ALL-SICCI3REv3aSSMI-vs-SIC0-2005-S
freqnorm
SIC count=334 bias=-0.150 rmse=3.018 mtsu=3.458

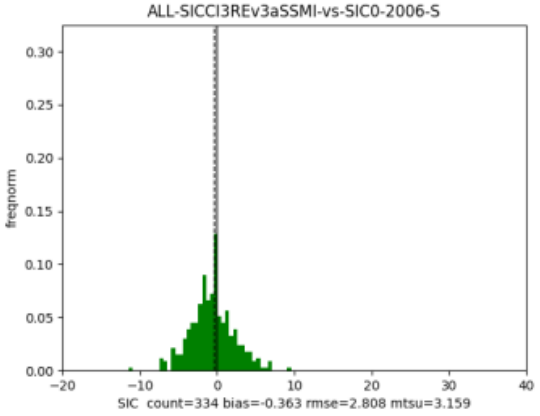
ALL-SICCI3REv3aSSMI-vs-SIC0-2006-S
freqnorm
SIC count=334 bias=-0.363 rmse=2.808 mtsu=3.159

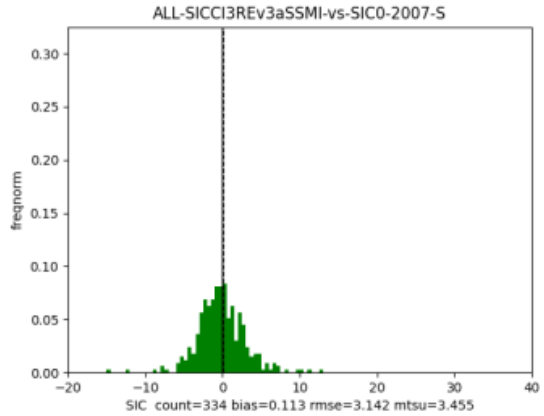
ALL-SICCI3REv3aSSMI-vs-SIC0-2007-S
freqnorm
SIC count=334 bias=0.113 rmse=3.142 mtsu=3.455

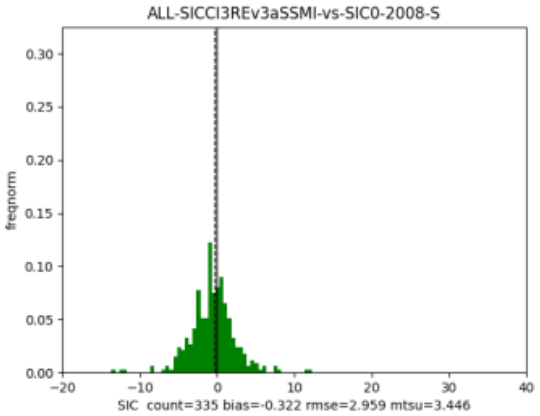
ALL-SICCI3REv3aSSMI-vs-SIC0-2008-S
freqnorm
SIC count=335 bias=-0.322 rmse=2.959 mtsu=3.446

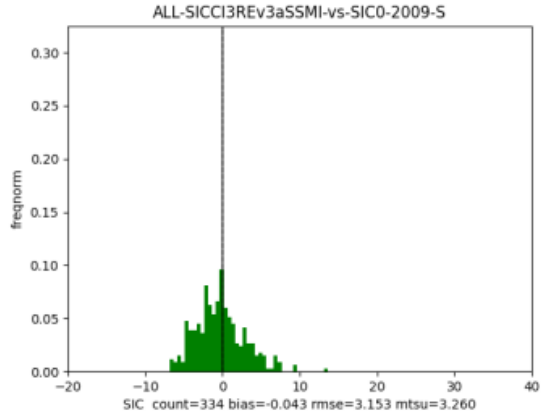
ALL-SICCI3REv3aSSMI-vs-SIC0-2009-S
freqnorm
SIC count=334 bias=-0.043 rmse=3.153 mtsu=3.260

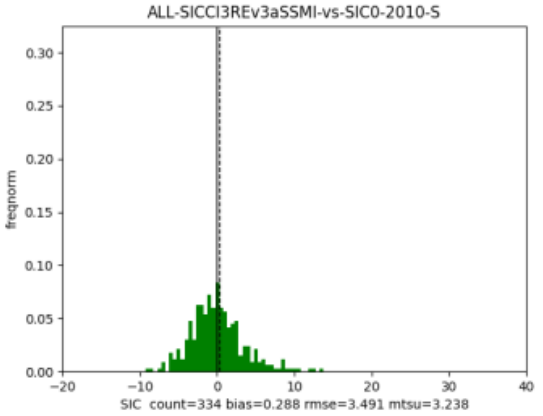
ALL-SICCI3REv3aSSMI-vs-SIC0-2010-S
freqnorm
SIC count=334 bias=0.288 rmse=3.491 mtsu=3.238

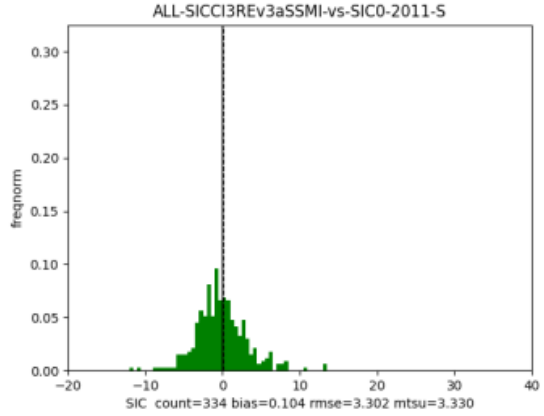
ALL-SICCI3REv3aSSMI-vs-SIC0-2011-S
freqnorm
SIC count=334 bias=0.104 rmse=3.302 mtsu=3.330

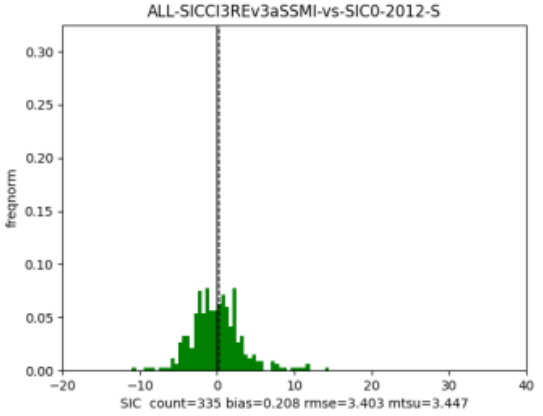
ALL-SICCI3REv3aSSMI-vs-SIC0-2012-S
freqnorm
SIC count=335 bias=0.208 rmse=3.403 mtsu=3.447

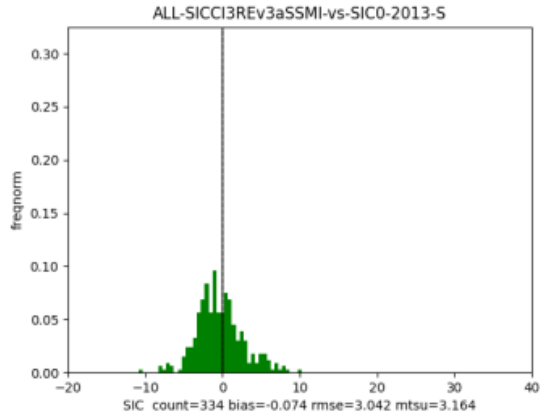
ALL-SICCI3REv3aSSMI-vs-SIC0-2013-S
freqnorm
SIC count=334 bias=-0.074 rmse=3.042 mtsu=3.164

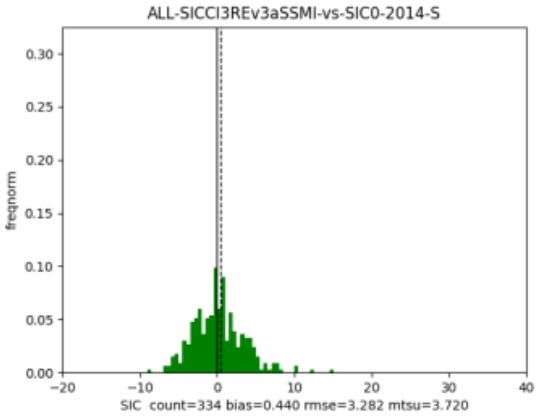
ALL-SICCI3REv3aSSMI-vs-SIC0-2014-S
freqnorm
SIC count=334 bias=0.440 rmse=3.282 mtsu=3.720

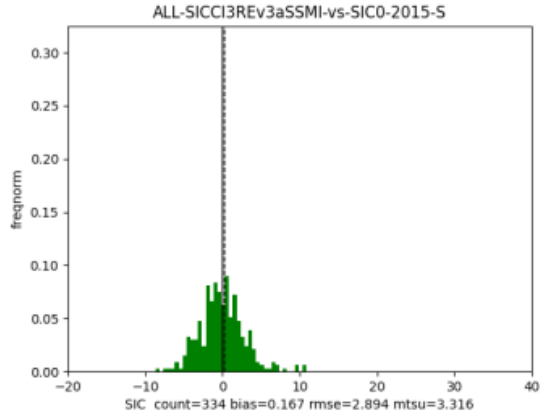
ALL-SICCI3REv3aSSMI-vs-SIC0-2015-S
freqnorm
SIC count=334 bias=0.167 rmse=2.894 mtsu=3.316

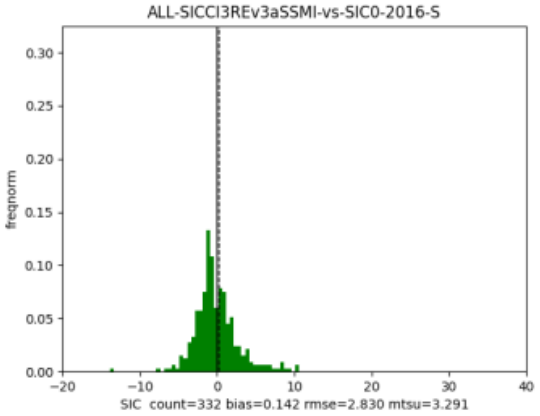
ALL-SICCI3REv3aSSMI-vs-SIC0-2016-S
freqnorm
SIC count=332 bias=0.142 rmse=2.830 mtsu=3.291

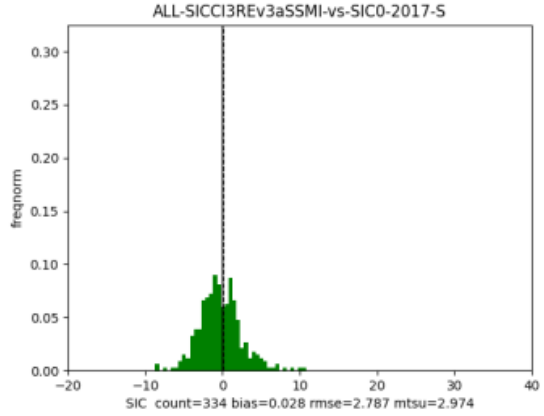
ALL-SICCI3REv3aSSMI-vs-SIC0-2017-S
freqnorm
SIC count=334 bias=0.028 rmse=2.787 mtsu=2.974

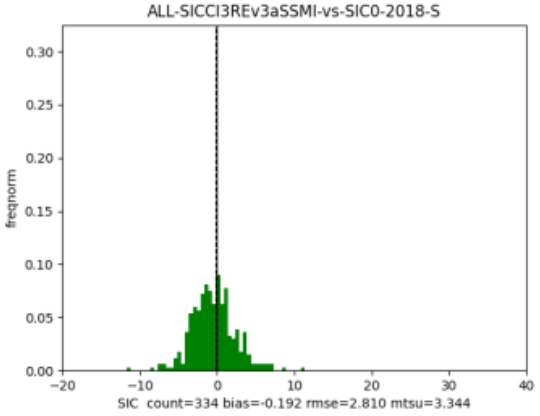
ALL-SICCI3REv3aSSMI-vs-SIC0-2018-S
freqnorm
SIC count=334 bias=-0.192 rmse=2.810 mtsu=3.344

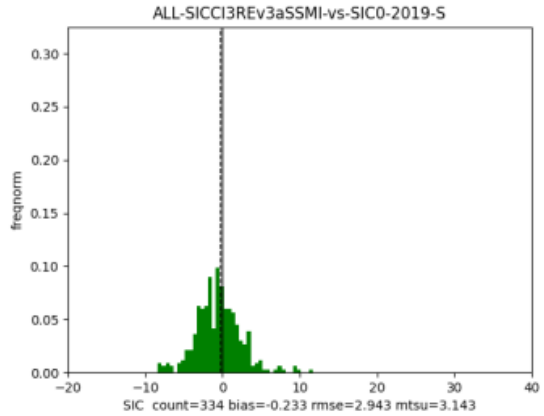
ALL-SICCI3REv3aSSMI-vs-SIC0-2019-S
freqnorm
SIC count=334 bias=-0.233 rmse=2.943 mtsu=3.143

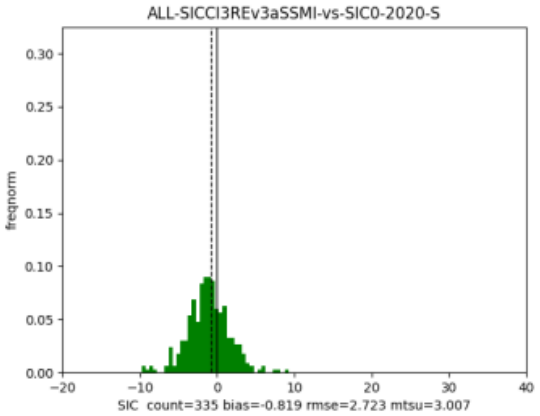
ALL-SICCI3REv3aSSMI-vs-SIC0-2020-S
freqnorm
SIC count=335 bias=-0.819 rmse=2.723 mtsu=3.007

APPENDIX C : SIC1 validation per year for the Northern Hemisphere (Histograms)

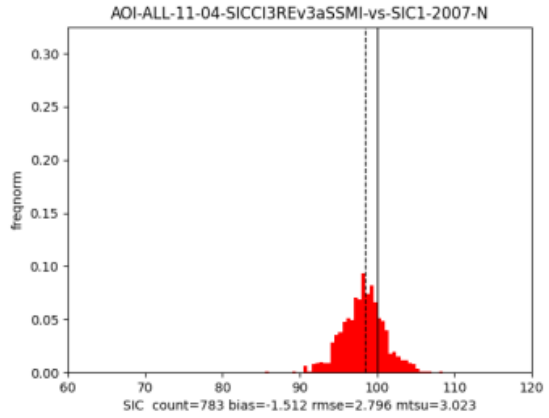

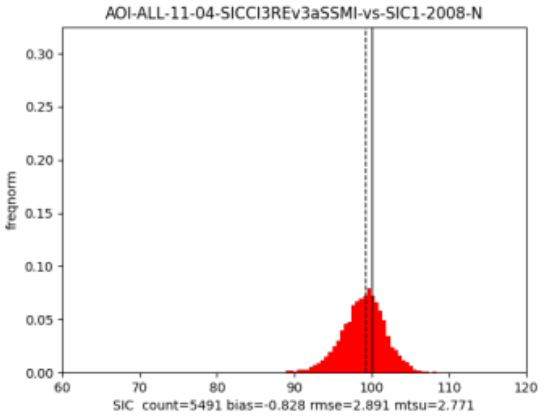

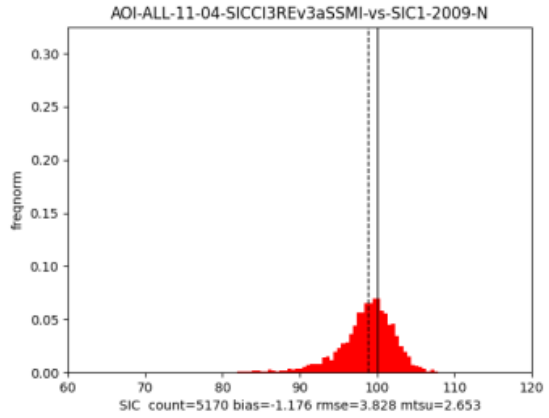

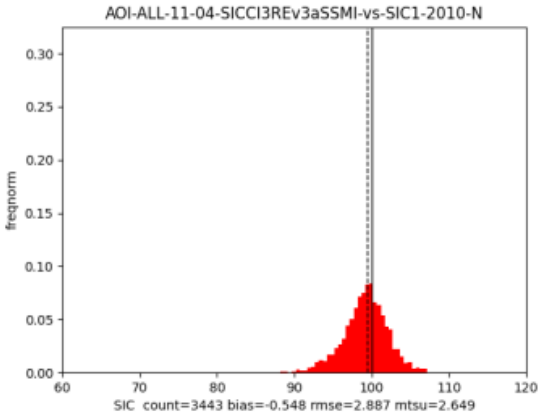

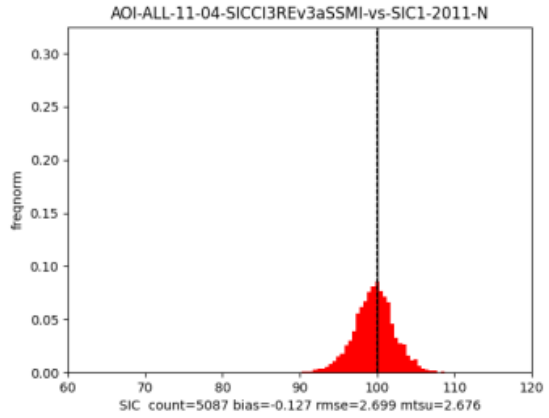

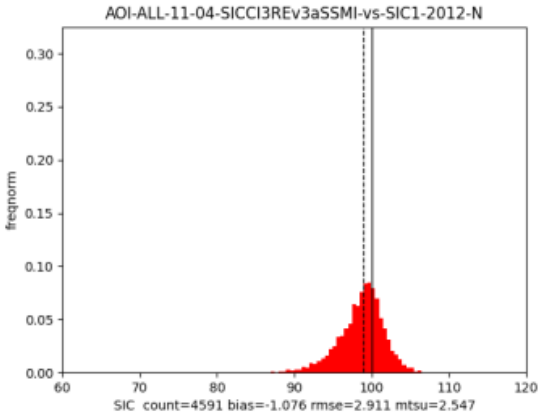

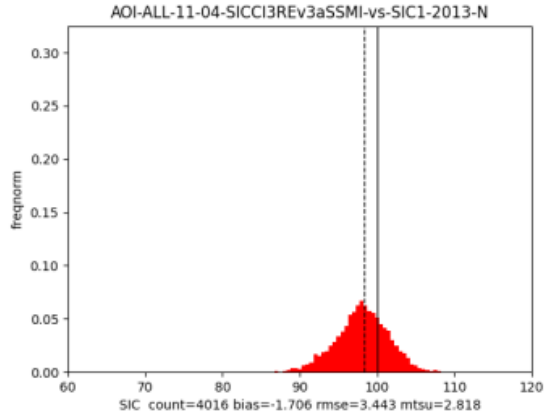
AOI-ALL-11-04-SICCI3REv3aSSMI-vs-SIC1-2013-N
freqnorm
SIC count=4016 bias=-1.706 rmse=3.443 mtsu=2.818

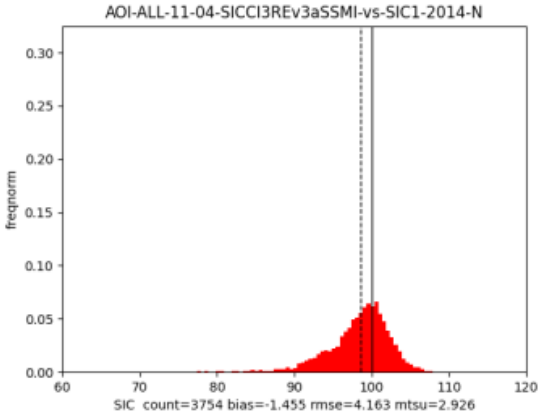
AOI-ALL-11-04-SICCI3REv3aSSMI-vs-SIC1-2014-N
freqnorm
SIC count=3754 bias=-1.455 rmse=4.163 mtsu=2.926

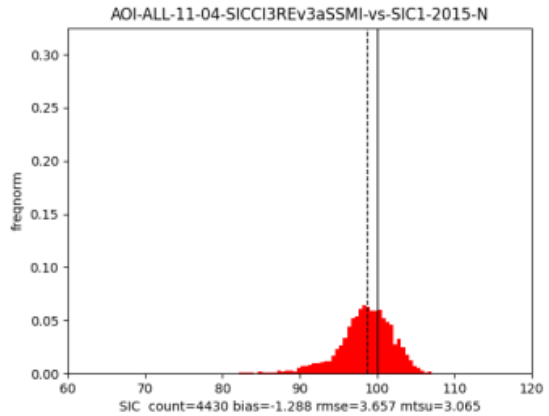
AOI-ALL-11-04-SICCI3REv3aSSMI-vs-SIC1-2015-N
freqnorm
SIC count=4430 bias=-1.288 rmse=3.657 mtsu=3.065

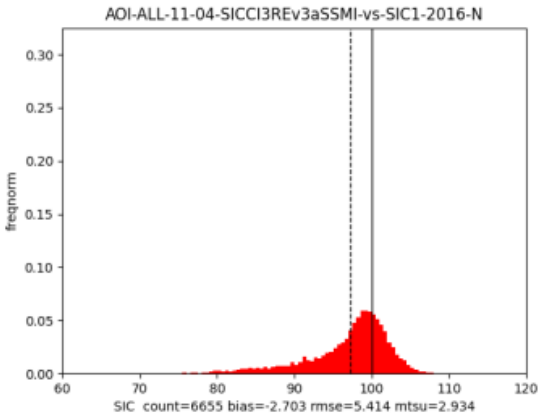
AOI-ALL-11-04-SICCI3REv3aSSMI-vs-SIC1-2016-N
freqnorm
SIC count=6655 bias=-2.703 rmse=5.414 mtsu=2.934

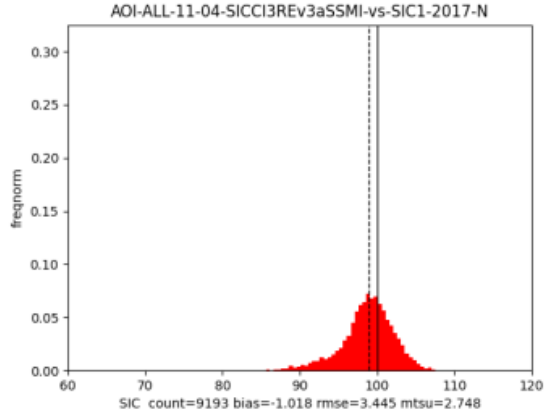
AOI-ALL-11-04-SICCI3REv3aSSMI-vs-SIC1-2017-N
freqnorm
SIC count=9193 bias=-1.018 rmse=3.445 mtsu=2.748

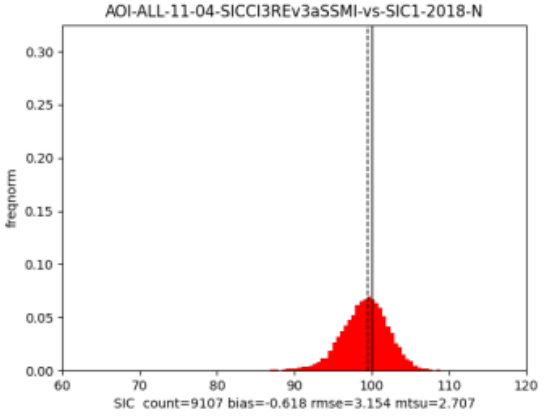
AOI-ALL-11-04-SICCI3REv3aSSMI-vs-SIC1-2018-N
freqnorm
SIC count=9107 bias=-0.618 rmse=3.154 mtsu=2.707

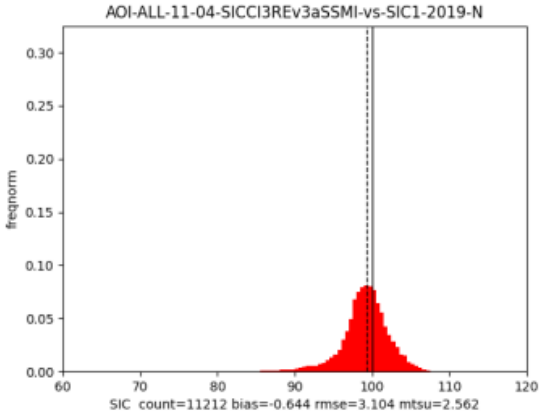
AOI-ALL-11-04-SICCI3REv3aSSMI-vs-SIC1-2019-N
freqnorm
SIC count=11212 bias=-0.644 rmse=3.104 mtsu=2.562

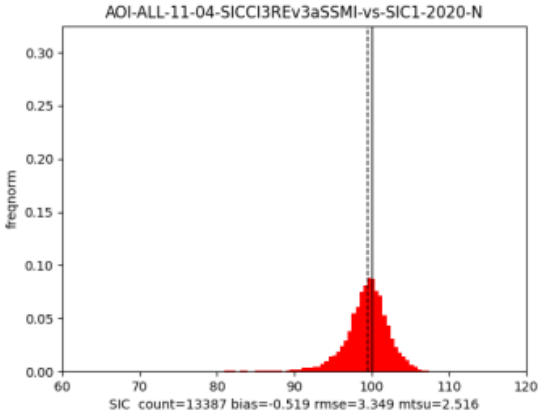
AOI-ALL-11-04-SICCI3REv3aSSMI-vs-SIC1-2020-N
freqnorm
SIC count=13387 bias=-0.519 rmse=3.349 mtsu=2.516

APPENDIX D : SIC1 validation per year for the Southern Hemisphere (Histograms)

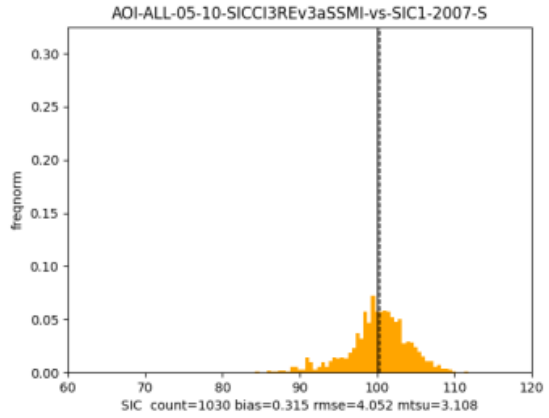

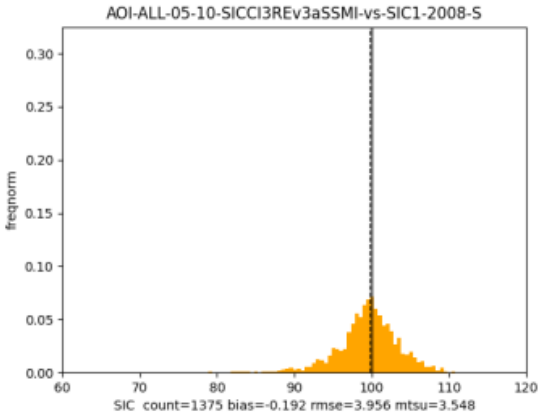

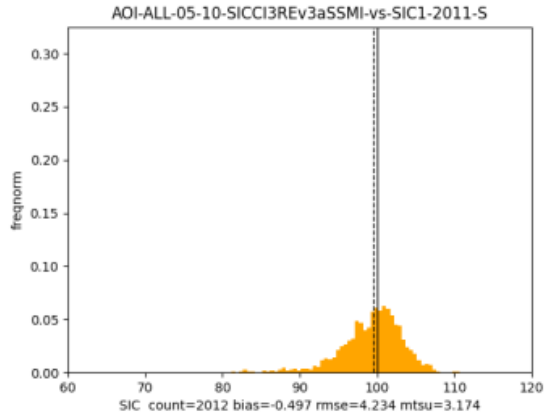

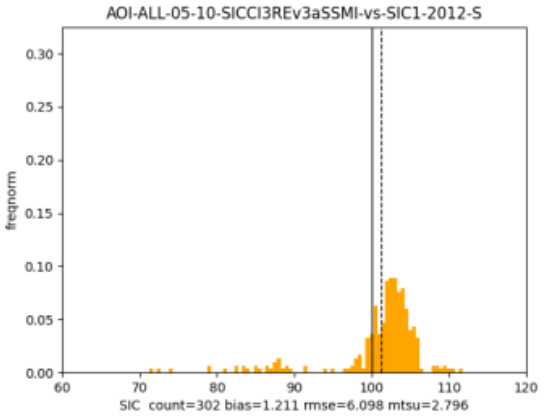

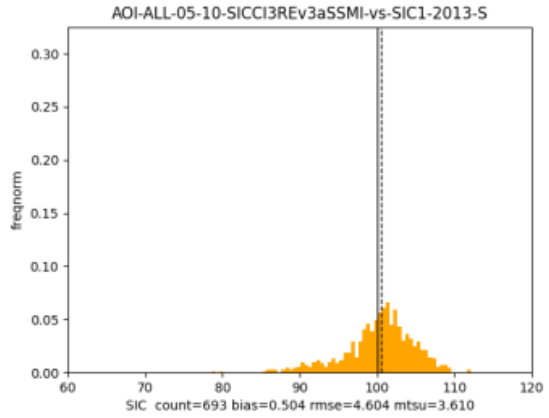

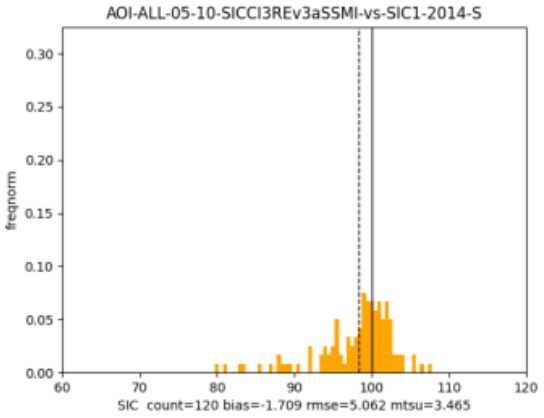

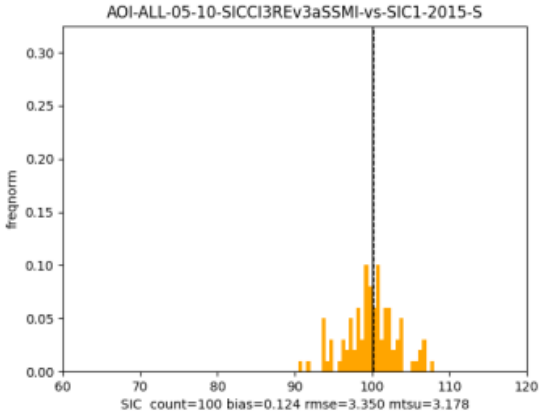
AOI-ALL-05-10-SICCI3REv3aSSMI-vs-SIC1-2015-S
freqnorm
SIC count=100 bias=0.124 rmse=3.350 mtsu=3.178

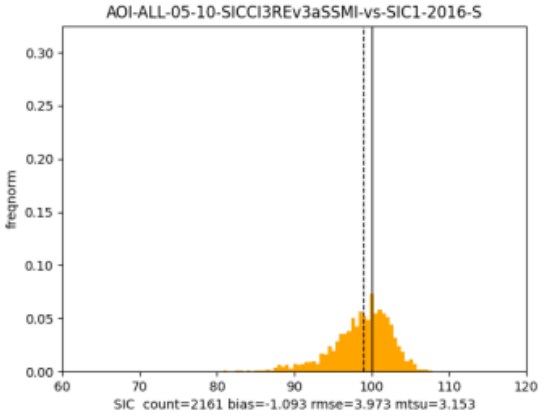
AOI-ALL-05-10-SICCI3REv3aSSMI-vs-SIC1-2016-S
freqnorm
SIC count=2161 bias=-1.093 rmse=3.973 mtsu=3.153

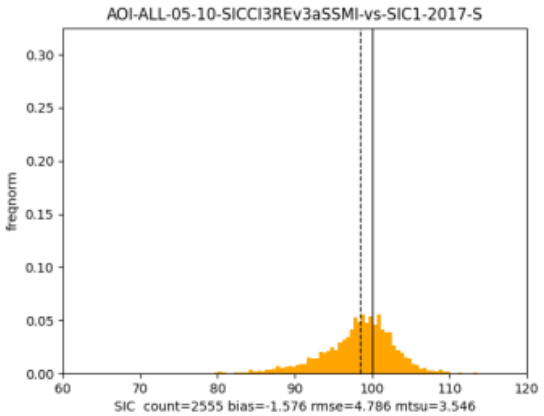
AOI-ALL-05-10-SICCI3REv3aSSMI-vs-SIC1-2017-S
freqnorm
SIC count=2555 bias=-1.576 rmse=4.786 mtsu=3.546

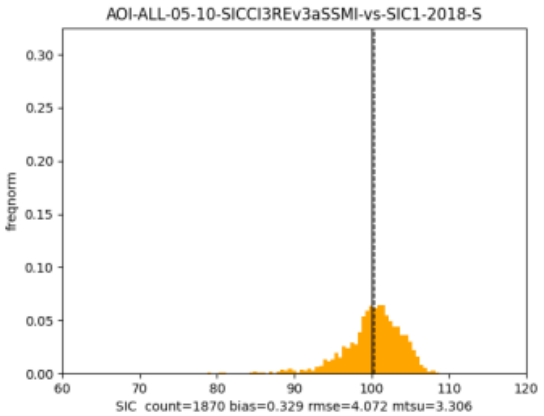
AOI-ALL-05-10-SICCI3REv3aSSMI-vs-SIC1-2018-S
freqnorm
SIC count=1870 bias=0.329 rmse=4.072 mtsu=3.306

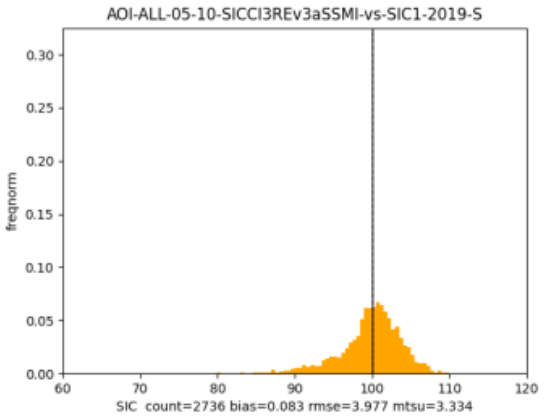
AOI-ALL-05-10-SICCI3REv3aSSMI-vs-SIC1-2019-S
freqnorm
SIC count=2736 bias=0.083 rmse=3.977 mtsu=3.334

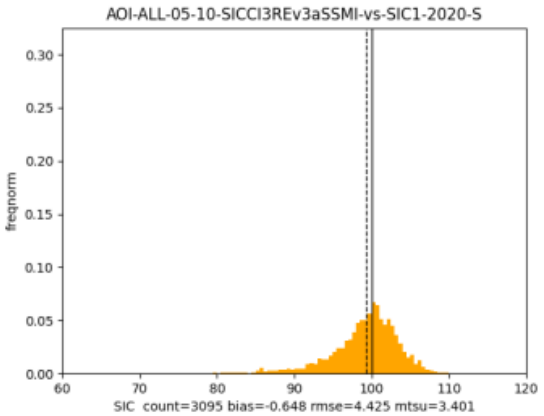
AOI-ALL-05-10-SICCI3REv3aSSMI-vs-SIC1-2020-S
freqnorm
SIC count=3095 bias=-0.648 rmse=4.425 mtsu=3.401

APPENDIX E : SIC1 validation per year for Baffin Bay (Histograms)

Note that the number of points used for validation of SIC1 in Baffin Bay is too low for analysis of the histograms in the first years.

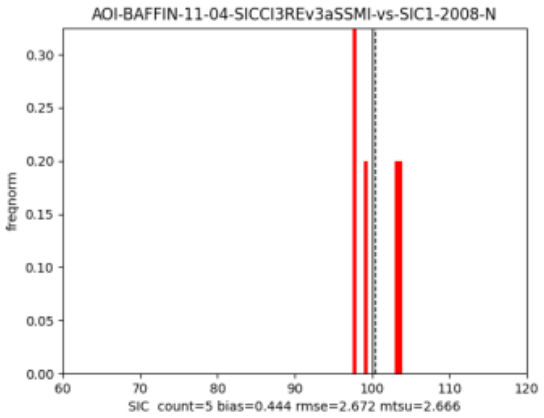

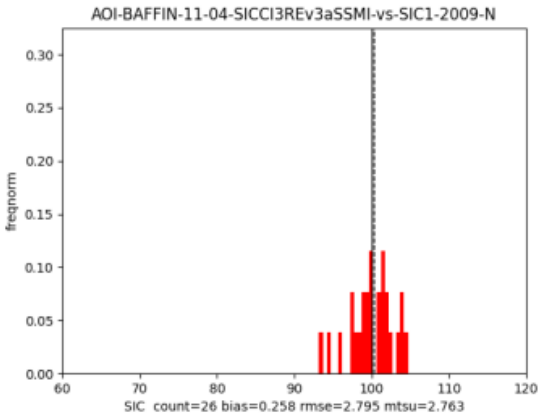

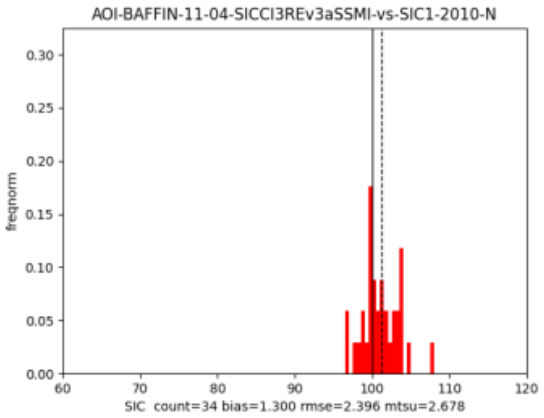

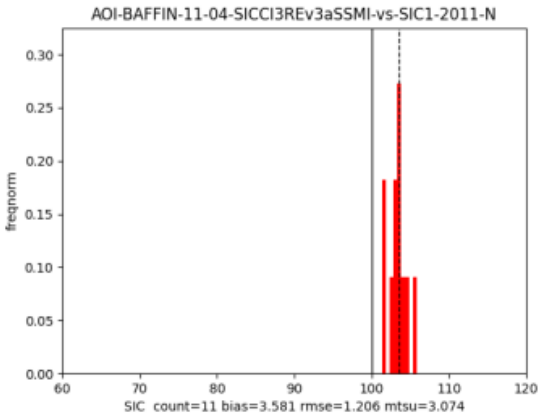

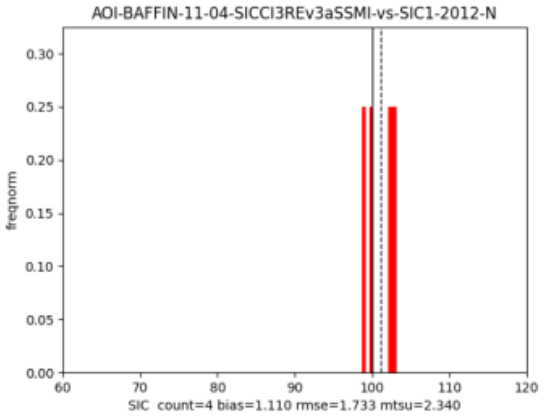

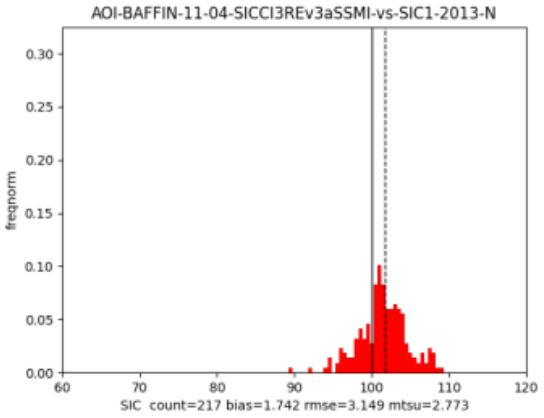

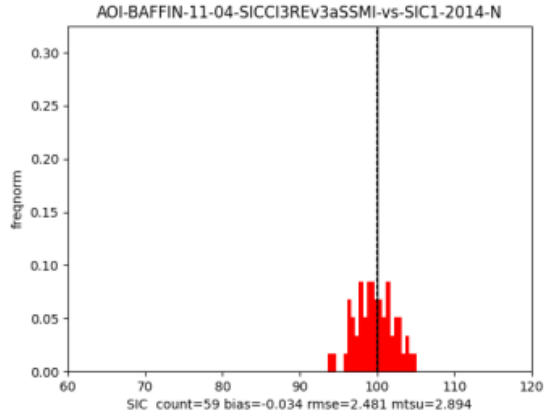
AOI-BAFFIN-11-04-SICCI3REv3aSSMI-vs-SIC1-2014-N
freqnorm
SIC count=59 bias=-0.034 rmse=2.481 mtsu=2.894

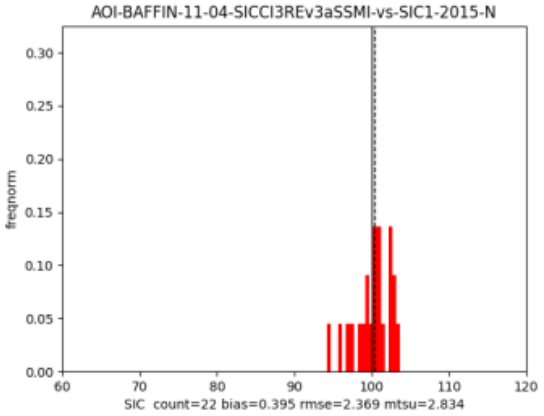
AOI-BAFFIN-11-04-SICCI3REv3aSSMI-vs-SIC1-2015-N
freqnorm
SIC count=22 bias=0.395 rmse=2.369 mtsu=2.834

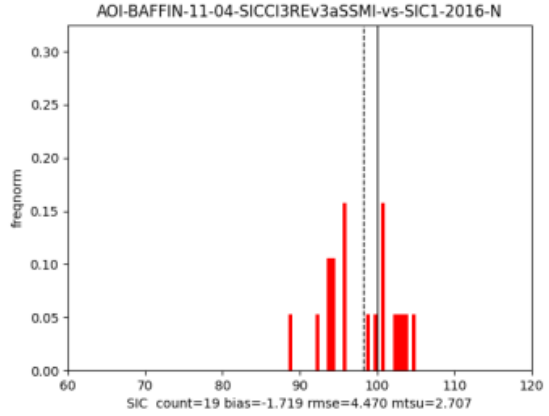
AOI-BAFFIN-11-04-SICCI3REv3aSSMI-vs-SIC1-2016-N
freqnorm
SIC count=19 bias=-1.719 rmse=4.470 mtsu=2.707

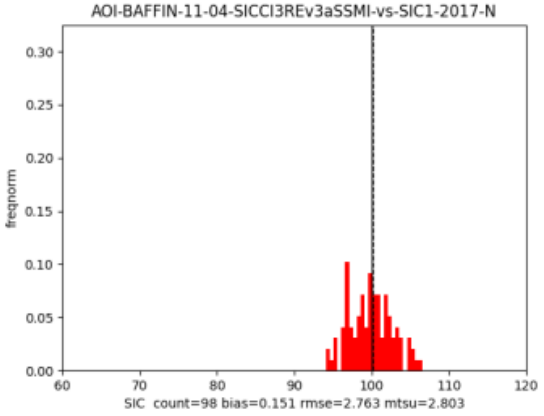
AOI-BAFFIN-11-04-SICCI3REv3aSSMI-vs-SIC1-2017-N
freqnorm
SIC count=98 bias=0.151 rmse=2.763 mtsu=2.803

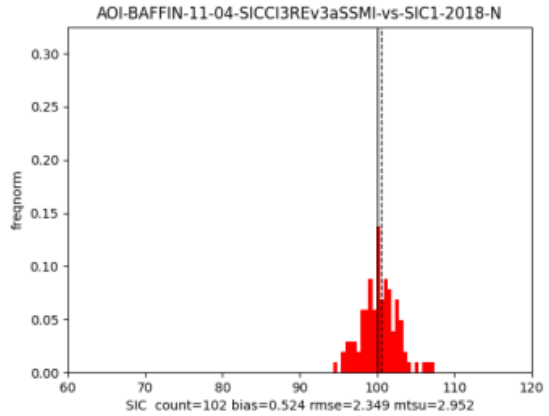
AOI-BAFFIN-11-04-SICCI3REv3aSSMI-vs-SIC1-2018-N
freqnorm
SIC count=102 bias=0.524 rmse=2.349 mtsu=2.952

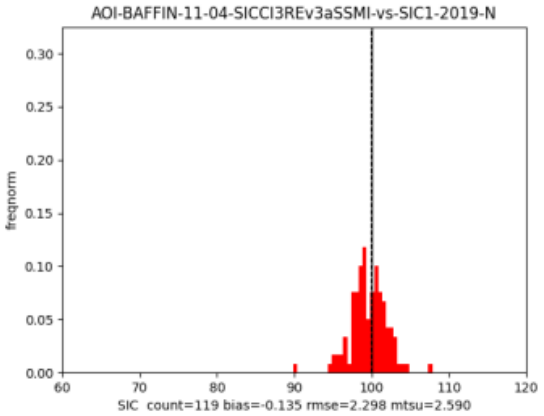
AOI-BAFFIN-11-04-SICCI3REv3aSSMI-vs-SIC1-2019-N
freqnorm
SIC count=119 bias=-0.135 rmse=2.298 mtsu=2.590

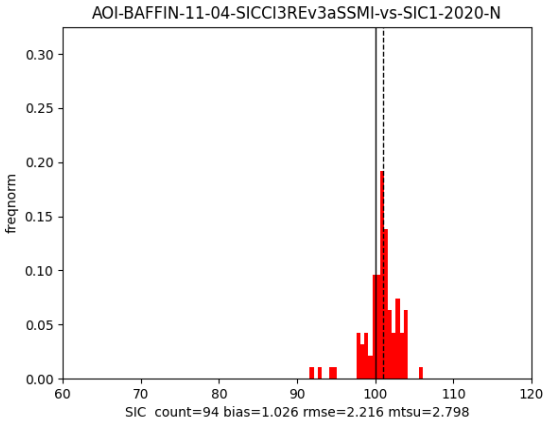
AOI-BAFFIN-11-04-SICCI3REv3aSSMI-vs-SIC1-2020-N
freqnorm
0.00
0.05
0.10
0.15
0.20
0.25
0.30
60
70
80
90
100
110
120
SIC count=94 bias=1.026 rmse=2.216 mtsu=2.798

APPENDIX F : SIC1 validation per year for Northern Beaufort Sea (Histograms)

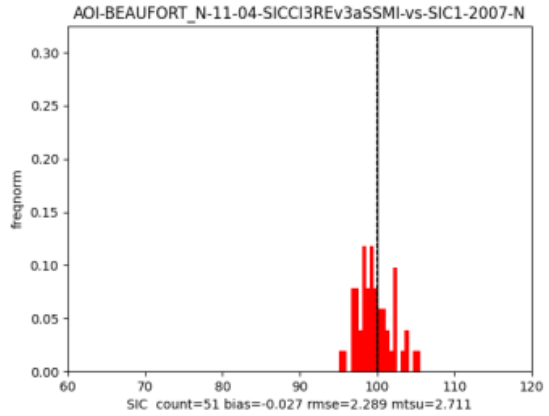

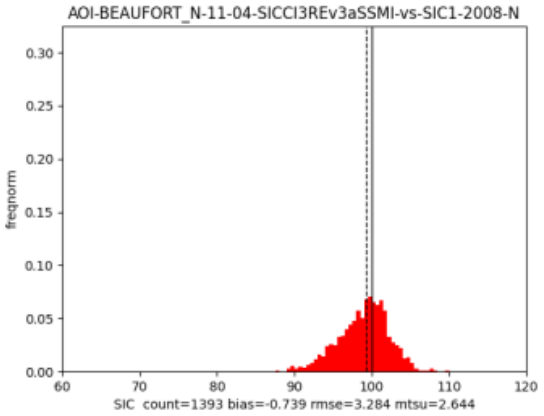

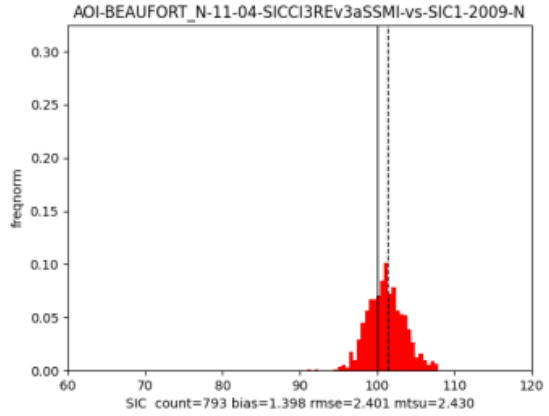

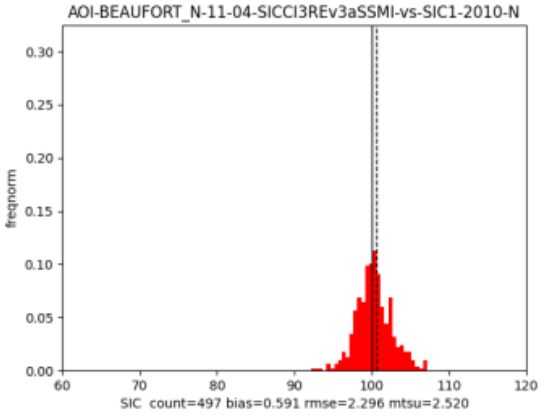

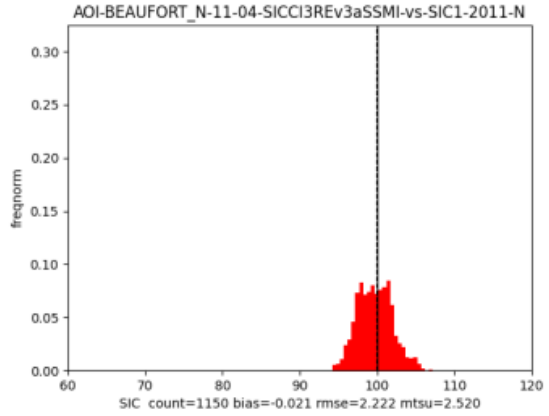

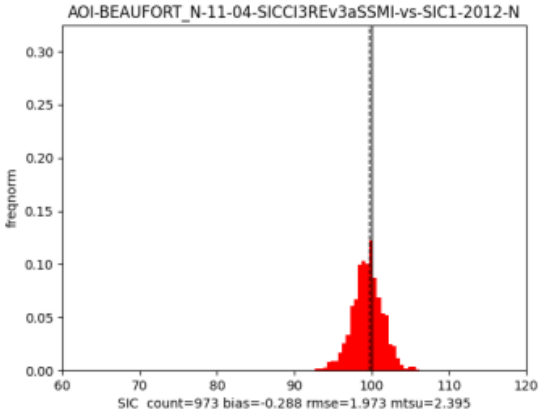

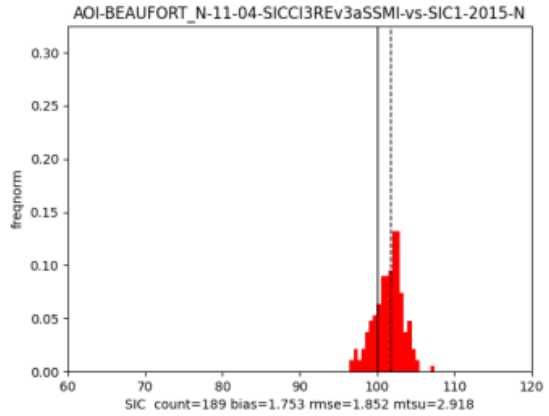
AOI-BEAUFORT_N-11-04-SICCI3REv3aSSMI-vs-SIC1-2015-N
freqnorm
SIC count=189 bias=1.753 rmse=1.852 mtsu=2.918

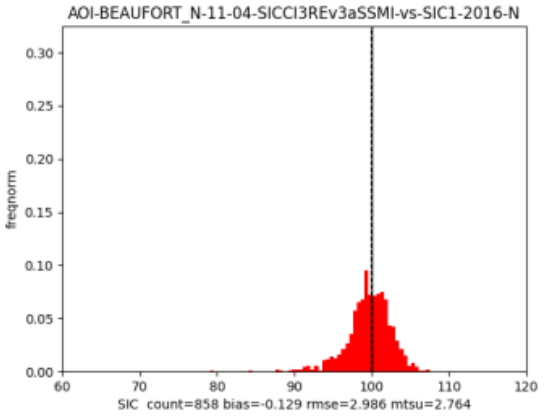
AOI-BEAUFORT_N-11-04-SICCI3REv3aSSMI-vs-SIC1-2016-N
freqnorm
SIC count=858 bias=-0.129 rmse=2.986 mtsu=2.764

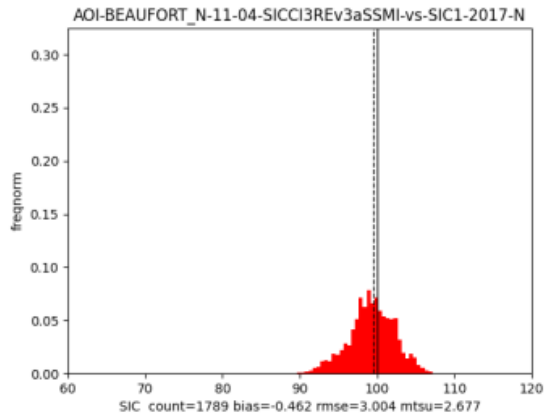
AOI-BEAUFORT_N-11-04-SICCI3REv3aSSMI-vs-SIC1-2017-N
freqnorm
SIC count=1789 bias=-0.462 rmse=3.004 mtsu=2.677

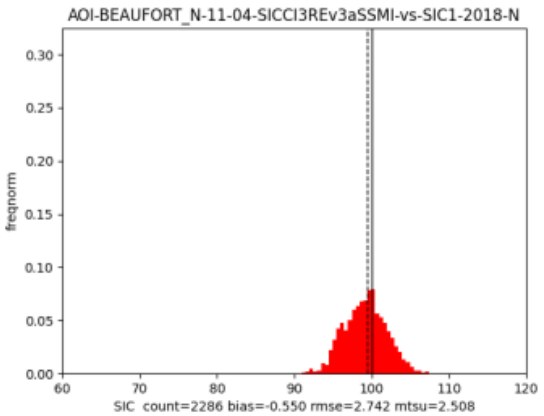
AOI-BEAUFORT_N-11-04-SICCI3REv3aSSMI-vs-SIC1-2018-N
freqnorm
SIC count=2286 bias=-0.550 rmse=2.742 mtsu=2.508

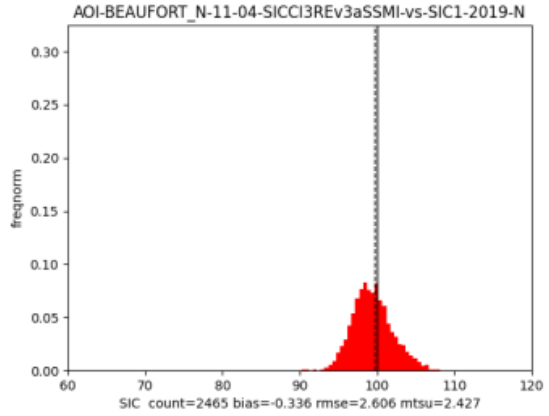
AOI-BEAUFORT_N-11-04-SICCI3REv3aSSMI-vs-SIC1-2019-N
freqnorm
SIC count=2465 bias=-0.336 rmse=2.606 mtsu=2.427

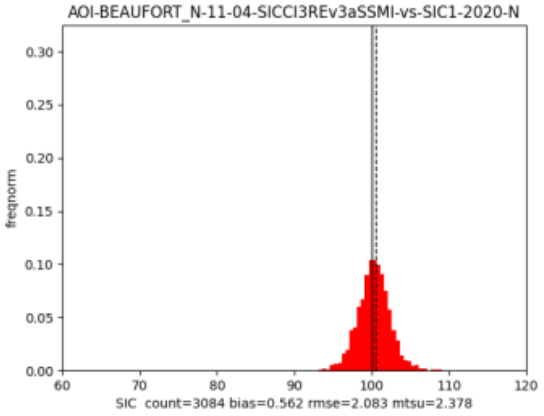
AOI-BEAUFORT_N-11-04-SICCI3REv3aSSMI-vs-SIC1-2020-N
freqnorm
SIC count=3084 bias=0.562 rmse=2.083 mtsu=2.378

APPENDIX G : SIC1 validation per year for the Southern Beaufort Sea (Histograms)

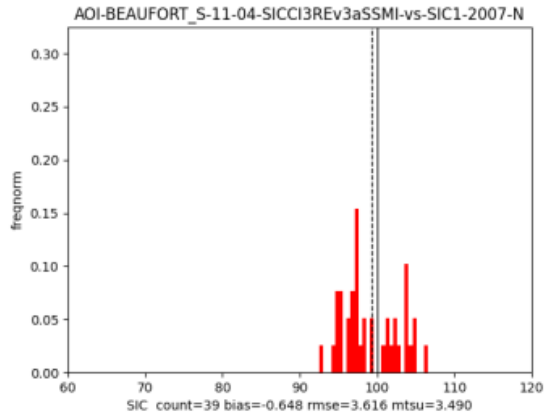

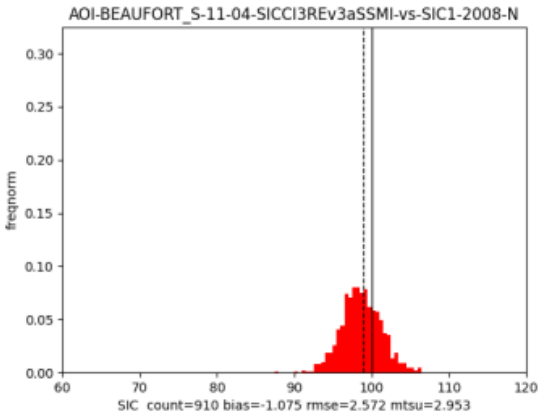

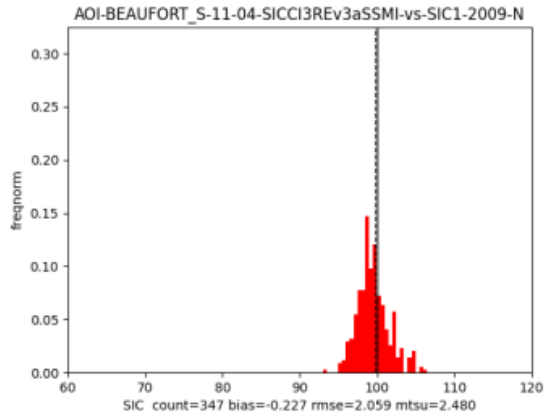

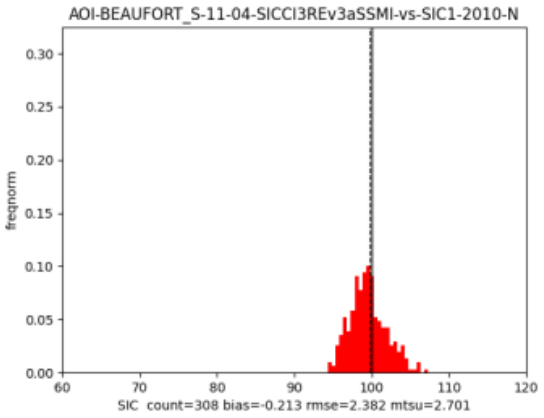

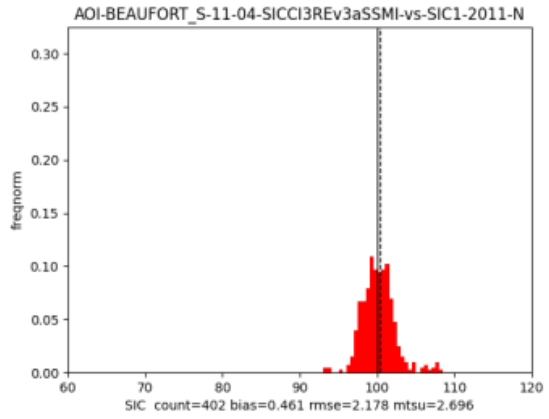

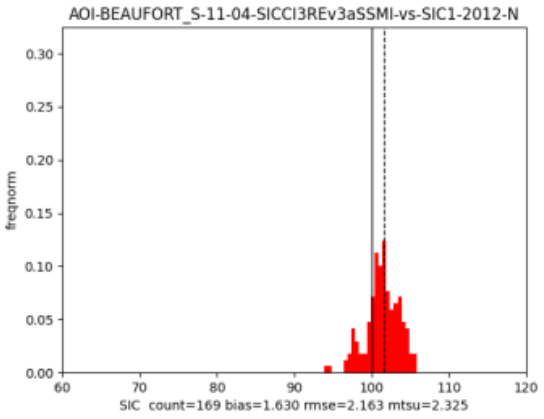

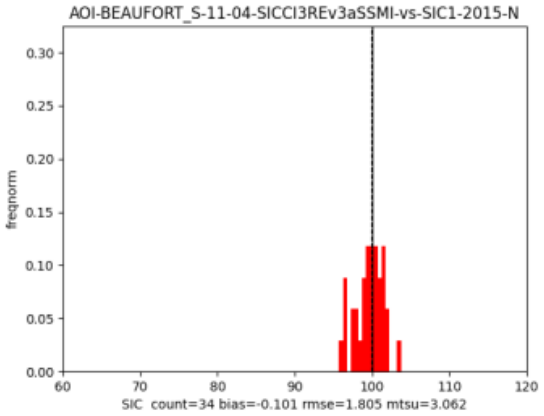
AOI-BEAUFORT_S-11-04-SICCI3REv3aSSMI-vs-SIC1-2015-N
freqnorm
SIC count=34 bias=-0.101 rmse=1.805 mtsu=3.062

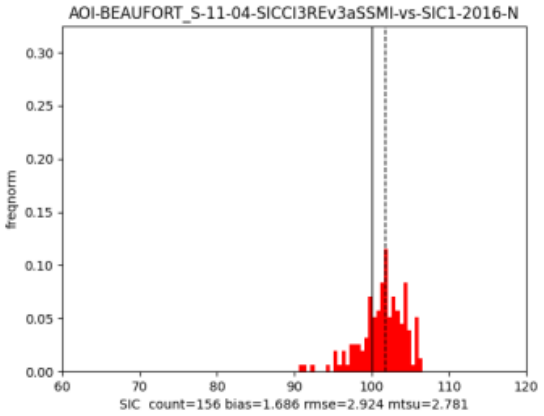
AOI-BEAUFORT_S-11-04-SICCI3REv3aSSMI-vs-SIC1-2016-N
freqnorm
SIC count=156 bias=1.686 rmse=2.924 mtsu=2.781

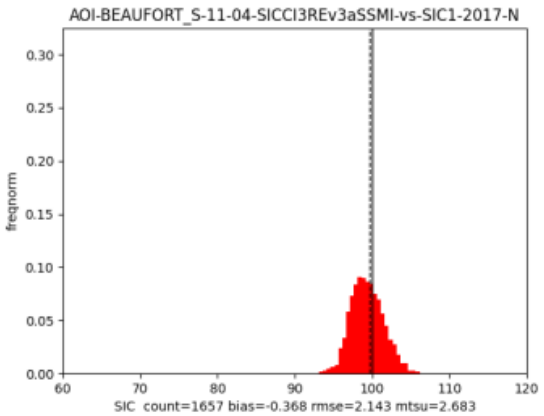
AOI-BEAUFORT_S-11-04-SICCI3REv3aSSMI-vs-SIC1-2017-N
freqnorm
SIC count=1657 bias=-0.368 rmse=2.143 mtsu=2.683

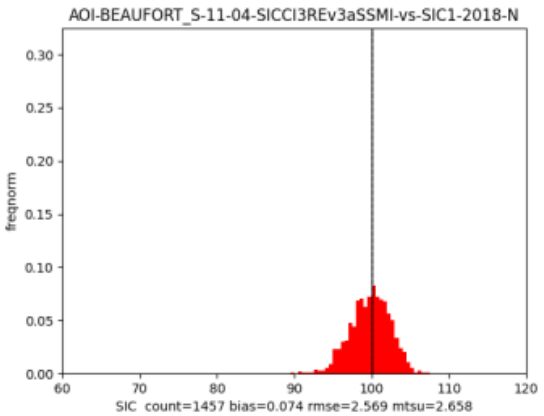
AOI-BEAUFORT_S-11-04-SICCI3REv3aSSMI-vs-SIC1-2018-N
freqnorm
SIC count=1457 bias=0.074 rmse=2.569 mtsu=2.658

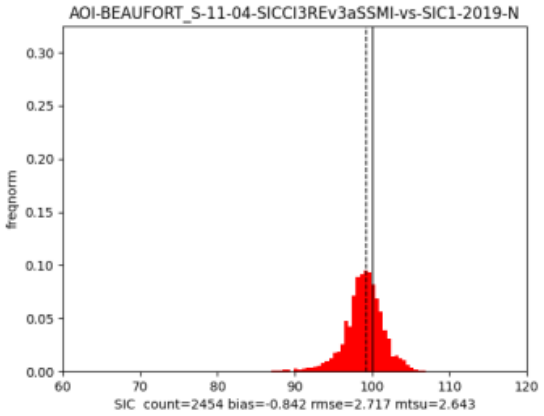
AOI-BEAUFORT_S-11-04-SICCI3REv3aSSMI-vs-SIC1-2019-N
freqnorm
SIC count=2454 bias=-0.842 rmse=2.717 mtsu=2.643

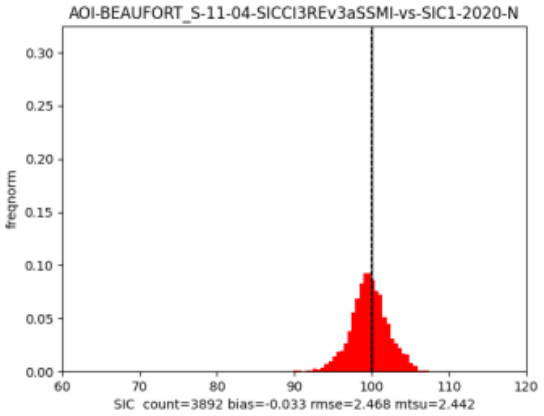
AOI-BEAUFORT_S-11-04-SICCI3REv3aSSMI-vs-SIC1-2020-N
freqnorm
SIC count=3892 bias=-0.033 rmse=2.468 mtsu=2.442

APPENDIX H : SIC1 validation per year for the Northern Kara Sea (Histograms)

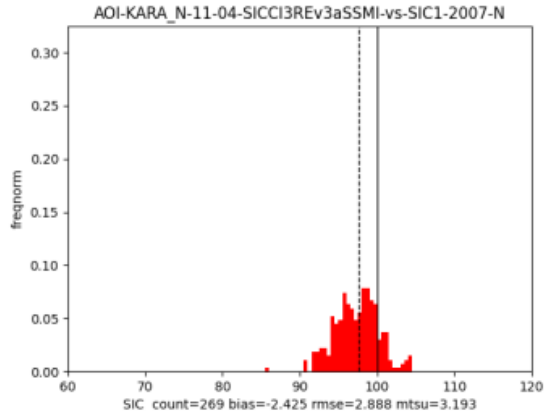

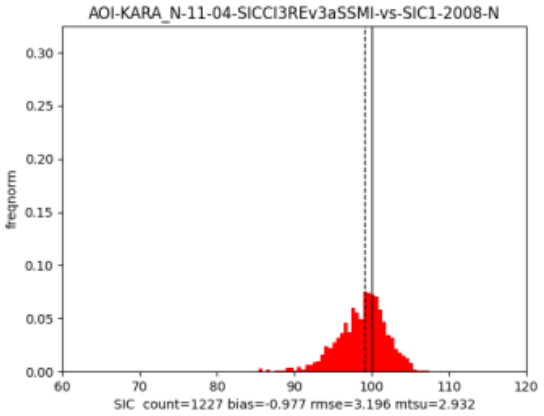

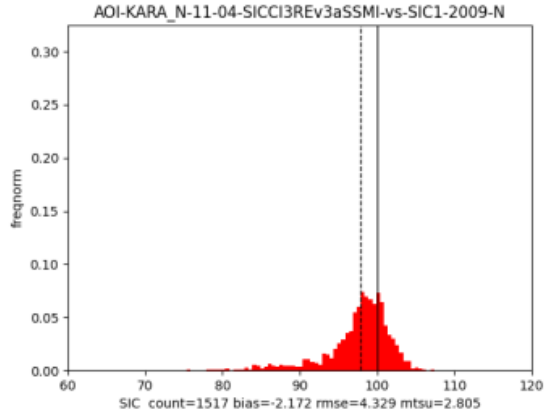

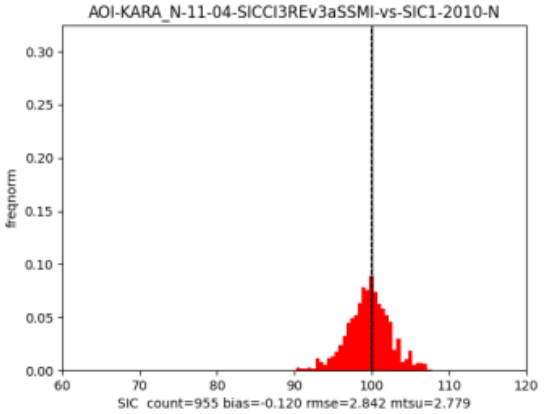

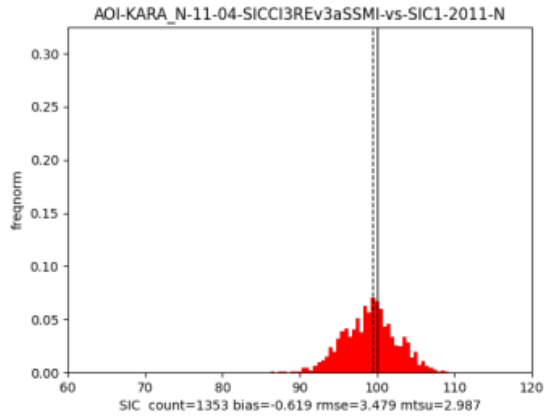

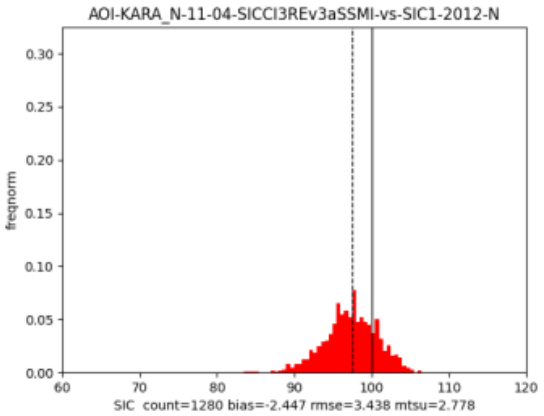

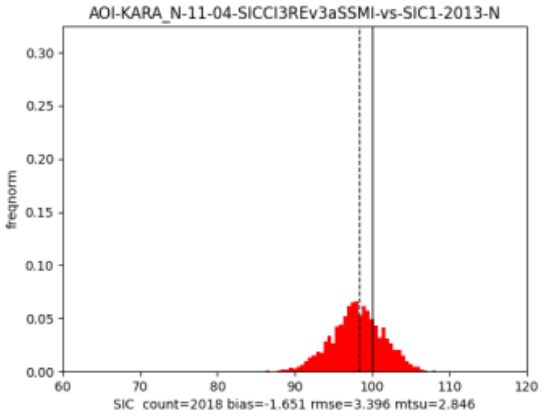
AOI-KARA_N-11-04-SICCI3REv3aSSMI-vs-SIC1-2013-N
freqnorm
SIC count=2018 bias=-1.651 rmse=3.396 mtsu=2.846

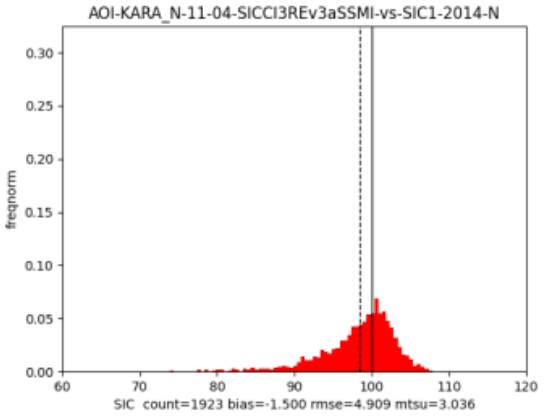
AOI-KARA_N-11-04-SICCI3REv3aSSMI-vs-SIC1-2014-N
freqnorm
SIC count=1923 bias=-1.500 rmse=4.909 mtsu=3.036

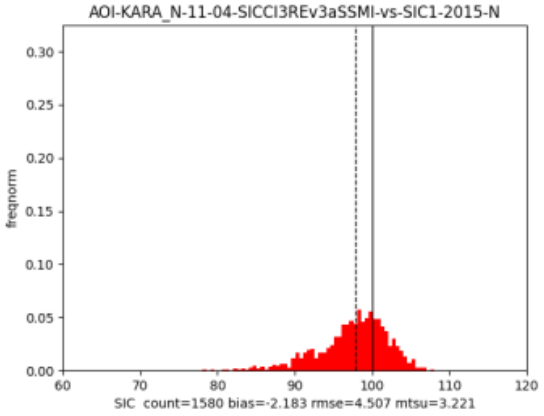
AOI-KARA_N-11-04-SICCI3REv3aSSMI-vs-SIC1-2015-N
freqnorm
SIC count=1580 bias=-2.183 rmse=4.507 mtsu=3.221

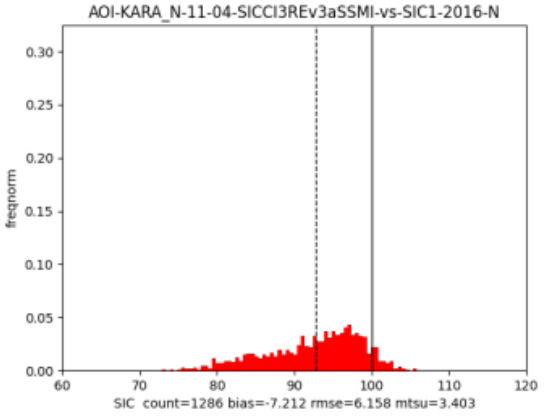
AOI-KARA_N-11-04-SICCI3REv3aSSMI-vs-SIC1-2016-N
freqnorm
SIC count=1286 bias=-7.212 rmse=6.158 mtsu=3.403

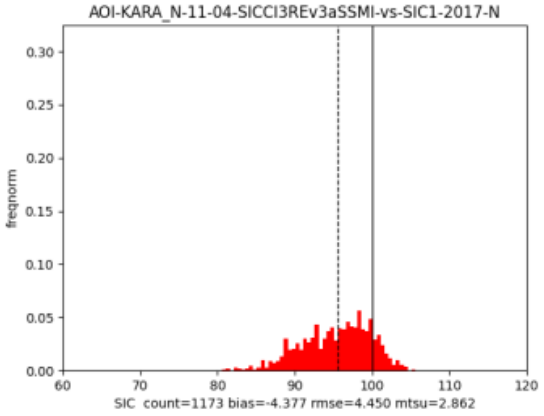
AOI-KARA_N-11-04-SICCI3REv3aSSMI-vs-SIC1-2017-N
freqnorm
SIC count=1173 bias=-4.377 rmse=4.450 mtsu=2.862

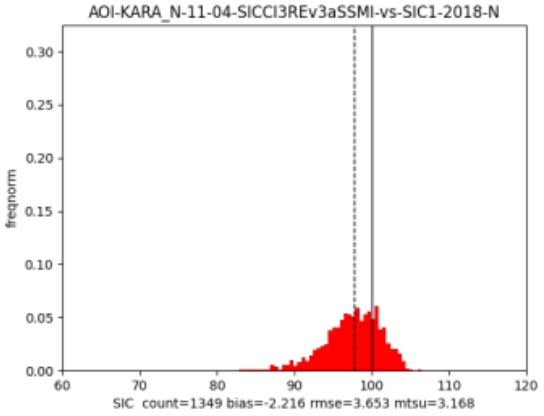
AOI-KARA_N-11-04-SICCI3REv3aSSMI-vs-SIC1-2018-N
freqnorm
SIC count=1349 bias=-2.216 rmse=3.653 mtsu=3.168

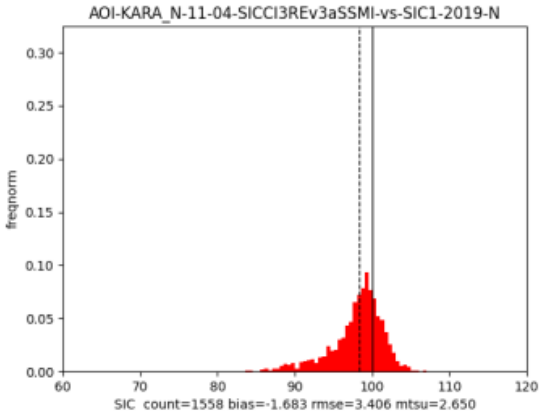
AOI-KARA_N-11-04-SICCI3REv3aSSMI-vs-SIC1-2019-N
freqnorm
0.30
0.25
0.20
0.15
0.10
0.05
0.00
60
70
80
90
100
110
120
SIC count=1558 bias=-1.683 rmse=3.406 mtsu=2.650

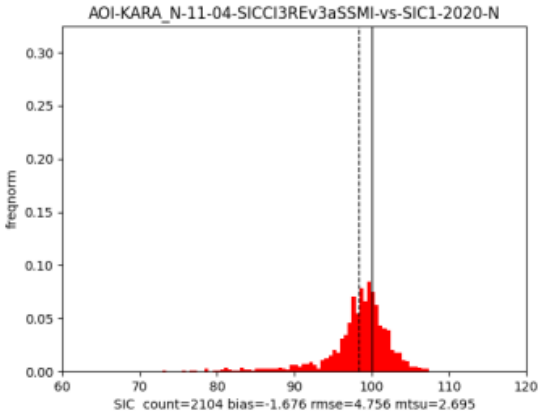
AOI-KARA_N-11-04-SICCI3REv3aSSMI-vs-SIC1-2020-N
freqnorm
0.30
0.25
0.20
0.15
0.10
0.05
0.00
60
70
80
90
100
110
120
SIC count=2104 bias=-1.676 rmse=4.756 mtsu=2.695

APPENDIX I : SIC1 validation per year for the Southern Kara Sea (Histograms)

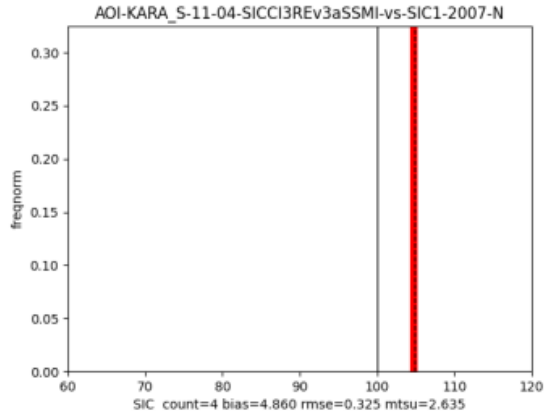

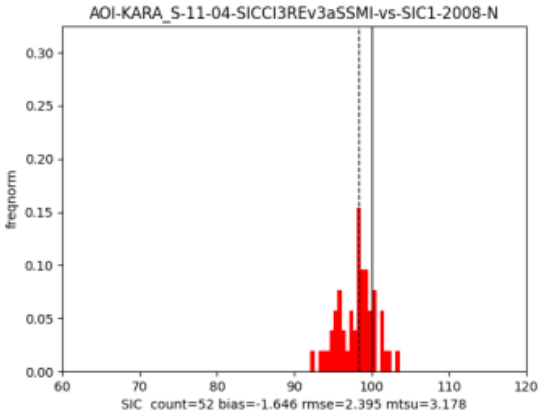

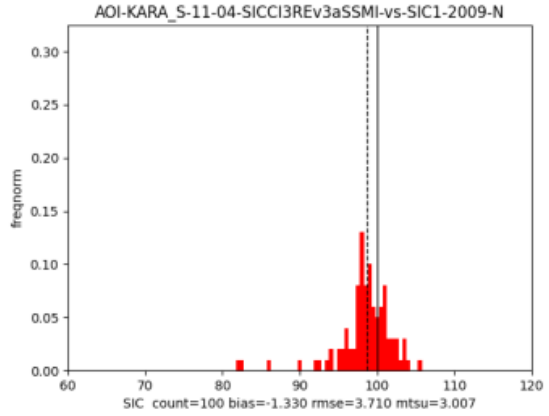

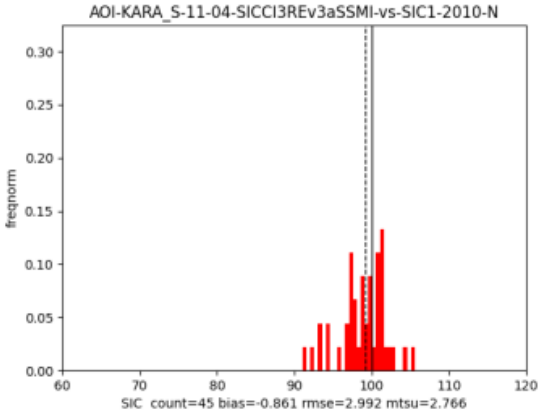

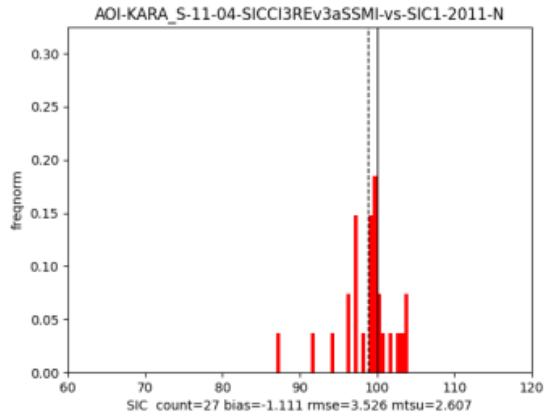

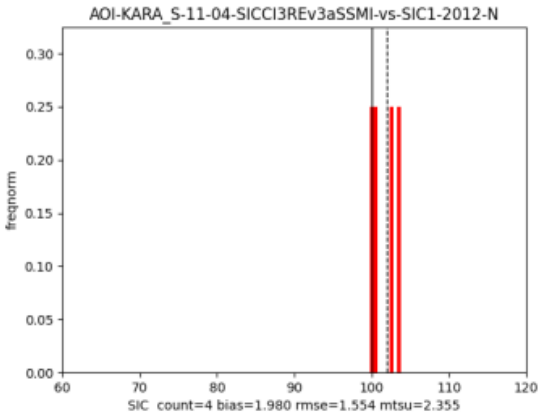

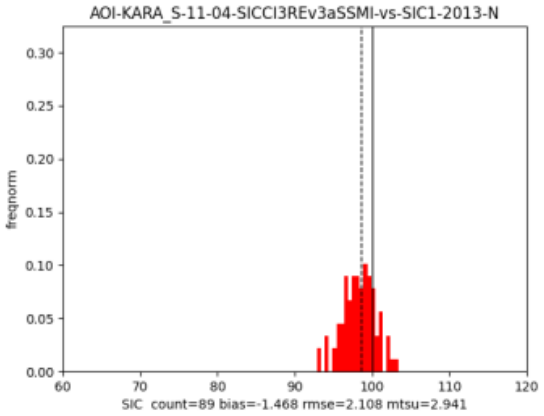
AOI-KARA_S-11-04-SICCI3REv3aSSMI-vs-SIC1-2013-N
freqnorm
SIC count=89 bias=-1.468 rmse=2.108 mtsu=2.941

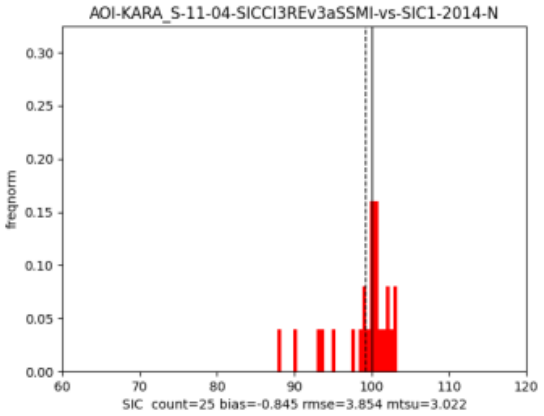
AOI-KARA_S-11-04-SICCI3REv3aSSMI-vs-SIC1-2014-N
freqnorm
SIC count=25 bias=-0.845 rmse=3.854 mtsu=3.022

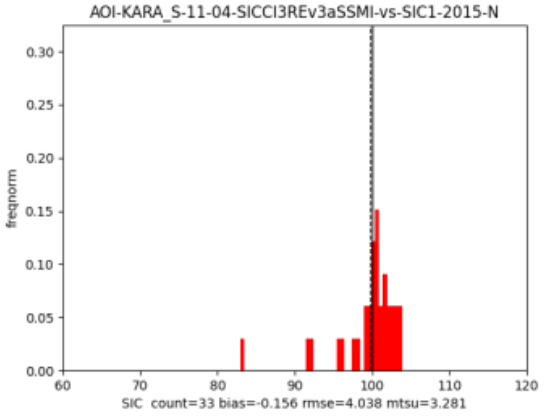
AOI-KARA_S-11-04-SICCI3REv3aSSMI-vs-SIC1-2015-N
freqnorm
SIC count=33 bias=-0.156 rmse=4.038 mtsu=3.281

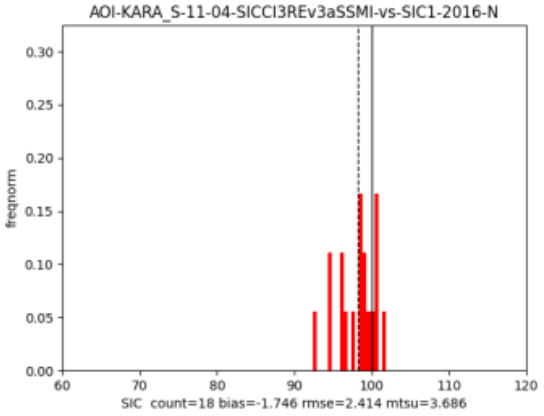
AOI-KARA_S-11-04-SICCI3REv3aSSMI-vs-SIC1-2016-N
freqnorm
SIC count=18 bias=-1.746 rmse=2.414 mtsu=3.686

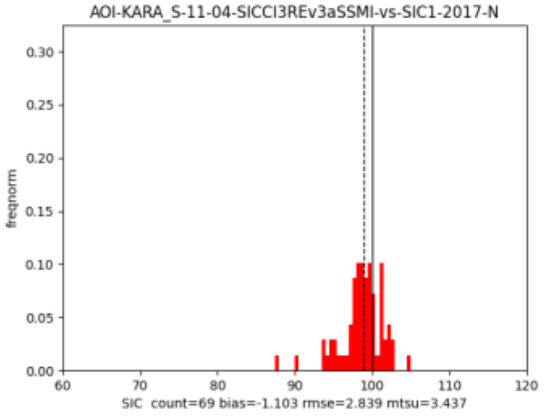
AOI-KARA_S-11-04-SICCI3REv3aSSMI-vs-SIC1-2017-N
freqnorm
SIC count=69 bias=-1.103 rmse=2.839 mtsu=3.437

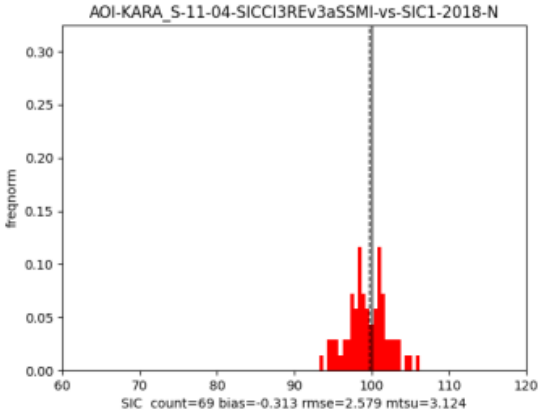
AOI-KARA_S-11-04-SICCI3REv3aSSMI-vs-SIC1-2018-N
freqnorm
SIC count=69 bias=-0.313 rmse=2.579 mtsu=3.124

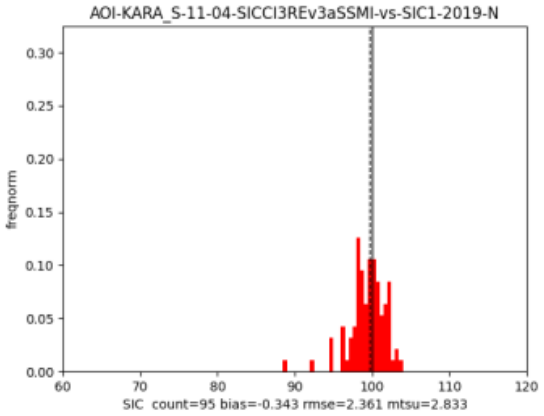
AOI-KARA_S-11-04-SICCI3REv3aSSMI-vs-SIC1-2019-N
freqnorm
0.30
0.25
0.20
0.15
0.10
0.05
0.00
60
70
80
90
100
110
120
SIC count=95 bias=-0.343 rmse=2.361 mtsu=2.833

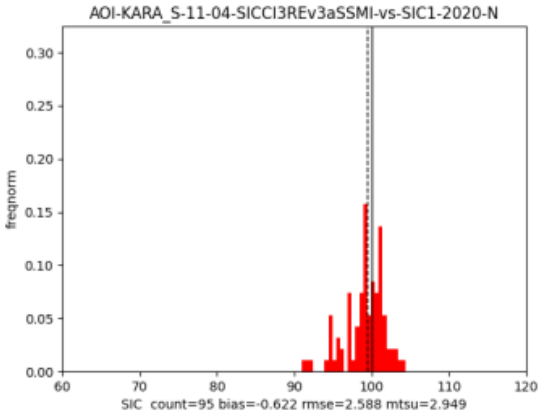
AOI-KARA_S-11-04-SICCI3REv3aSSMI-vs-SIC1-2020-N
freqnorm
0.30
0.25
0.20
0.15
0.10
0.05
0.00
60
70
80
90
100
110
120
SIC count=95 bias=-0.622 rmse=2.588 mtsu=2.949

APPENDIX J : SIC1 validation per year for the Northern Laptev Sea (Histograms)

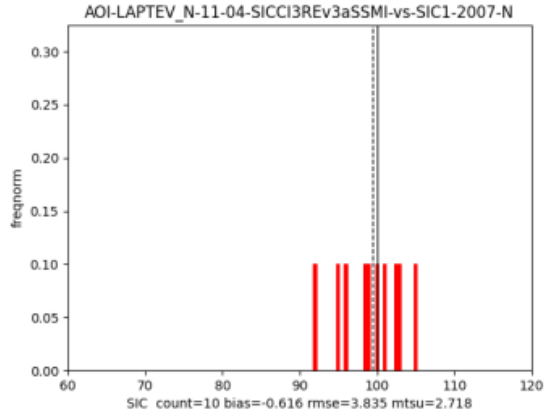

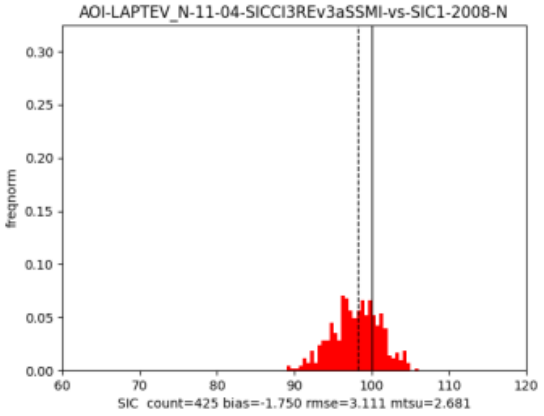

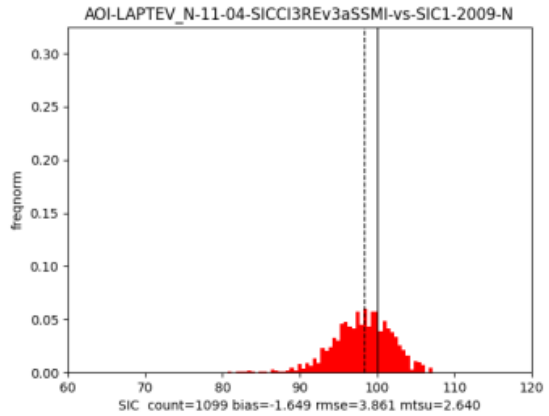

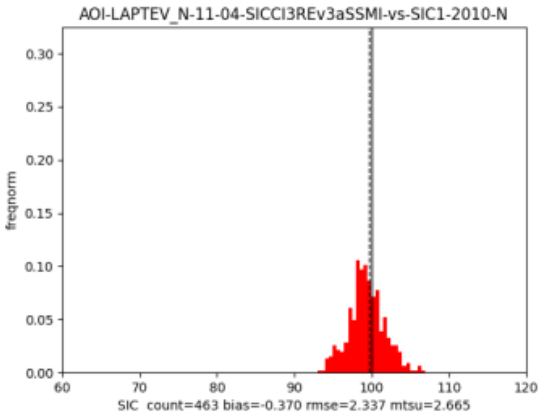

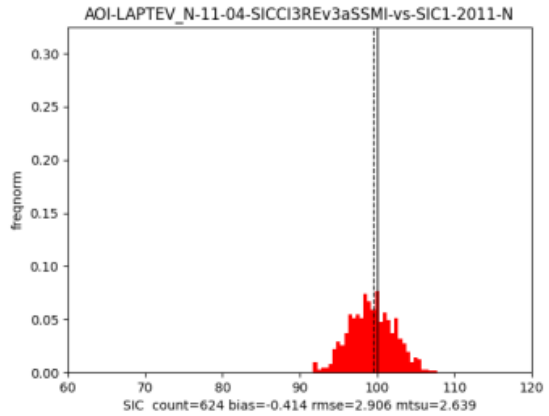

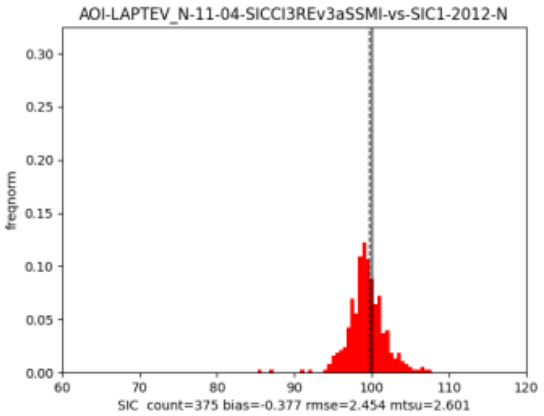

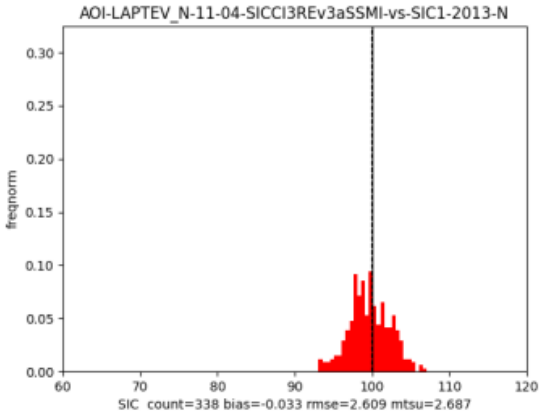
AOI-LAPTEV_N-11-04-SICCI3REv3aSSMI-vs-SIC1-2013-N
freqnorm
SIC count=338 bias=-0.033 rmse=2.609 mtsu=2.687

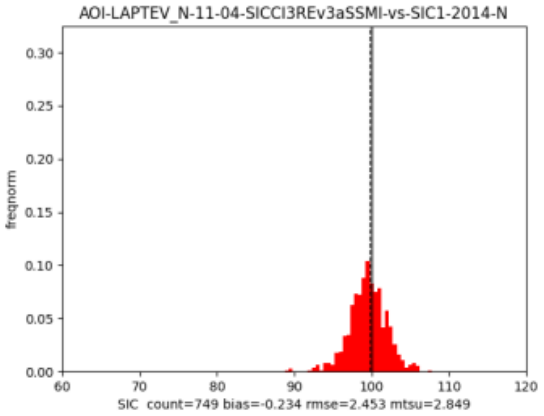
AOI-LAPTEV_N-11-04-SICCI3REv3aSSMI-vs-SIC1-2014-N
freqnorm
SIC count=749 bias=-0.234 rmse=2.453 mtsu=2.849

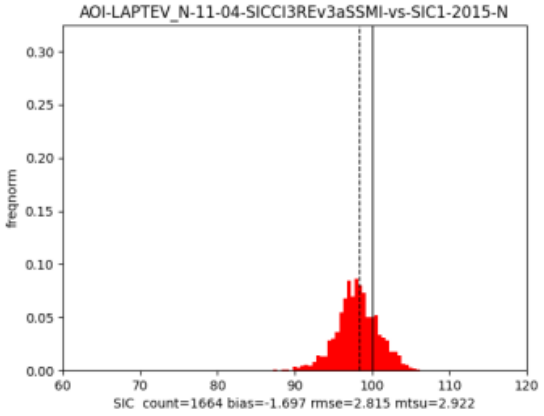
AOI-LAPTEV_N-11-04-SICCI3REv3aSSMI-vs-SIC1-2015-N
freqnorm
SIC count=1664 bias=-1.697 rmse=2.815 mtsu=2.922

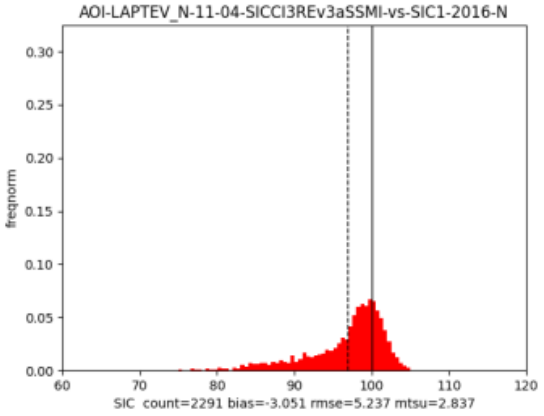
AOI-LAPTEV_N-11-04-SICCI3REv3aSSMI-vs-SIC1-2016-N
freqnorm
SIC count=2291 bias=-3.051 rmse=5.237 mtsu=2.837

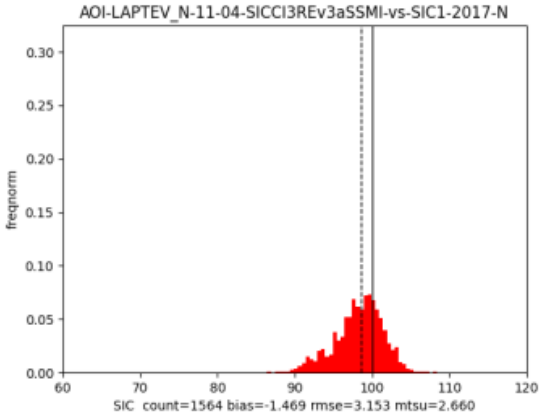
AOI-LAPTEV_N-11-04-SICCI3REv3aSSMI-vs-SIC1-2017-N
freqnorm
SIC count=1564 bias=-1.469 rmse=3.153 mtsu=2.660

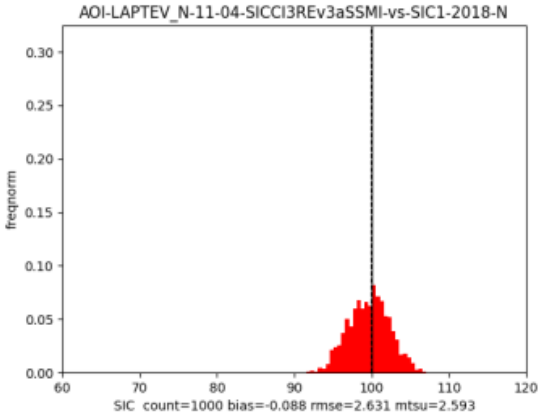
AOI-LAPTEV_N-11-04-SICCI3REv3aSSMI-vs-SIC1-2018-N
freqnorm
SIC count=1000 bias=-0.088 rmse=2.631 mtsu=2.593

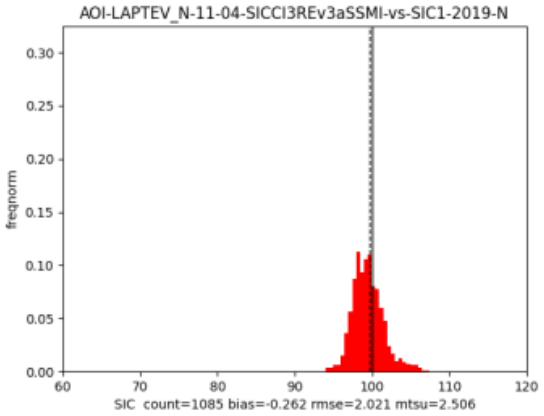
AOI-LAPTEV_N-11-04-SICCI3REv3aSSMI-vs-SIC1-2019-N
freqnorm
0.30
0.25
0.20
0.15
0.10
0.05
0.00
60
70
80
90
100
110
120
SIC count=1085 bias=-0.262 rmse=2.021 mtsu=2.506

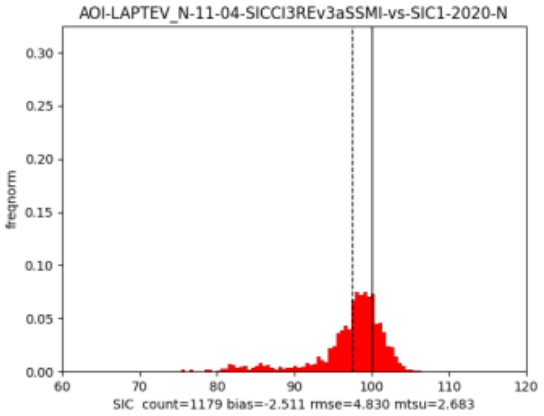
AOI-LAPTEV_N-11-04-SICCI3REv3aSSMI-vs-SIC1-2020-N
freqnorm
0.30
0.25
0.20
0.15
0.10
0.05
0.00
60
70
80
90
100
110
120
SIC count=1179 bias=-2.511 rmse=4.830 mtsu=2.683

APPENDIX K : SIC1 validation per year for North Greenland region (Histograms)

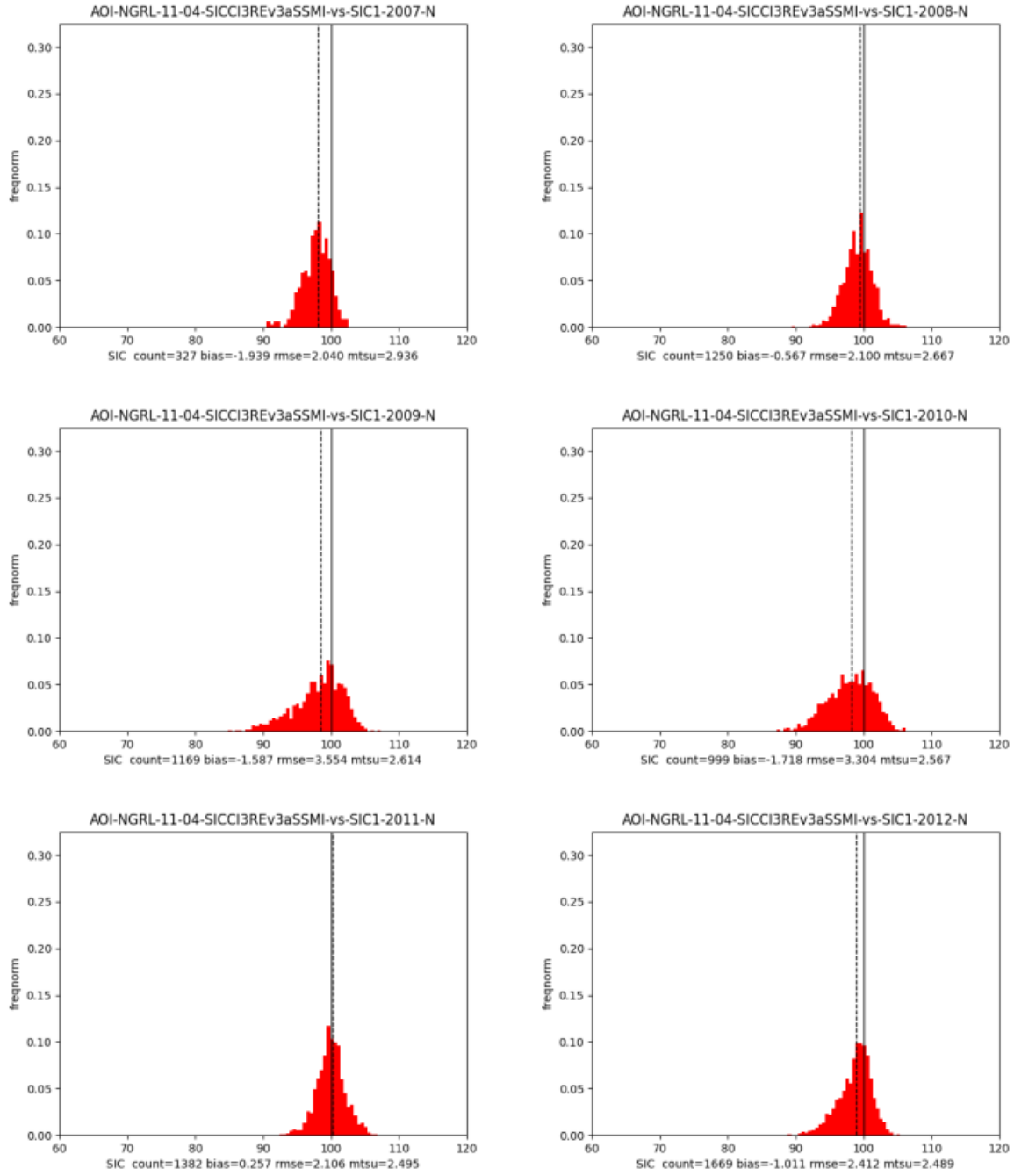

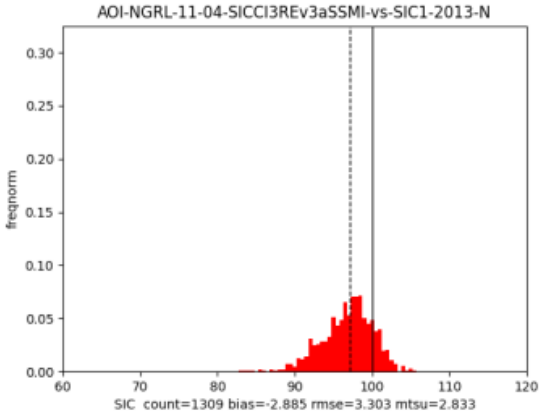
AOI-NGRL-11-04-SICCI3REv3aSSMI-vs-SIC1-2013-N
freqnorm
SIC count=1309 bias=-2.885 rmse=3.303 mtsu=2.833

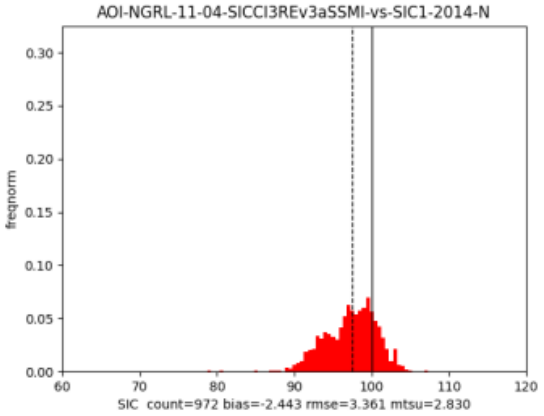
AOI-NGRL-11-04-SICCI3REv3aSSMI-vs-SIC1-2014-N
freqnorm
SIC count=972 bias=-2.443 rmse=3.361 mtsu=2.830

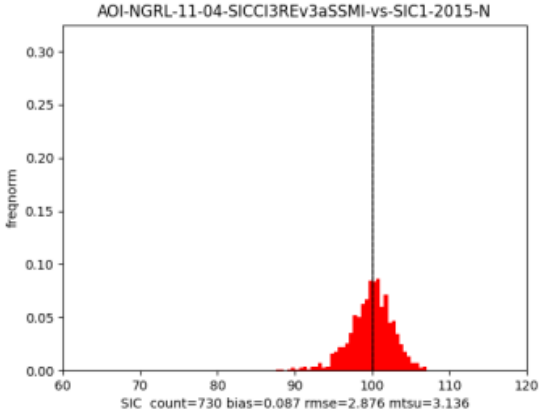
AOI-NGRL-11-04-SICCI3REv3aSSMI-vs-SIC1-2015-N
freqnorm
SIC count=730 bias=0.087 rmse=2.876 mtsu=3.136

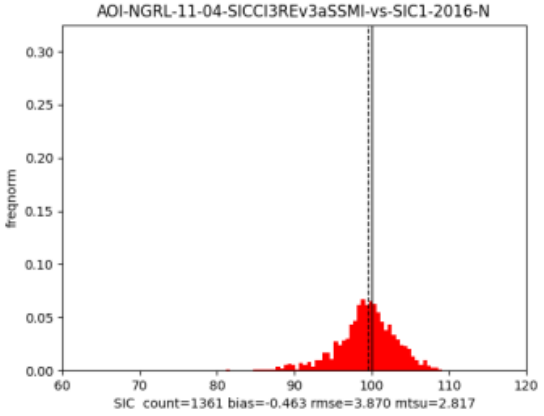
AOI-NGRL-11-04-SICCI3REv3aSSMI-vs-SIC1-2016-N
freqnorm
SIC count=1361 bias=-0.463 rmse=3.870 mtsu=2.817

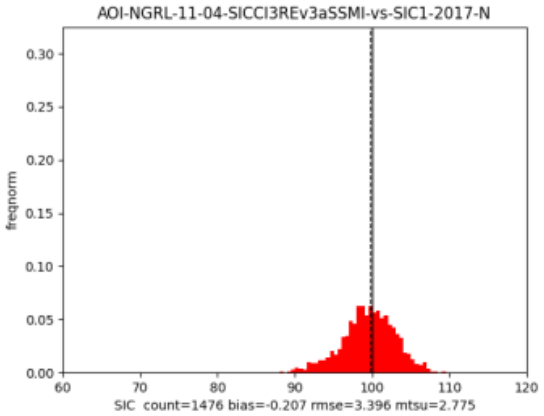
AOI-NGRL-11-04-SICCI3REv3aSSMI-vs-SIC1-2017-N
freqnorm
SIC count=1476 bias=-0.207 rmse=3.396 mtsu=2.775

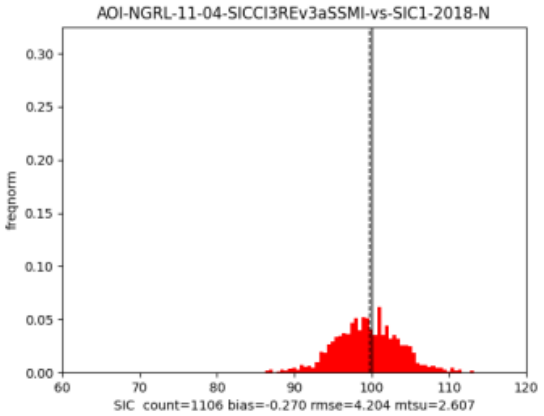
AOI-NGRL-11-04-SICCI3REv3aSSMI-vs-SIC1-2018-N
freqnorm
SIC count=1106 bias=-0.270 rmse=4.204 mtsu=2.607

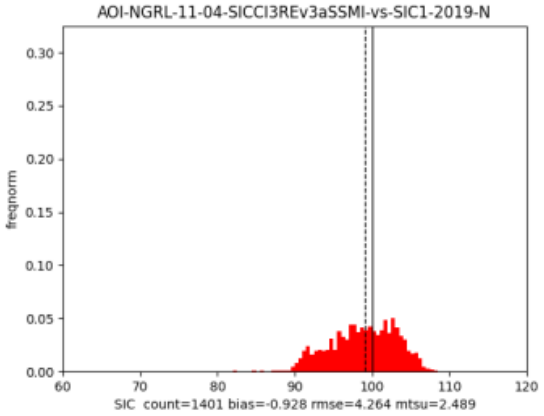
AOI-NGRL-11-04-SICCI3REv3aSSMI-vs-SIC1-2019-N
freqnorm
0.30
0.25
0.20
0.15
0.10
0.05
0.00
60
70
80
90
100
110
120
SIC count=1401 bias=-0.928 rmse=4.264 mtsu=2.489

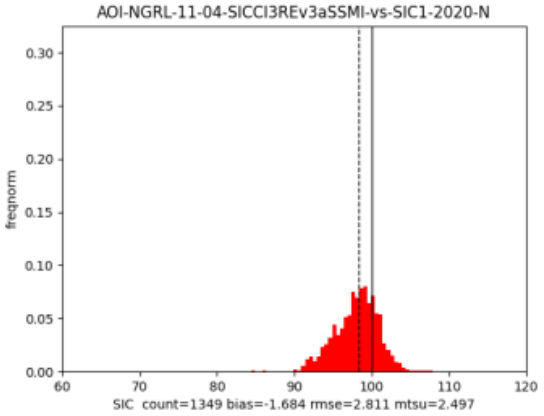
AOI-NGRL-11-04-SICCI3REv3aSSMI-vs-SIC1-2020-N
freqnorm
0.30
0.25
0.20
0.15
0.10
0.05
0.00
60
70
80
90
100
110
120
SIC count=1349 bias=-1.684 rmse=2.811 mtsu=2.497

APPENDIX L : SIC1 validation per year for the Ross Sea (Histograms)

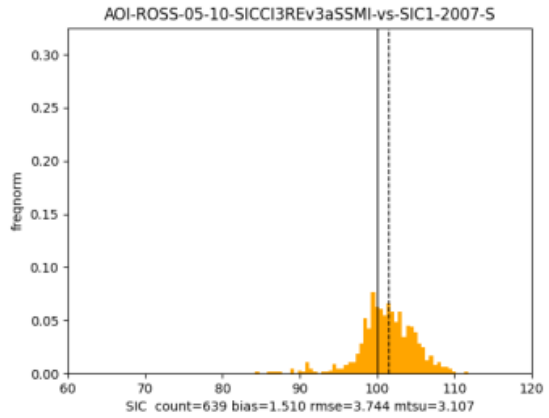

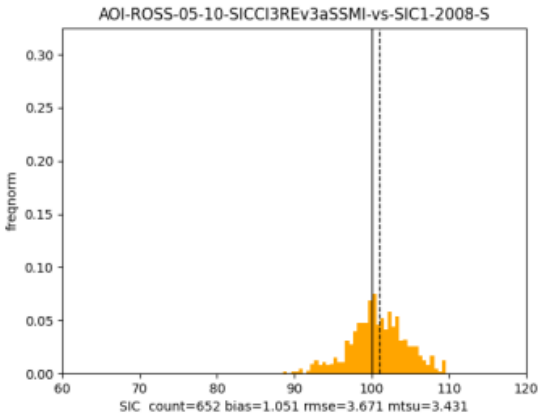

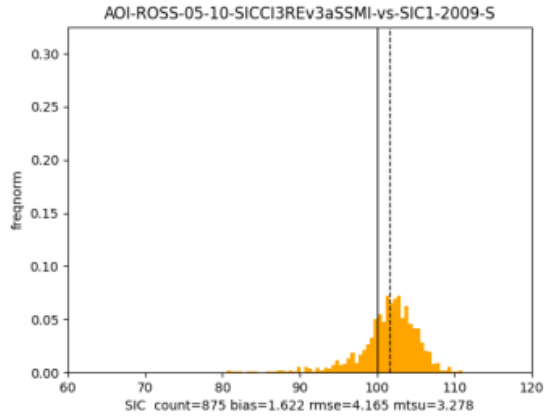

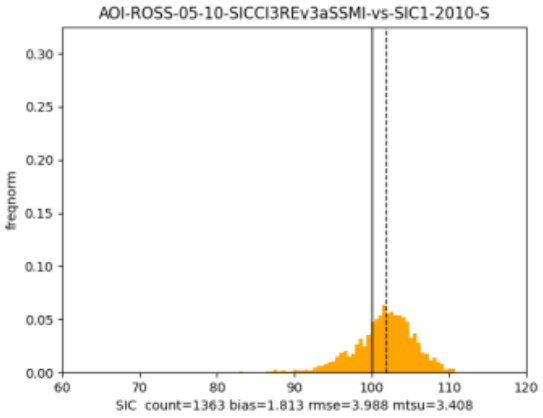

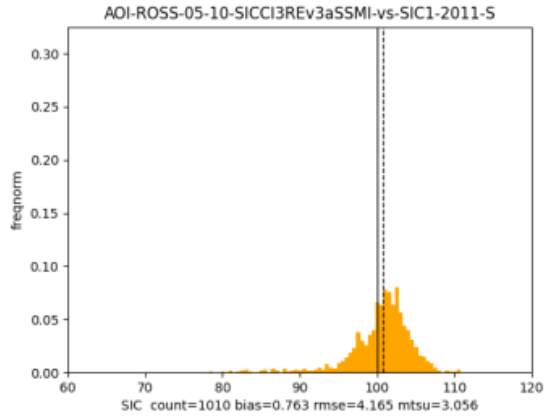

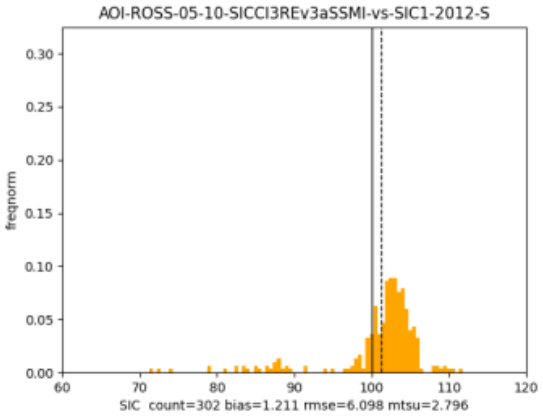

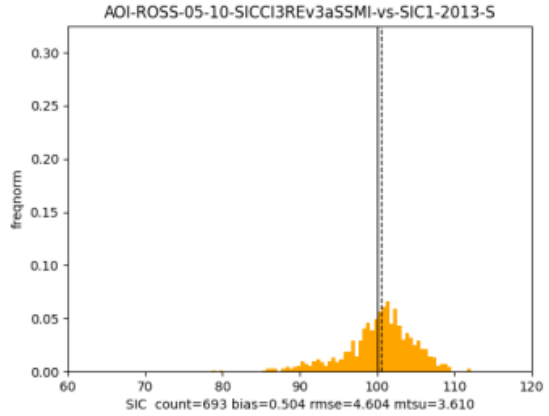
AOI-ROSS-05-10-SICCI3REv3aSSMI-vs-SIC1-2013-S
freqnorm
SIC count=693 bias=0.504 rmse=4.604 mtsu=3.610

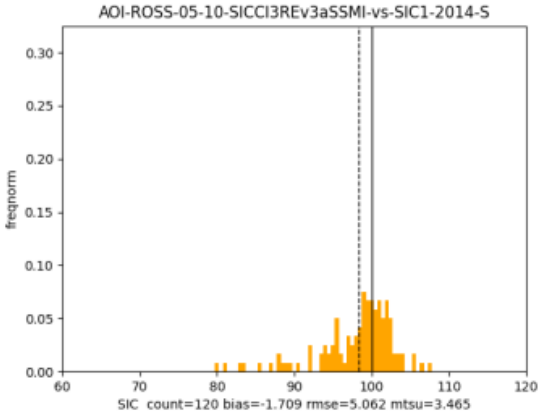
AOI-ROSS-05-10-SICCI3REv3aSSMI-vs-SIC1-2014-S
freqnorm
SIC count=120 bias=-1.709 rmse=5.062 mtsu=3.465

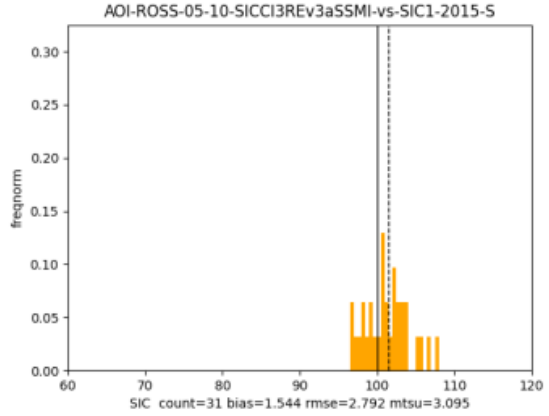
AOI-ROSS-05-10-SICCI3REv3aSSMI-vs-SIC1-2015-S
freqnorm
SIC count=31 bias=1.544 rmse=2.792 mtsu=3.095

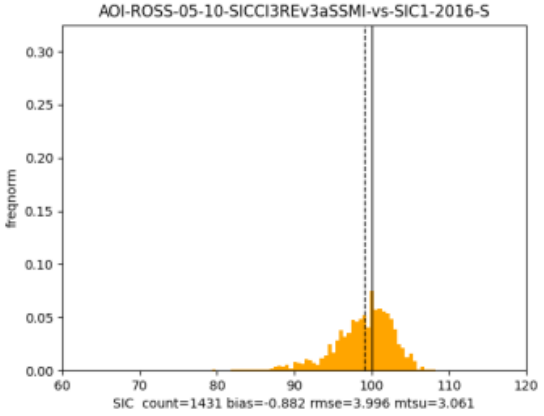
AOI-ROSS-05-10-SICCI3REv3aSSMI-vs-SIC1-2016-S
freqnorm
SIC count=1431 bias=-0.882 rmse=3.996 mtsu=3.061

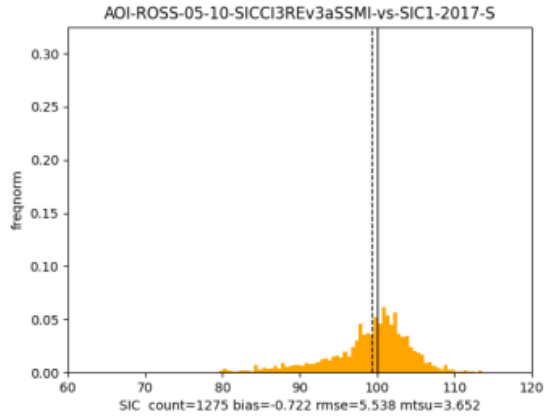
AOI-ROSS-05-10-SICCI3REv3aSSMI-vs-SIC1-2017-S
freqnorm
SIC count=1275 bias=-0.722 rmse=5.538 mtsu=3.652

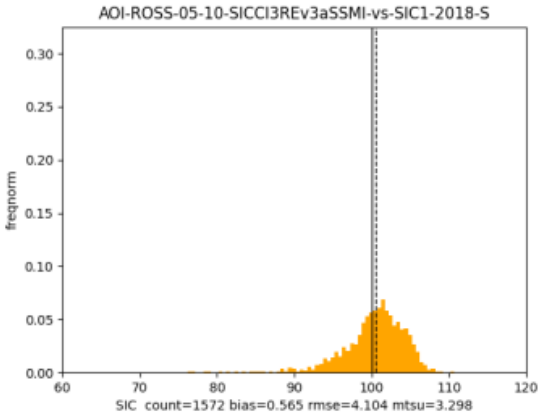
AOI-ROSS-05-10-SICCI3REv3aSSMI-vs-SIC1-2018-S
freqnorm
SIC count=1572 bias=0.565 rmse=4.104 mtsu=3.298

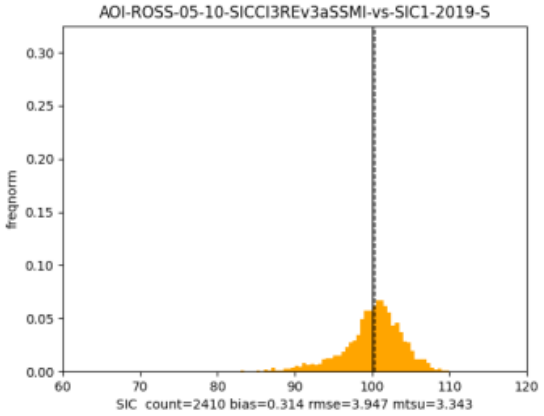
AOI-ROSS-05-10-SICCI3REv3aSSMI-vs-SIC1-2019-S
freqnorm
0.30
0.25
0.20
0.15
0.10
0.05
0.00
60
70
80
90
100
110
120
SIC count=2410 bias=0.314 rmse=3.947 mtsu=3.343

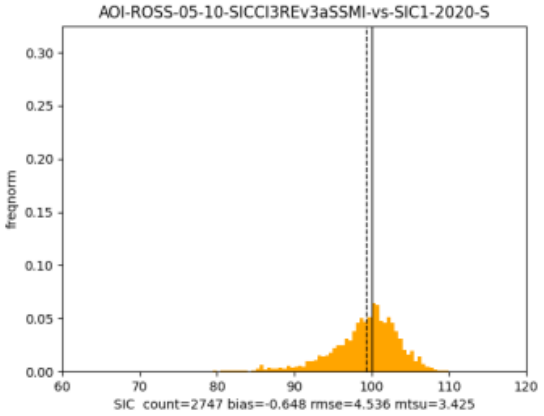
AOI-ROSS-05-10-SICCI3REv3aSSMI-vs-SIC1-2020-S
freqnorm
0.30
0.25
0.20
0.15
0.10
0.05
0.00
60
70
80
90
100
110
120
SIC count=2747 bias=-0.648 rmse=4.536 mtsu=3.425

APPENDIX M : SIC1 validation per year for the Weddell Sea (Histograms)

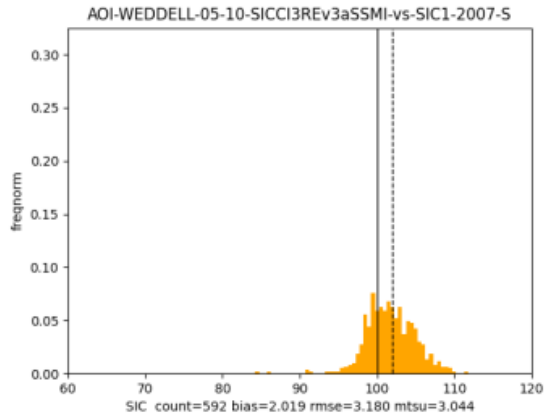

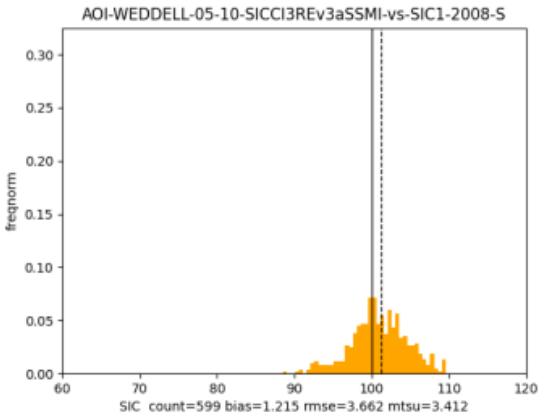

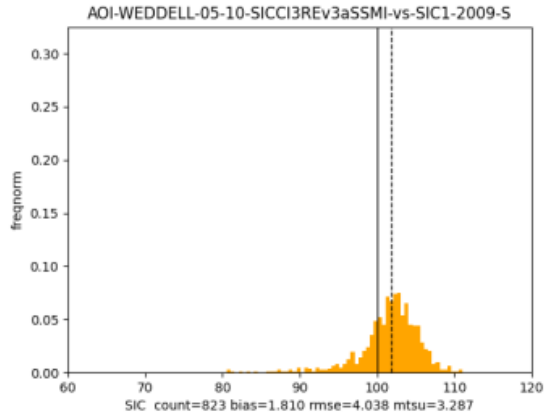

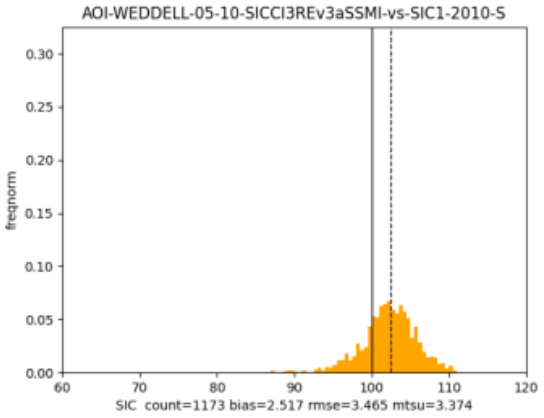

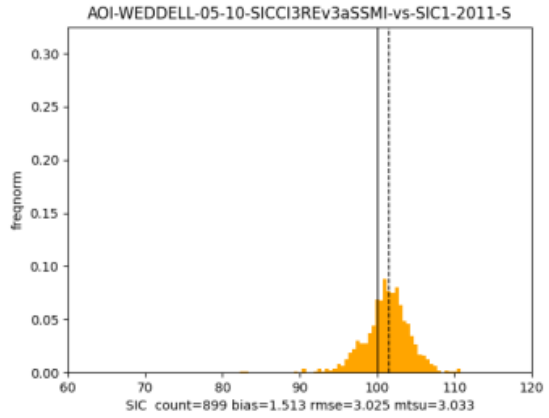

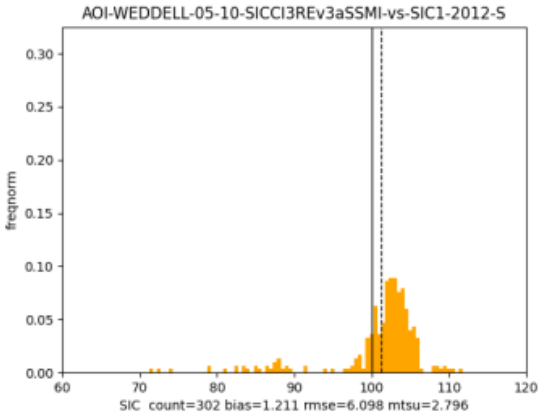

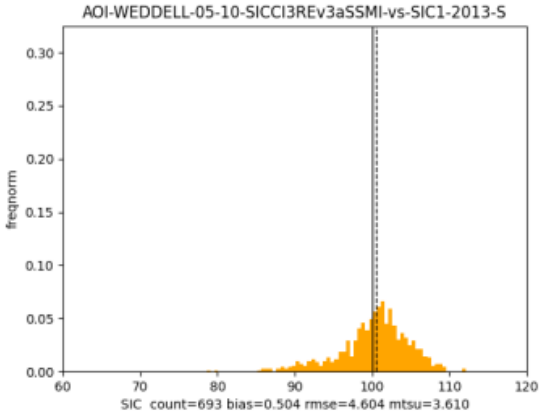
AOI-WEDDELL-05-10-SICCI3REv3aSSMI-vs-SIC1-2013-S
freqnorm
SIC count=693 bias=0.504 rmse=4.604 mtsu=3.610

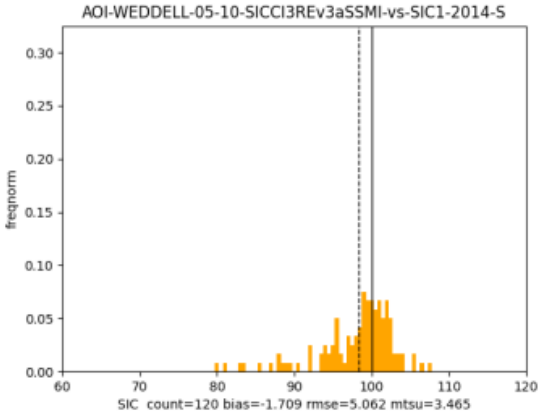
AOI-WEDDELL-05-10-SICCI3REv3aSSMI-vs-SIC1-2014-S
freqnorm
SIC count=120 bias=-1.709 rmse=5.062 mtsu=3.465

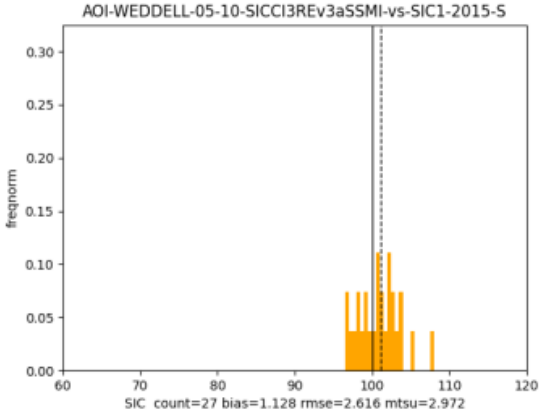
AOI-WEDDELL-05-10-SICCI3REv3aSSMI-vs-SIC1-2015-S
freqnorm
SIC count=27 bias=1.128 rmse=2.616 mtsu=2.972

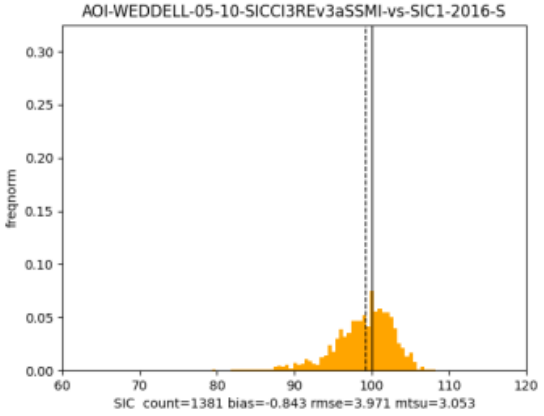
AOI-WEDDELL-05-10-SICCI3REv3aSSMI-vs-SIC1-2016-S
freqnorm
SIC count=1381 bias=-0.843 rmse=3.971 mtsu=3.053

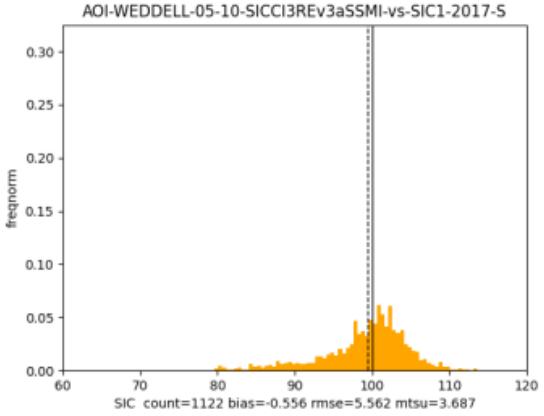
AOI-WEDDELL-05-10-SICCI3REv3aSSMI-vs-SIC1-2017-S
freqnorm
SIC count=1122 bias=-0.556 rmse=5.562 mtsu=3.687

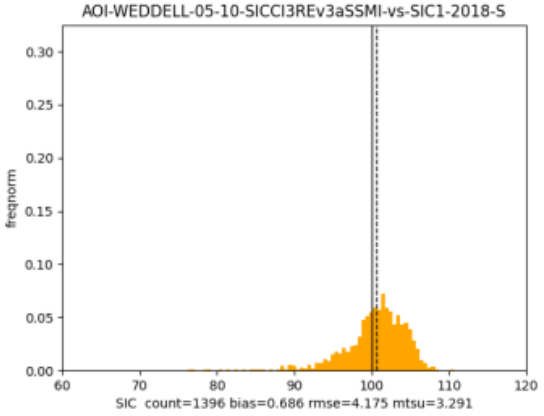
AOI-WEDDELL-05-10-SICCI3REv3aSSMI-vs-SIC1-2018-S
freqnorm
SIC count=1396 bias=0.686 rmse=4.175 mtsu=3.291

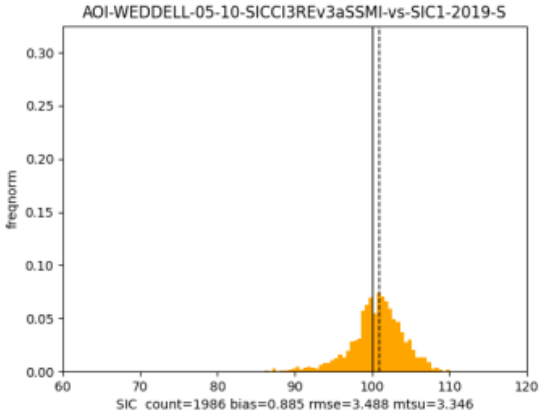
AOI-WEDDELL-05-10-SICCI3REv3aSSMI-vs-SIC1-2019-S
freqnorm
0.30
0.25
0.20
0.15
0.10
0.05
0.00
60
70
80
90
100
110
120
SIC count=1986 bias=0.885 rmse=3.488 mtsu=3.346

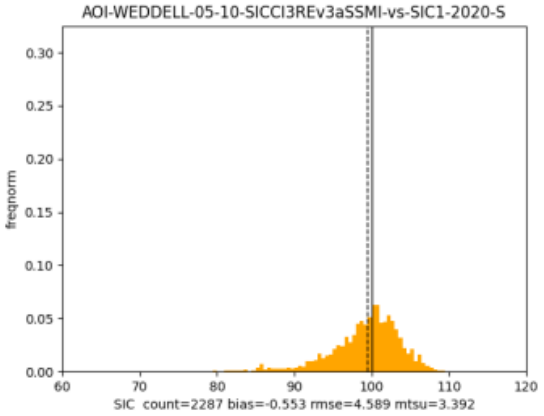
AOI-WEDDELL-05-10-SICCI3REv3aSSMI-vs-SIC1-2020-S
freqnorm
0.30
0.25
0.20
0.15
0.10
0.05
0.00
60
70
80
90
100
110
120
SIC count=2287 bias=-0.553 rmse=4.589 mtsu=3.392